

**The removal of anionic surfactant from commercial laundry  
wastewater with reverse osmosis membrane**

by

**Bradley Gareth Morris**

**A thesis submitted in fulfilment of the requirements for the degree**

**Master of Engineering: Chemical Engineering**

in the

Faculty of Engineering and the Built Environment

at the

Cape Peninsula University of Technology

Supervisor: Dr M Aziz

January 2020

**CPUT copyright information**

The dissertation/thesis may not be published either in part (in scholarly, scientific or technical journals), or as a whole (as a monograph), unless permission has been obtained from the University

## Declaration

I, Bradley Gareth Morris, declare that the contents of this dissertation/thesis represent my own unaided work, and that the dissertation/thesis has not previously been submitted for academic examination towards any qualification. Furthermore, it represents my own opinions and not necessarily those of the Cape Peninsula University of Technology.

Signed



Date

January 2020

## Abstract

Fresh, clean water has always been critical for the world's social development. The current water scarcity will only worsen unless measures are put in place to either reduce water usage or clean and reuse greywater. In areas with limited water resources, affordable technologies can be used to treat greywater and increase the water supply.

Greywater sources that can be reused include domestic, hospital and industrial laundry wastewater. These wastewaters contain different chemicals such as organic and inorganic constituents, which make it difficult to treat. Microfiltration and ultrafiltration are examples of physical filtration processes that can reduce turbidity and pathogens sufficiently, but struggle to remove organics. Therefore, implementing an additional step such as reverse osmosis (RO) could be the solution in the removal of harmful chemicals in greywater.

Unfortunately, the salts that are removed from the water, precipitate on the membrane surface, thus, decreasing the overall process efficiency, due to fouling and scaling. Scaling causes decline in permeation flux, degeneration of membranes, production loss and higher operating costs. This occurrence of fouling cannot be completely isolated; however, it can be minimised. There are two approaches for dealing with the fouling effect, namely, minimization and remediation. Remediation focuses more on frequent chemical cleaning. By using suitable pre-treatment measurements upstream of RO, scale formation can be minimised.

In this study, the use of a commercial antiscalant was examined in the treatment of laundry wastewater influent. The removal of anionic surfactants and COD's from this effluent with a low-pressure, extra low energy, reverse osmosis membrane for reuse application was investigated. The effect of different laundry detergent feed concentrations on operational parameters such as the membrane salt rejection and permeate flow rate (flux) was also analysed. The effect of different antiscalant concentrations to minimise scaling was also evaluated. Membrane fouling and remediation was evaluated by selected membrane surface characteristics.

Model laundry wastewater was treated using a bench-scale reverse osmosis unit. The effects of laundry detergent concentration and antiscalant dosage on the permeate flow rate (flux) and rejection characteristics of the membrane were examined. Removal efficiencies for surfactant and COD concentration were analysed as an indication of membrane performance. A detailed examination of membrane fouling was done by investigating membrane surface characteristics

using Scanning Electron Microscopy (SEM); Attenuated Total Reflection-Fourier Transform Infrared Spectroscopy (ATR-FTIR) and Energy Dispersive X-Ray Spectroscopy (EDX), before and after antiscalant addition. Design Expert 11 was used to generate a predictive model to describe the behaviour of permeate flux decline over time.

ATR-FTIR revealed all the characteristic peaks on a virgin extra low energy (XLE) polyamide thin film composite membrane, in its clean state. It was observed that more foulant is deposited onto the surface of membranes with lower or no antiscalant dosage compared to the higher antiscalant dosed membranes. A morphological change of the membranes was observed using SEM analysis. The hindered attachment of scalant on the surface of the membranes resulted in a much lower rate of flux decline when compared to membranes with no antiscalant addition. EDX revealed that the amount of carbon decreased with an increase in laundry detergent amount (concentration). This could be due to the carbonyl group present in the PA layer being masked by the foulant layer.

The flux decline could be associated with the fouling phenomenon caused by the accumulation of anionic surfactant molecules on the membrane surface, where the build-up of a concentration polarisation layer and/ the or the entrapment in the polyamide layer.

Surfactant rejection exceeded 99.8% in almost all the experimental runs over a range of varied feed concentrations. An average COD removal throughout was 91-96%. It must be noted that the COD removal during the Percentage removal (COD and average EC) of the membranes are all significantly high, between 96-98% removal for average EC and between 91-96% removal for COD, however it was observed that membranes with membranes with no anti-scalant addition performed slightly better than membranes with anti-scalant dosing.

It was observed that the predictive model successfully described the permeate flux decline of laundry wastewater using an RO membrane within the design space of the model. It can be confirmed that the membrane performance investigated using model laundry wastewater could be improved when using commercial antiscalant.

## Research Outputs

- Kasongo, G; Steenberg, C; **Morris, B**; Kapenda, G; Jacobs, N & Aziz, M; 2019; Surface grafting of polyvinyl alcohol (PVA) cross-linked with glutaraldehyde (GA) to improve resistance to fouling of aromatic polyamide thin-film composite reverse osmosis membranes using municipal membrane bioreactor effluent, *IWA: Water Practice, and Technology*, 14 (3), 614-626 [ISSN 1751-321X / DOI.org/10.2166/wpt.2019.047]
- **Morris, B**; Aziz, M & Kasongo, G. 2020, The remediation of laundry wastewater with aromatic polyamide thin-film composite reverse osmosis membranes for recycling application. *Environmental Science and Pollution Research*, Submitted 02 March 2020 [Paper ID.: ESPR-D-20-02522]
- **Morris B** & Aziz M; 2020, The removal of COD and anionic surfactants from laundry wastewater using extra low energy reverse osmosis membrane for reuse application, Proceedings of the WISA 2020 Conference [Johannesburg, South Africa, Sandton Convention Centre, 31 May – 4 June 2020]. Paper No. 113

## Acknowledgements

**I thank God for giving me the strength to succeed with this project, for protecting me, and blessing me with my family and friends.**

This research project was undertaken within the Chemical Engineering Department at the Cape Peninsula University of Technology between January 2018 and January 2020.

I want to express my gratitude to the following people for their contributions towards the completion of this thesis:

My Supervisor, Dr Mujahid Aziz, for his incomparable supervision, persistent guidance, motivation, encouragement and technical expertise in the field of this research. I am thankful for his sustained academic, moral and fatherly assistance throughout my academic journey. "It's been an honour and privilege to have you as my supervisor, Sir."

My Co-supervisor Prof S Ntwampe for his assistance

The technical and administrative staff in the Chemical Engineering Department Mrs Hannelene Small, Mrs Elizma Alberts and Mr Alwyn Bester, always willing to assist.

The Environmental Engineering Research Group (*EnvERG*) for their support. A special thanks to Ntobu Divine Luboya and Franklin Elenga Ewe, assisting with the practical work.

Mrs Miranda Waldron at Electron Microscope Unit, the University of Cape Town and Dr Helen Pfukwa at Polymer Science, University of Stellenbosch.

All my family members, brother bear, Dylan Morris and his wife Danica Morris, Aunts and Uncles, and friends for their moral support, prayers and encouragement.

Monique Dagnin and family, Thea, Lance and Leandri, thank you for your unconditional love and support.

My parents, for their continued moral and financial support and for those who have passed on.

## **Dedication**

To my parents and role models, Glen Morris and Vida Morris for their endless love, support, encouragement and inspiration. This achievement would not be possible without you.

I am forever grateful for your presence in my life

**Thank You, Mommy and Daddy!**

# Table of Contents

List of Figures .....	xii
List of Photos .....	xiv
List of Tables.....	xv
List of Symbols .....	xvii
List of Abbreviations .....	xviii
<b>CHAPTER 1.....</b>	<b>1</b>
<b>Introduction.....</b>	<b>1</b>
<b>1 Introduction.....</b>	<b>2</b>
<b>1.1 Background .....</b>	<b>2</b>
<b>1.2 Laundry wastewater treatment processes .....</b>	<b>3</b>
1.2.1 Problems related to the discharge of Laundry wastewater effluent .....	3
1.2.2 Reverse Osmosis Membranes .....	4
1.2.3 Fouling and Scaling.....	4
1.2.4 Remediation of membrane scaling.....	5
<b>1.3 Research Problem .....</b>	<b>6</b>
<b>1.4 Research topic.....</b>	<b>6</b>
<b>1.5 Research questions .....</b>	<b>6</b>
<b>1.6 Aim and objectives .....</b>	<b>6</b>
<b>1.7 Delineation.....</b>	<b>7</b>
<b>1.8 Thesis Outline.....</b>	<b>8</b>
<b>CHAPTER 2.....</b>	<b>9</b>
<b>2 Literature Review .....</b>	<b>10</b>
<b>2.1 Water shortages .....</b>	<b>10</b>
<b>2.2 Laundry Wastewater and Composition .....</b>	<b>11</b>
<b>2.3 Technologies for the treatment of Laundry Wastewater .....</b>	<b>13</b>



2.3.1	Biological Treatments .....	13
2.3.2	Chemical Treatments .....	13
2.3.3	Physical Treatments .....	13
<b>2.4</b>	<b>Reasons for treating Laundry Wastewater .....</b>	<b>14</b>
2.4.1	Environmental Concerns .....	14
2.4.2	Economic Viability .....	14
<b>2.5</b>	<b>Membrane Technology.....</b>	<b>16</b>
<b>2.6</b>	<b>Membrane configuration.....</b>	<b>17</b>
2.6.1	Hollow fine fibre .....	17
2.6.2	Plate and frame membranes.....	19
2.6.3	Tubular membranes .....	20
2.6.4	Spiral wound membranes .....	20
<b>2.7</b>	<b>Membrane types based on pore sizes .....</b>	<b>22</b>
2.7.1	Microfiltration and Ultrafiltration .....	22
2.7.2	Nanofiltration .....	23
2.7.3	Reverse Osmosis.....	23
<b>2.8</b>	<b>Filtration system in the treatment of laundry wastewater .....</b>	<b>25</b>
<b>2.9</b>	<b>Reverse Osmosis membrane fouling.....</b>	<b>29</b>
<b>2.10</b>	<b>Type of foulants .....</b>	<b>30</b>
2.10.1	Biofouling .....	30
2.10.2	Organic fouling .....	30
2.10.3	Inorganic scaling .....	30
2.10.4	Colloidal fouling.....	31
<b>2.11</b>	<b>Factors affecting Scaling .....</b>	<b>32</b>
<b>2.12</b>	<b>Scale Control Techniques.....</b>	<b>33</b>
2.12.1	Altering feed water characteristics .....	33
2.12.2	Optimisation of operating parameters and system design .....	34
2.12.3	Antiscalant addition .....	35
<b>2.13</b>	<b>RO Process parameters.....</b>	<b>36</b>
2.13.1	Flux .....	36
2.13.2	Salt Rejection.....	36

2.13.3	Pressure .....	37
2.13.4	Recovery .....	37
2.13.5	Temperature.....	37
2.13.6	pH .....	37
<b>2.14</b>	<b>Membrane Surface Characterization .....</b>	<b>38</b>
2.14.1	Fourier Transform Infra-Red Spectroscopy .....	38
2.14.2	Nuclear Magnetic Resonance Spectroscopy .....	40
2.14.3	X-ray Photon Spectroscopy .....	40
2.14.4	Atomic Force Microscopy.....	40
2.14.5	Scanning Electron Microscopy and Energy Dispersive X-ray Spectroscopy .....	41
<b>CHAPTER 3.....</b>	<b>.....</b>	<b>43</b>
<b>3</b>	<b>Research Methodology .....</b>	<b>44</b>
<b>3.1</b>	<b>Introduction .....</b>	<b>44</b>
<b>3.2</b>	<b>RO system process description .....</b>	<b>45</b>
3.2.1	Experimental Set-up .....	45
3.2.2	RO System Operation .....	48
3.2.3	RO Cell Start up procedure.....	48
3.2.4	Membrane cleaning .....	50
3.2.5	Membrane replacement .....	50
3.2.6	Equipment used during RO operation.....	52
3.2.7	COD and surfactant analysis.....	53
3.2.8	Make-up of the simulated feed.....	55
<b>3.3</b>	<b>Anti-Scalant Addition .....</b>	<b>56</b>
<b>3.4</b>	<b>Membrane Surface Characterization .....</b>	<b>57</b>
3.4.1	ATR-FTIR Analysis .....	57
3.4.2	SEM-EDS Analysis .....	57
<b>CHAPTER 4.....</b>	<b>.....</b>	<b>58</b>
<b>4</b>	<b>Results and Discussion .....</b>	<b>59</b>
<b>4.1</b>	<b>Membrane Surface Characterisation .....</b>	<b>59</b>
4.1.1	ATR-FTIR Analysis .....	59
4.1.2	SEM-EDX Analysis .....	63

<b>4.2</b>	<b>RO Process performance .....</b>	<b>69</b>
4.2.1	The flux performances during the fouling test.....	69
4.2.2	Flux Decline Ratio .....	72
4.2.3	Salt rejection & Surfactant and COD removal .....	74
<b>4.3</b>	<b>Development of Permeate Flux Decline Model .....</b>	<b>77</b>
4.3.1	Permeate Flux Decline Model Validation .....	80
4.3.2	Effect of process parameters on Permeate Flux Decline .....	81
<b>CHAPTER 5.....</b>	<b>.....</b>	<b>86</b>
<b>5</b>	<b>Conclusion and Recommendations.....</b>	<b>87</b>
5.1	Conclusion.....	87
5.2	Recommendations .....	89
<b>References.....</b>	<b>.....</b>	<b>90</b>
<b>Appendices.....</b>	<b>.....</b>	<b>101</b>
Appendix A.....	.....	102
Appendix A.1.....	.....	103
	<b>RO cell experimental runs with 13.2 mL Laundry Detergent and 0 ppm anti-scalant .....</b>	<b>103</b>
Appendix A.2.....	.....	109
	<b>RO cell experimental runs with 13.2 mL Laundry Detergent and 4 ppm anti-scalant .....</b>	<b>109</b>
Appendix A.3.....	.....	115
	<b>RO cell experimental runs with 13.2 mL Laundry Detergent and 8 ppm anti-scalant .....</b>	<b>115</b>
Appendix B.....	.....	121
Appendix B.1 .....	.....	122
	<b>RO cell experimental runs with 19.8 mL Laundry Detergent and 0 ppm anti-scalant .....</b>	<b>122</b>
Appendix B.2.....	.....	128
	<b>RO cell experimental runs with 19.8 mL Laundry Detergent and 4 ppm anti-scalant .....</b>	<b>128</b>
Appendix B.3.....	.....	134
	<b>RO cell experimental runs with 19.8 mL Laundry Detergent and 8 ppm anti-scalant .....</b>	<b>134</b>
Appendix C.....	.....	140
Appendix C.1.....	.....	141

<b>RO cell experimental runs with 26.4 mL Laundry Detergent and 0 ppm anti-scalant .....</b>	<b>141</b>
Appendix C.2 .....	147
<b>RO cell experimental runs with 26.4 mL Laundry Detergent and 4 ppm anti-scalant .....</b>	<b>147</b>
Appendix C.3 .....	153
<b>RO cell experimental runs with 26.4 mL Laundry Detergent and 8 ppm anti-scalant .....</b>	<b>153</b>
Appendix D .....	159
<b>RO cell experimental Long run with 13.2 mL Laundry Detergent and 0 ppm anti-scalant .....</b>	<b>159</b>
Appendix E .....	163
<b>RO cell experimental Long run with 13.2 mL Laundry Detergent and 8 ppm anti-scalant .....</b>	<b>163</b>
Appendix F .....	167
<b>Sample calculations of RO parameters .....</b>	<b>167</b>
Appendix G .....	169
<b>COD and Surfactant data .....</b>	<b>169</b>
Appendix H .....	171
<b>Testing procedure of physical and chemical parameters.....</b>	<b>171</b>
Appendix I .....	173
<b>EDX Raw Data .....</b>	<b>173</b>
Appendix J .....	186
<b>ATR FTIR Raw Data .....</b>	<b>186</b>

## List of Figures

Figure 2-1: Schematic representation of the membrane process (Adapted from Puretec, (n.d.) )	16
Figure 2-2: Shell-side feed design (Baker, 2012; Berk, 2018; Judd, 2010)	18
Figure 2-3: Bore-side feed design (Baker, 2012; Berk, 2018; Judd, 2010)	18
Figure 2-4: Schematic representation of a plate and frame module (Baker, 2012)	19
Figure 2-5: Diagram of a tubular ultrafiltration system (Baker, 2012)	20
Figure 2-6: Schematic representation of a spiral wound membrane (Baker, 2012)	21
Figure 2-7: Schematic representation of scaling	32
Figure 2-8: Basic operation of an ATR-FTIR system (Johnson et al., 2018)	39
Figure 2-9: Characteristics of functional groups frequencies on FTIR spectra (Coates, 2006)	39
Figure 2-10: SEM images (a) biofouled NF-4040 membrane used for reclaimed water treatment and (b) virgin XLE membrane (Advanced Water Technology Center, 2015)	42
Figure 2-11: EDS spectrum of a fouled MF membrane (Advanced Water Technology Center, 2015)	42
Figure 3-1: Schematic representation of the RO PFD	47
Figure 3-2: Timeline during the fouling experimental runs using the RO cell	48
Figure 3-3: Typical Sepa CF Cell Body Assembly (Sterlite Corporation, 2015)	49
Figure 3-4: Chemical structure of a polyamide composite RO membrane composition (Kucera, 2015)	51
Figure 3-5: Cylindrical beaker (Left) and stop watch (right)	52
Figure 3-6: YSI Eco Sense EC300 conductivity meter model use during the experiments	52
Figure 3-7: Anionic Surfactant Portable Photometer (left) and reagents (right)	53
Figure 3-8: Vitec 3000 23kg pail (Left) and Pipette (Right)	56
Figure 4-1: Full ATR-FTIR Spectra for Virgin membrane	60
Figure 4-2: Zoomed in ATR-FTIR Spectra for varying concentrations of laundry detergent. A: 13.2 mL; B: 19.8 mL; C: 26.4 mL & D: Long Run 1 (0 ppm anti-scalant) and long run 2 (8 ppm anti-scalant)	61
Figure 4-3: Membranes with 13.2 mL Laundry Detergent at various antiscalant dosages- A: 0 ppm; B: 4 ppm & C: 8 ppm	63
Figure 4-4: Membranes with 19.8 mL Laundry Detergent at various anti-scalant dosages- D: 0 ppm; E: 4 ppm & F: 8 ppm	63
Figure 4-5: Membranes with 26.4 mL Laundry Detergent at various anti-scalant dosages- G: 0 ppm; H: 4 ppm & I: 8 ppm	64

Figure 4-6: Long Run 1 (No anti-scalant); K: Long Run 2 (Anti-scalant- 8 ppm) & L: Virgin membrane.....	64
Figure 4-7: EDX analysis of membrane: 13.2 mL Laundry Detergent .....	65
Figure 4-8: EDX analysis of membrane: 19.8 mL Laundry Detergent .....	66
Figure 4-9: EDX analysis of membrane: 26.4 mL Laundry Detergent .....	66
Figure 4-10: EDX analysis of Virgin membrane; Long run 1 (0 ppm anti-scalant) and Long run 2 (8 ppm anti-scalant) .....	67
Figure 4-11: Time dependent average permeate flux of membrane: 13.2 mL Laundry Detergent .....	69
Figure 4-12: Time dependent average permeate flux of membrane: 19.8 mL Laundry Detergent .....	70
Figure 4-13: Time dependent average permeate flux of membrane: 26.4 mL Laundry Detergent .....	70
Figure 4-14: Time dependent average permeate flux of membranes for Long Run 1 and Long Run 2 .....	71
Figure 4-15: Flux decline Ratio at the end of the experiment .....	72
Figure 4-16: Flux Decline Ratio over time of membranes- A: 13.2 mL Laundry detergent; B: 19.8 mL Laundry detergent; C: 26.4 mL Laundry detergent & D: Long Runs.....	73
Figure 4-17: Average EC Salt Rejection for all experiments.....	74
Figure 4-18: COD and Surfactant removal percentages at varying dosages of anti-scalant- A: 13.2 mL Laundry Detergent; B: 19.8 mL Laundry Detergent; C: 26.4 mL Laundry Detergent & D: Long Runs.....	75
Figure 4-19: Normal plot of residuals for flux model .....	80
Figure 4-20: Predicted values vs Actual values .....	80
Figure 4-21: Perturbation graph of factor interaction .....	81
Figure 4-22: Interaction graph between the different factors and permeate flux decline .....	82
Figure 4-23: 2D contour plots showing the influence of increasing time as well as the effects of changes in laundry detergent amount and anti-scalant dosage .....	84
Figure 4-24: 3D contour plots showing the influence of increasing time as well as the effects of changes in laundry detergent amount and anti-scalant dosage .....	85
Figure A.1-1: Permeate flux decline of experimental run and duplication.....	108
Figure A.2-1: Permeate flux decline of experimental run and duplication.....	114
Figure A.3-1: Permeate flux decline of experimental run and duplication.....	120
Figure B.1-1: Permeate flux decline of experimental run and duplication.....	127

Figure B.2-1: Permeate flux decline of experimental run and duplication.....	133
Figure B.3-1: Permeate flux decline of experimental run and duplication.....	139
Figure C.1-1: Permeate flux decline of experimental run and duplication .....	146
Figure C.2-1: Permeate flux decline of experimental run and duplication .....	152
Figure C.3-1: Permeate flux decline of experimental run and duplication .....	158
Figure D-1: Permeate flux decline of experimental run.....	162
Figure E-1: Permeate flux decline of experimental run .....	166
Figure I-1: EDX Spectrum (virgin).....	174
Figure I-2: EDX Spectrum (long run 1) .....	175
Figure I-3: EDX Spectrum (long run 2) .....	176
Figure I-4: EDX Spectrum (13.2 ml Laundry detergent; 0 ppm anti-scalant dosage) .....	177
Figure I-5: EDX Spectrum (13.2 ml Laundry detergent; 4 ppm anti-scalant dosage) .....	178
Figure I-6: EDX Spectrum (13.2 ml Laundry detergent; 8 ppm anti-scalant dosage) .....	179
Figure I-7: EDX Spectrum (19.8 ml Laundry detergent; 0 ppm anti-scalant dosage) .....	180
Figure I-8: EDX Spectrum (19.8 ml Laundry detergent; 4 ppm anti-scalant dosage) .....	181
Figure I-9: EDX Spectrum (19.8 ml Laundry detergent; 8 ppm anti-scalant dosage) .....	182
Figure I-10: EDX Spectrum (26.4 ml Laundry detergent; 0 ppm anti-scalant dosage) .....	183
Figure I-11: EDX Spectrum (26.4 ml Laundry detergent; 4 ppm anti-scalant dosage) .....	184
Figure I-12: EDX Spectrum (26.4 ml Laundry detergent; 8 ppm anti-scalant dosage) .....	185
Figure J-1: Zoomed in ATR-FTIR Spectra for varying concentrations of Anti-scalant. A: 0 ppm; B: 4 ppm; C: 8 ppm & D: Long Runs.....	190

## List of Photos

Photo 3-1: RO Cell system (Lab 1.18, New Chemical Engineering Building, CPUT Bellville, October 2019).....	45
Photo 3-2: Synthetic laundry wastewater.....	55

## List of Tables

Table 2-1: Simulated laundry wastewater feed composition (Boddu et al., 2016) .....	11
Table 2-2: Characteristics of domestic, industrial and hospital laundries wastewaters (Manouchehri & Kargari, 2017) .....	12
Table 2-3: Toxic effects of laundry water constituents (Sumisha et al., 2015) .....	15
Table 2-4: Characteristic features of micro- and ultrafiltration (Friedrich & Pinnekamp, 2003)...	22
Table 2-5: Characteristic features of nanofiltration (Friedrich & Pinnekamp, 2003) .....	23
Table 2-6: Characteristic feature of reverse osmosis (Friedrich & Pinnekamp, 2003) .....	24
Table 2-7: Summary of previous membrane studies with various pollutant removals .....	27
Table 3-1: RO system equipment .....	46
Table 3-2: Operating limits of the Filmtec XLE-4040 PA TFC membrane (Lenntech, n.d.) .....	51
Table 3-3: RO system operating conditions .....	51
Table 3-4: Experiment summary .....	54
Table 3-5: Synthetic feed solution composition .....	55
Table 4-1: ANOVA Response for Cubic model .....	78
Table A.1-1: Membrane specification and initial operating conditions of experimental run. ....	104
Table A.1-2: Experimental run .....	105
Table A.1-3: Experimental run duplicate .....	106
Table A.1-4: Average experimental flux and FDR .....	108
Table A.2-1: Membrane specification and initial operating conditions of experimental run. ....	110
Table A.2-2: Experimental run .....	111
Table A.2-3: Experimental run duplicate .....	112
Table A.2-4: Average experimental flux and FDR .....	114
Table A.3-1: Membrane specification and initial operating conditions of experimental run. ....	116
Table A.3-2: Experimental run .....	117
Table A.3-3: Experimental run duplicate .....	118
Table A.3-4: Average experimental flux and FDR .....	120
Table B.1-1: Membrane specification and initial operating conditions of experimental run. ....	123
Table B.1-2: Experimental run .....	124
Table B.1-3: Experimental run duplicate .....	125
Table B.1-4: Average experimental flux and FDR .....	127
Table B.2-1: Membrane specification and initial operating conditions of experimental run. ....	129
Table B.2-2: Experimental run .....	130
Table B.2-3: Experimental run duplicate .....	131



Table B.2-4: Average experimental flux and FDR .....	133
Table B.3-1: Membrane specification and initial operating conditions of experimental run. ....	135
Table B.3-2: Experimental run .....	136
Table B.3-3: Experimental run duplicate.....	137
Table B.3-4: Average experimental flux and FDR .....	139
Table C.1-1: Membrane specification and initial operating conditions of experimental run. ....	142
Table C.1-2: Experimental run .....	143
Table C.1-3: Experimental run duplicate.....	144
Table C.1-4: Average experimental flux and FDR .....	146
Table C.2-1: Membrane specification and initial operating conditions of experimental run. ....	148
Table C.2-2: Experimental run .....	149
Table C.2-3: Experimental run duplicate.....	150
Table C.2-4: Average experimental flux and FDR .....	152
Table C.3-1: Membrane specification and initial operating conditions of experimental run. ....	154
Table C.3-2: Experimental run .....	155
Table C.3-3: Experimental run duplicate.....	156
Table C.3-4: Average experimental flux and FDR .....	158
Table D-1: Membrane specification and initial operating conditions of experimental run. ....	160
Table D-2: Experimental run .....	161
Table E-1: Membrane specification and initial operating conditions of experimental run. ....	164
Table E-2: Experimental run .....	165
Table G-1: COD and Surfactant data.....	170
Table J-1: FTIR data (virgin; 13.2 ml laundry detergent @ 0ppm, 4ppm, 8ppm anti-scalant) ..	187
Table J-2: FTIR data (long run 1; 19.8ml laundry detergent @ 0ppm, 4ppm, 8ppm anti-scalant) .....	188
Table J-3: FTIR data (long run 2; 26.4ml laundry detergent @ 0ppm, 4ppm, 8ppm anti-scalant) .....	189

## List of Symbols

Area (m <sup>2</sup> )	A
Conductivity (μS)	EC
Water flux (L.m <sup>-2</sup> hr <sup>-1</sup> )	J
Molecular weight (g/mol)	Mw
Pressure (bar)	P
Salt rejection (%)	R
Temperature (°C)	T
Time (hours)	t
Time interval (min)	Δt
Volume (L)	V
<i>Subscripts</i>	
Feed	f
Permeate	p
Time dependant	<i>wf</i>
Initial water	<i>wi</i>
Time dependant	<i>wt</i>

## List of Abbreviations

AFM	Atomic Force Microscopy
ANSI	American National Standards Institute
ATR	Attenuated Total Reflection
ASB	Anaerobic Sludge Blanket
BOD	Biochemical Oxygen Demand
BSE	Back Scattered Electrons
COD	Chemical Oxygen Demand
CW	Constructed Wetland
DI	De-Ionised
DIN	German Institute for Standardisation
DO	Dissolved Oxygen
EC	Electrical Conductivity
EDS	Energy Dispersive X-Ray Spectroscopy
EfOM	Effluent Organic Matter
EPS	Extracellular Polymeric Substances
FTIR	Fourier Transform Infrared Spectrometer
GAC	Granular Activated Carbon
HEDP	Hydroxyethylidene Diphosphonic
IR	Infra-Red
LAS	Linear Alkylbenzene Sulfonate
MBAS	Methylene Blue Active Substance
MBR	Membrane Bioreactor
MF	Microfiltration
NF	Nanofiltration
NMR	Nuclear Magnetic Resonance
NOM	Natural Organic Matter
NSF	National Sanitation Foundation
PA	Polyamide
PES	Polyethersulfone
PSF	Polysulfone
PVP	Polyvinylpyrrolidone
RBC	Rotating Biological Contactor

RO	Reverse Osmosis
SBR	Sequencing Batch Reactor
SDS	Sodium Dodecyl Sulfonate
SE	Second Electrons
SEM	Scanning Electron Microscopy
SHMP	Sodium Hexometaphosphate
SPM	Scanning Probe Microscopy
TA	Total Alkalinity
TDS	Total Dissolved Solids
TFC	Thin Film Composite
TH	Total Hardness
TOC	Total Organic Carbon
TOG	Total Oil and Grease
TP	Total Phosphorous
TSS	Total Suspended Solids
UF	Ultrafiltration
XPS	X-Ray Photoelectron Spectroscopy

# **CHAPTER 1**

## **Introduction**

# 1 Introduction

## 1.1 Background

Although approximately 70% of the earth is covered in water, only 0.03% thereof is usable freshwater (Manouchehri & Kargari, 2017). Considering the inconsistency of water availability, it is important for the successful management of this limited resource (UNESCO, 2003). Two factors affect this limited resource; population and water usage. According to the United Nations University (Guppy & Anderson, 2017), the use of water is growing twice as fast as the global population. The current water scarcity will only worsen unless measures are put in place to either reduce water usage or clean and reuse greywater.

In areas with limited water resources, affordable technologies can be used to treat greywater and increase the water supply; however, only 8% of municipal and industrial wastewater in low-income countries is currently treated (Guppy & Anderson, 2017). Greywater sources that can be reused include domestic, industrial, hospital and laundry wastewater (Boddu et al., 2016). Manouchehri & Kargari (2017) explains that laundry wastewaters contain different substances such as organic (fat, grease, oil, soaps, detergents, chlorinated and aromatic solvents, and biological substances) and inorganic (metal ions and particles, heavy metals, sand and soil dust), which make them difficult to treat. Microfiltration and Ultrafiltration are examples of physical filtration measures that can reduce turbidity and pathogens sufficiently, but struggle to remove organics — thus causing the product water to be less microbiologically stable, which results in the excessive formation of disinfection by-products in addition to chemical disinfectants (Li et al., 2009). Therefore, implementing a tertiary process such as reverse osmosis (RO) can be valuable to assist in the removal of harmful chemicals in greywater. One of the major obstacles of RO is membrane fouling.

Membrane fouling is the accumulation of unwanted constituents on the membrane surface. It is divided into two components, external (surface) and internal fouling (Antony et al., 2011). Fouling cannot be completely removed; however, it can be minimized. There are two approaches for dealing with the fouling effect, minimization and remediation. Remediation focuses more on frequent chemical cleaning (Saqib & Aljundi, 2016). As a result of fouling, scale formation has been a drawback in RO operation because scaling causes decline in permeation flux, degeneration of membrane, production loss and higher operating costs. By using suitable pre-treatment measurements upstream of reverse osmosis (RO), scale formation can be minimised (Antony et al., 2011).

## **1.2 Laundry wastewater treatment processes**

Large amounts of wastewater are produced during the laundering process. In order for soil to be broken down and separated from woven fibres, various factors need to work in synergy. These factors are known as “the Sinner” parameters. For effective cleaning to take place over time, mechanical, thermal and chemical energy is required (Sostar-Turk et al., 2005).

Laundry detergents are comprised of different chemicals at various concentrations, depending on the items to be cleaned and how soiled the items are. Along with bleach and water softeners, surfactants are also present. Surfactant molecules are able to attach to and solubilise oils in the soil. This makes surfactants unique in the effective cleaning and removal of soils (Sostar-Turk et al., 2005).

Conventional wastewater treatment methods including coagulation, flotation, adsorption, chemical (Myburgh et al., 2019) and biological treatment (Kasongo et al., 2019) could be applied for the treatment of laundry wastewater. Future innovation for treating laundry wastewater will be focused around in situ resource recovery. This means that treatments are directly incorporated within laundering systems. In terms of energy requirements and configurations of modules, membrane filtration is a viable wastewater treatment (Giagnorio et al., 2017). In a study conducted by Forstmeier et al. (2005) an integrated treatment solution based on membrane units was studied to recover water in liquid detergent production.

### **1.2.1 Problems related to the discharge of Laundry wastewater effluent**

In some cases, wastewater is discarded in rivers, lakes and oceans without being properly treated. Laundry detergents have been identified as one of the main sources of domestic, commercial and industrial pollution, especially in large cities. Surfactants in pollution can cause drastic changes in biota because many organisms depend on water surface tension. Anionic surfactants can attach themselves to biological molecules. Binding to proteins and peptides modify the polypeptide chain and consequently changes the surface charge of a molecule. This change in biological function can cause toxic effects on ecosystems and changes in biodiversity (Braga & Varesche, 2014).

Because of its ability to remove water-insoluble substances like oily stains, sodium dodecylbenzene sulfonate (SDS), also known as linear alkylbenzene sulfonates (LAS), is the most commonly used anionic surfactant in laundry detergent. Biodegradation of LAS compounds negatively affect the environment and organisms within said system. Under aerobic conditions, large amounts of bio-available oxygen are consumed consequently increasing the chemical oxygen demand (COD) (Ramcharan & Bissessur, 2017). Typically, laundry

wastewaters have a COD, Biochemical Oxygen Demand (BOD) and Total Suspended Solids (TSS) level of 5000, 1300 and 1000 ppm, respectively, but in some scenarios, a COD level of 20000 ppm is also observed (Manouchehri & Kargari, 2017).

The chronic toxicity of anionic surfactants occurs at concentrations greater than 0.1 mg/L. Singh et al. (2002) tested seven surfactants for toxicity on six freshwater microbes and observed that cationic surfactants were more toxic than anionic and followed with non-ionic surfactants.

### **1.2.2 Reverse Osmosis Membranes**

Reverse osmosis is becoming more popular worldwide in industrial wastewater and desalination applications due to the distinctive property of RO membranes to produce pure water by rejecting inorganic species. A semi-permeable membrane separates dissolved constituents present in the feed water from the pure water utilizing pressure as the driving force. RO takes advantage of size properties, charge properties and physical-chemical interactions between constituents present in solvent and membrane surface to achieve high rejection (Malaeb & Ayoub, 2011; Tang et al., 2011; Antony et al., 2011). Nanofiltration membranes attain considerable retention performances for substances with a molar mass of 200 g/mol and more, while reverse osmosis membranes also retain dissolved organic components with a molar mass of 100-150 g/mol nearly completely (Friedrich & Pinnekamp, 2003).

### **1.2.3 Fouling and Scaling**

According to Malaeb & Ayoub (2011), fouling is the accumulation of unwanted deposits on the membrane surface, which leads to the decrease of permeation flux and salt rejection.

Fouling in RO can be classified into four types, i) colloidal/particulate fouling as a result of colloidal/particulate accumulation, ii) organic fouling is due to deposition of organic macromolecules, iii) inorganic fouling resulting from precipitation of inorganic salts and iv) biofouling as a result of microorganisms (Saqib & Aljundi, 2016; Antony et al., 2011; Matin et al., 2019).

Scale formation comprises of intricate phenomenon focussed around crystallization and transport mechanisms. When the saturation limit is exceeded and the solution is supersaturated, crystallization or precipitation then occurs. Surface crystallization and bulk crystallization are the two pathways through which scale forms. Scaling is a combination of these two mechanisms and is affected by the surface structure of the membrane and operating conditions of the system (Antony et al., 2011; Matin et al., 2019).



#### **1.2.4 Remediation of membrane scaling**

Applying the following scale reducing methods can assist as follows:

- i. Optimising the operating parameters by adjusting the feed characteristics based on varying concentrations.
- ii. The addition of an appropriate antiscalant that will remediate fouling

Selecting one of these applications depends on the nature of the feed water, membrane compatibility with acid or scale inhibitor and operating cost (Antony et al., 2011).

One advantage of antiscalants is the low dosage levels needed (sub-stoichiometric amounts), which results in minimal impact on the quality of the feed water. As explained by Asadollahi et al. (2017), the inhibition of scale formation does not involve bond formation or breaking between the antiscalant and the scale-forming constituent. Scale inhibition occurs by unsettling one or more aspects of the crystallisation process.

### **1.3 Research Problem**

As environmental regulations tighten, the concern of reducing the surfactant concentration and COD levels in effluent streams from laundry wastewaters before discharge into municipal wastewater treatment plants, increases. Linear alkylbenzene sulfonates are the most abundant anionic surfactant utilised in laundry detergents and are difficult to remediate with the current conventional activated sludge process (CAS) utilised at most municipal. Based on previous literature, microfiltration and ultrafiltration as a primary removal step are inadequate for the removal of anionic surfactants. Using reverse osmosis with thin film composite membranes is a possible solution for anionic surfactant removal. RO do have its disadvantages when it comes to industrial effluent treatment in the form of membrane fouling.

### **1.4 Research topic**

The treatment of laundry wastewaters studies is few, making this area very attractive for more research, especially from a zero discharge water cycle perspective. According to Manouchehri & Kargari (2017), coagulations, flotation and membrane bioreactor processes are some of the most effective treatment methods. Reports by Šostar-Turk et al. (2005) indicated that membrane technology is an effective approach for the removal of surfactants. Ultrafiltration followed by ion-exchange with magnetic resin can also be an effective physico-chemical method, exclusively for the removal of anionic surfactant from laundry waste stream.

### **1.5 Research questions**

- i. Can a standalone RO bench scale system reduce anionic surfactant concentration effectively from laundry wastewater?
- ii. What effect will the feed detergent concentration have on the permeate flow rate (flux) and rejection at stipulated plant parameters?
- iii. Could a known industrial antiscalant reduce inevitable membrane scaling?

### **1.6 Aim and objectives**

The aim of this study is to investigate the removal of anionic surfactants and COD in laundry wastewater with a low-pressure and low energy-intensive thin film composite polyamide reverse osmosis membrane using a RO bench-scale unit for compliant effluent discharge and or recycle application.

Primary Objective:

The research objective is the removal of anionic surfactants and COD with an RO bench-scale unit

The secondary objectives are as follows:

- i. Investigate the effect of different laundry detergent feed concentrations on operational parameters such as the membrane salt rejection and permeate flow rate (flux)
- ii. Evaluate the effect of different antiscalant concentrations to minimise scaling
- iii. Determine membrane fouling and remediation by evaluating selected membrane surface characteristics.

### **1.7 Delineation**

This study was focused on the investigation of the removal of anionic surfactants and COD from laundry wastewater using a low pressure and low energy RO membrane for municipal discharge or recycle application.

The effects of laundry detergent concentrations in the feed on the permeate flux and salt rejection were examined. The effect a commercial antiscalant to minimise scaling and improve membrane performance was evaluated. Quantitative analysis investigating membrane surface characteristics with the usage of Scanning Electron Microscopy (SEM); Attenuated Total Reflection-Fourier Transform Infrared Spectroscopy (ATR-FTIR) and Energy Dispersive X-Ray Spectroscopy (EDX), before and after antiscalant addition, were applied. All other variables are delineated.

## **1.8 Thesis Outline**

- Chapter 1** provides a detailed background of the entire thesis, calls attention to key points of this study such as the objectives, research question and significance of the study;
- Chapter 2** gives an in-depth detail of literature study in relation to the different topics linked to this topic;
- Chapter 3** gives details of the procedures, equipment and apparatus used for data acquisition;
- Chapter 4** discusses different results obtained from experimental runs;
- Chapter 5** concludes the research based on the results achieved and gives recommendations.

# **CHAPTER 2**

## **Literature Review**

## **2 Literature Review**

### **2.1 Water shortages**

More than 2 billion people are affected by water shortages in over forty countries. It is estimated that 1.1 billion people have limited drinking water sources, and 2.4 billion people do not have provision for sanitation. Consequently, this can lead to increased spread of disease, lessened food security and conflict, as countries compete for freshwater sources (UNESCO, 2003; Guppy & Anderson, 2017; Wu, 2019).

For active and healthy life, people require a minimum annual per capita water requirement of 1,700 cubic metres of drinking water. Currently, developing countries are struggling to meet this requirement. It is predicted that by 2050, 25% of the global population is likely to live in countries battling with water insecurity (UNESCO, 2003).

South Africa is a water-scarce country. According to Donnenfeld et al. (2018) at present, more than 60% of South Africa's rivers are overexploited. One-quarter of its river ecosystems are crucially endangered and one-third of the country's main rivers are in good state. There are affordable technologies that could be used to help produce secondary and tertiary potable water while ensuring water security for future generations (Myburgh et al., 2019).

Since there is no organization which represents the South African laundry industry, data is limited regarding the water and wastewater practices. The Bidvest Laundry Group is the leader in the laundry sector, with facilities across the country (Welz & Muanda, 2018).

Domestic laundering significantly affects water resources, environment and municipal wastewater treatment facilities. In South Africa between 4% and 22% of household water is used for laundering in a standard household. On average about 52 L of potable water is used for laundering every day, per person (Welz & Muanda, 2018).

## 2.2 Laundry Wastewater and Composition

A large amount of laundry wastewater is produced during the laundering process. In order for soil to be broken down and separated from woven fibres, various factors need to work in synergy. For effective cleaning to take place over time, mechanical, thermal and chemical energy is required (Šostar-Turk et al., 2005).

Laundry detergents are comprised of different chemicals at various concentrations, depending on the items to be cleaned and how soiled they are. Along with bleach and water softeners, surfactants are also present. Surfactant molecules are able to attach to and solubilise oils in the soil. This makes surfactants unique in the effective cleaning and removal of soils (Šostar-Turk et al., 2005).

In a study conducted by Boddu et al. (2016), a simulated laundry wastewater was created as part of a simulated grey water feed where the effect of pre-treatments on RO was the focus. A simulated laundry wastewater feed can be found in Table 2-1.

Laundry wastewaters are not easily treated due to the different inorganic and organic substances removed from the soils and residue left behind from laundry detergents and fabric softeners. Table 2-2 gives characteristics of household, hospital and industrial laundry wastewaters, respectively.

**Table 2-1: Simulated laundry wastewater feed composition (Boddu et al., 2016)**

Chemical	Amount/ 100 Litre Deionised Water	Amount/ ±300L Deionised Water
Liquid detergent	13.2 mL	40 mL
Fabric Softener	7 mL	21 mL
Test Dust	10 g	30 g
Na <sub>2</sub> SO <sub>4</sub>	1.33 g	4 g
NaHCO <sub>3</sub>	0.667 g	2 g
Na <sub>2</sub> HPO <sub>4</sub>	1.33 g	4 g

**Table 2-2: Characteristics of domestic, industrial and hospital laundries wastewaters (Manouchehri & Kargari, 2017)**

Parameters	Domestic laundry	Industrial laundry	Hospital laundry
pH	9.3 - 10	9 - 11	11.4 -11.6
EC, $\mu\text{S}/\text{cm}$	190- 1400	640-3000	808-2000
TDS, mg/L	400-6000	420	456-800
TSS, mg/L	200-987	4-7000	66-71
TH, mg/L $\text{CaCO}_3$	-	44	53-68
TA, mg/L $\text{CaCO}_3$	83- 200	128	302-375
TOG, mg/L	8.0-35	71.5-11790	25-26
Phosphate, mg/L	4-27.6	3.43	10.8-167
$\text{BOD}_5$ , mg/L	48-1200	218-9810	44-50
COD, mg/L	375-4155	80-212000	477-876
Turbidity, NTU	14-400	40–150	87.9



## **2.3 Technologies for the treatment of Laundry Wastewater**

Conventional wastewater treatment methods include coagulation, flotation, adsorption, chemical and biological treatment. They could all be applied for the treatment of laundry wastewater (Giagnorio et al., 2017).

Technologies used for greywater treatments include physical, chemical, and biological systems. Most of these technologies are preceded by a solid-liquid separation step as pre-treatment and followed by a disinfection step as post-treatment. To avoid the clogging pre-treatments such as septic tanks, filter bags, screens and filters are applied to reduce the amount of particles, oil and grease. The disinfection step is used to meet the microbiological requirements (Li et al., 2009).

### **2.3.1 Biological Treatments**

According to Li et al. (2009), there are several biological processes, including rotating biological contactor (RBC), sequencing batch reactor (SBR), anaerobic sludge blanket (ASB), constructed wetland (CW) and membrane bioreactors (MBR), have been applied for greywater treatment. The biological processes were often preceded by a physical pre-treatment steps such as sedimentation or screening. Aside from the MBR process, most of the biological processes are followed by a filtration step (for example sand filtration) and or a disinfection step to meet the non-potable reuse standards.

### **2.3.2 Chemical Treatments**

Very few chemical processes were reported for greywater treatments and reuses. The chemical processes applied for grey water treatments include coagulation, photo-catalytic oxidation, ion exchange and granular activated carbon (Li et al., 2009).

### **2.3.3 Physical Treatments**

The physical treatments include coarse sand and soil filtration and membrane filtration, followed mostly by a disinfection step. The coarse filter alone has limited effect on the removal of the pollutants present in the greywater (Li et al., 2009; Wu, 2019).

## **2.4 Reasons for treating Laundry Wastewater**

### **2.4.1 Environmental Concerns**

As environmental regulations tighten, concern increases about reducing the surfactant concentration in effluent streams. It has been reported that the wastewater from a laundry, where very dirty items are being washed, contains mineral oils, heavy metals and dangerous substances that have COD values of 1200–20,000 mg O<sub>2</sub>/L. (Šostar-Turk et al., 2005).

Membrane processes offer a number of advantages over conventional water and wastewater treatment processes including fulfilment of higher standards; reducing environmental impact of effluents; land requirements and the possibility to use mobile treatment units. Bhattacharyya et al. (1978) showed that the recycled ultra-filtrate from laundry and shower wastewater could be used as non-potable water. Physically filtered wastewater with various types of ceramic membranes from a resort complex can be used effectively in creating recycled wastewater for such secondary purposes. Industrial laundries have a variety of opportunities to recycle/reuse water at their facilities (Šostar-Turk et al., 2005).

### **2.4.2 Economic Viability**

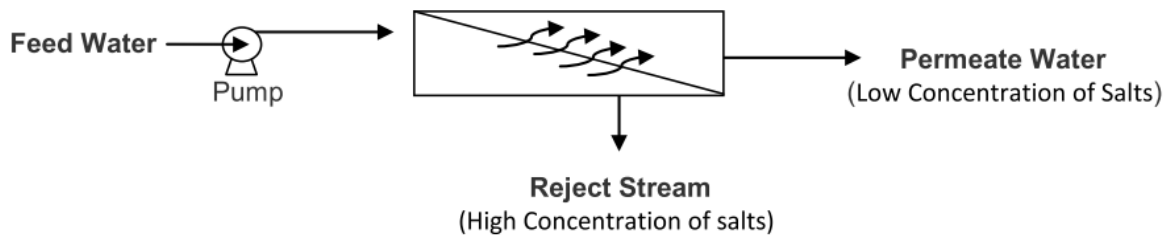
A study of the possibility for wastewater reuse is essential because of its large quantities in the laundering process of industrial laundries. Laundry wastewater possesses the potential for reclamation and reuse. Such reclamation and reuse of laundry discharge is important to save water supply and significantly improve urban environments with limited freshwater resources (Andersen et al., 2002).

**Table 2-3: Toxic effects of laundry water constituents (Sumisha et al., 2015)**

Source of pollutants	Effects
Surfactant	<p>The surfactants had both high or moderate toxicity and most toxic (mmol/L) components. They contributed between 10.4% and 98.8% of the toxicity of the detergents with a mean contribution of 40.7%.</p> <p>Surfactants create a bacterial population rise, transmitting through the food chain to protozoa, which are more sensitive to laundry wash toxins</p> <p>Linear alkyl benzene sulfonate (LAS) is the widest spread anionic surfactant and its concentration may vary from 17 to 1024 ppm. It is derived from petroleum bi-products, is quite rapidly degraded aerobically, but only very slowly or not at all under anaerobic conditions. It generates carcinogenic and toxic by-products.</p>
Detergents	<p>All detergents will destroy fish mucus membranes and gills to some degree. The gills may lose natural oils, interrupting oxygen transfer. Damaged mucus membranes leave fish susceptible to bacteria and parasites. Detergents are toxic to fish near 15 ppm, killing fish eggs at 5 ppm and cause endocrine disrupting and estrogenic effects in fish.</p>
Oil/grease	<p>Laundry water contains 8–35 mg/L of oil/grease. It adversely affect the aesthetic merit, water transparency and Dissolved Oxygen (DO) content in the water</p>

## 2.5 Membrane Technology

Membrane technology has gained significant importance globally because of its broad range of applications. It is a physical process in which the membranes work like a filter in order to separate material mixtures. Membranes have a unique ability to control the permeation rate of certain components through the membrane. During the process, substances are not thermally, chemically, or biologically modified. It is common in wastewater treatment for membrane technology to be used in combination with other purification treatments (Baker, 2012; Friedrich & Pinnekamp, 2003).



**Figure 2-1: Schematic representation of the membrane process (Adapted from Puretec, (n.d.) )**

Membrane processes microfiltration, ultrafiltration, nanofiltration, and reverse osmosis are characterised according to size or molar mass of substances to be separated. Depending on the task at hand, and type of water to be treated, though, each membrane process has its advantages and disadvantages.

In comparison to other greywater treatment technologies, membrane-based processes are advantageous as mentioned below:

- i. Based on pore size and particle size or molar mass, membranes offer a permanent barrier to suspended particles which improves quality of treated greywater;
- ii. Membrane processes can achieve better greywater treatment efficiency with economic feasibility;
- iii. Due to their compact nature, membrane systems do not require much space (Wu, 2019).

A major challenge in membrane technology is membrane fouling. As explained by Wu (2019) membrane fouling results in higher maintenance cost and more energy required. Understanding membrane fouling mechanisms is significantly important in order to decide on a suitable control strategy and essentially alleviate fouling. Research and development in this area is necessary to allow membrane technology to compete with other treatment processes for greywater treatment (Wu, 2019).

## **2.6 Membrane configuration**

According to Friedrich & Pinnekamp (2003) with respect to how they are manufactured, there are two basic membrane forms: tubular and flat membranes

The module is the arrangement membranes in an engineered unit. The type of module used is important for the efficiency of operation. Modules are created in a number of arrangements to adapt to the process and meet what is required of the end use.

Factors such as the separation layer, the component density and, with the tubular diaphragms, regarding the diameter various module arrangements are characterized. Based on performance and operation and the module costs, certain module types are preferred depending on the waste water to be treated.

### **2.6.1 Hollow fine fibre**

There are two basic geometries when it comes to hollow fibre membrane modules. The first is the shell-side feed design. A loop or a closed bundle of fibres is held in a pressurized vessel; permeate passes through the fibres wall and exits through the open fibres ends. This design allows large membrane areas to be contained in an inexpensive system (Baker, 2012; Berk, 2018; Judd, 2010).

Bore-side feed type is the second type of hollow fibres module. The fibres in this design are open at both sides, and the feed fluid is circulated through the bore of the fibres.

As stated by Baker (2012) the advantage of hollow fibre modules is the ability to pack a very large membrane area into a single module. As the diameter of the fibres in the module increases, the membrane area decreases. Capillary ultrafiltration membrane modules have almost the same area as equivalent-sized spiral-wound modules.

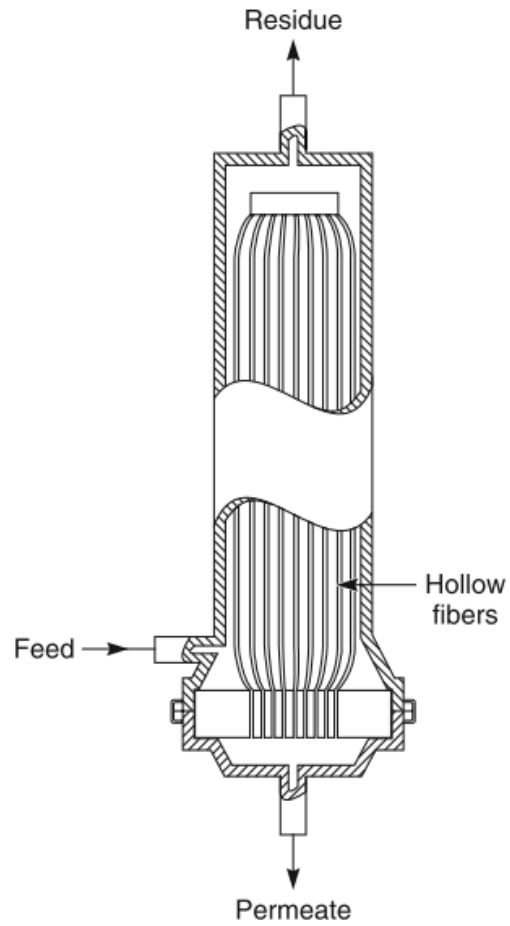


Figure 2-2: Shell-side feed design (Baker, 2012; Berk, 2018; Judd, 2010)

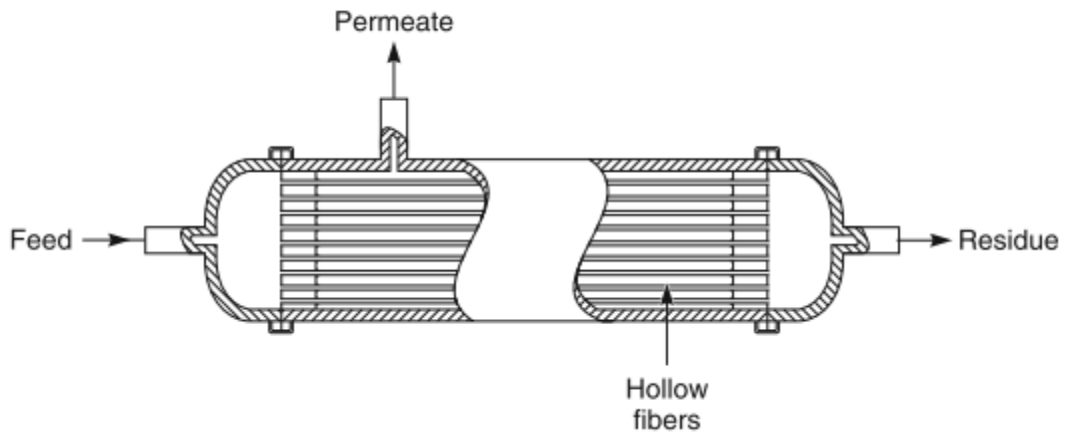


Figure 2-3: Bore-side feed design (Baker, 2012; Berk, 2018; Judd, 2010)

### 2.6.2 Plate and frame membranes

One of the earliest types of membrane systems were plate-and-frame modules. Membrane, feed spacers, and product spacers are layered together between two frames. While the feed mixture is forced across the membrane surface, permeate passes through the membrane, and is collected in a manifold (Baker, 2012; Berk, 2018; Judd, 2010).

Plate-and-frame units are expensive compared to other modules, and leaks through the gaskets pose an issue for each plate. Applications of plate-and-frame modules are in electro dialysis and pervaporation systems. They are also used for Reverse Osmosis and Ultrafiltration applications with feeds high in foulants (Baker, 2012; Berk, 2018; Judd, 2010).

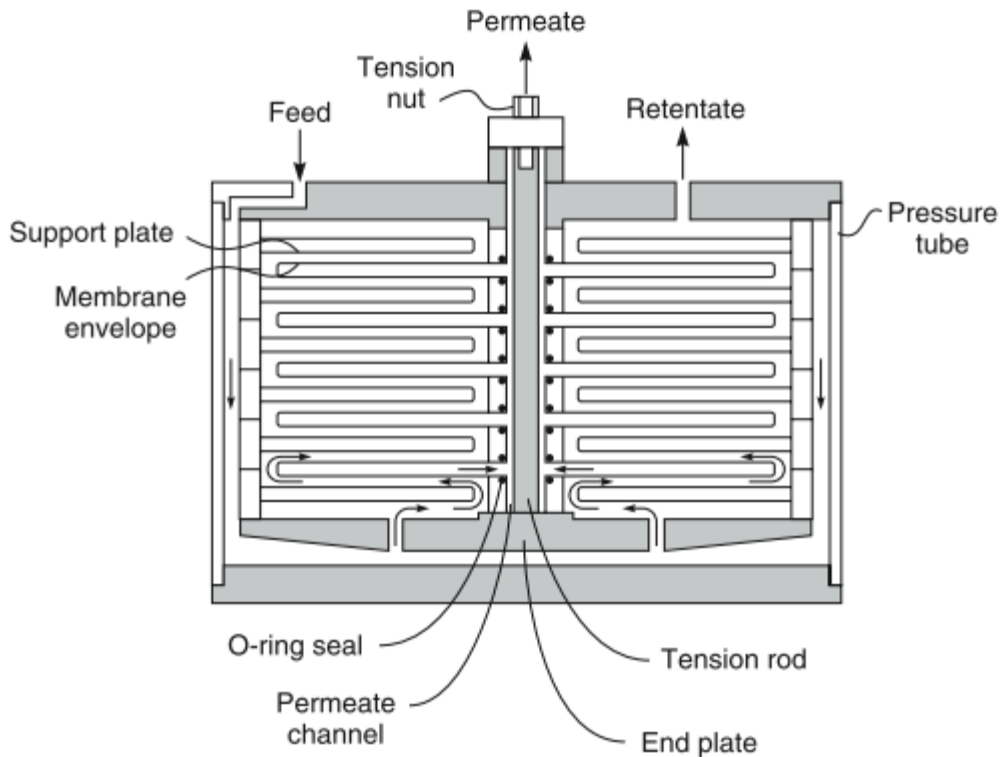


Figure 2-4: Schematic representation of a plate and frame module (Baker, 2012)

### 2.6.3 Tubular membranes

Tubular modules have resistance to membrane fouling due to good fluid hydrodynamics. The tubes are made of a porous paper or fibreglass support with the membrane on the inside of the tubes. This creates an increased membrane area in the same size module housing. In a typical tubular membrane system, tubes are folded in series. Permeate is extracted from each tube and sent to a permeate collector (Baker, 2012).

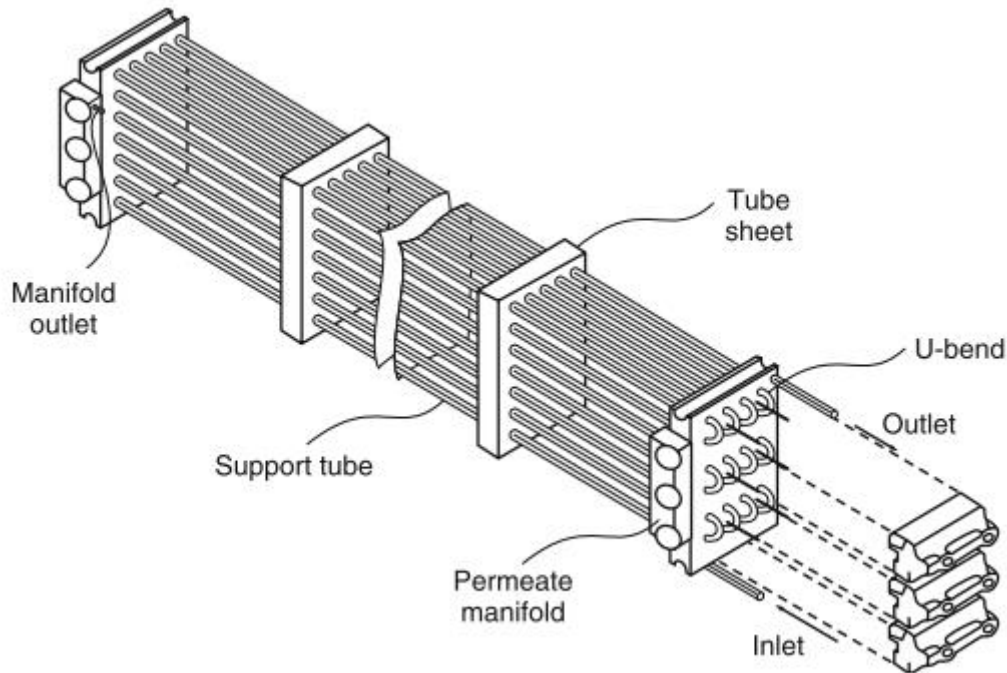


Figure 2-5: Diagram of a tubular ultrafiltration system (Baker, 2012)

### 2.6.4 Spiral wound membranes

Spiral wound membranes consist of layers of spacers and flat sheet membranes wound around a perforated central collection tube, which is encased by a tubular pressure vessel. Feed passes axially down the module across the membrane. This type of module is used in a wide range of applications, for example, nanofiltration modules to remove divalent ions from hard drinking water (Baker, 2012).



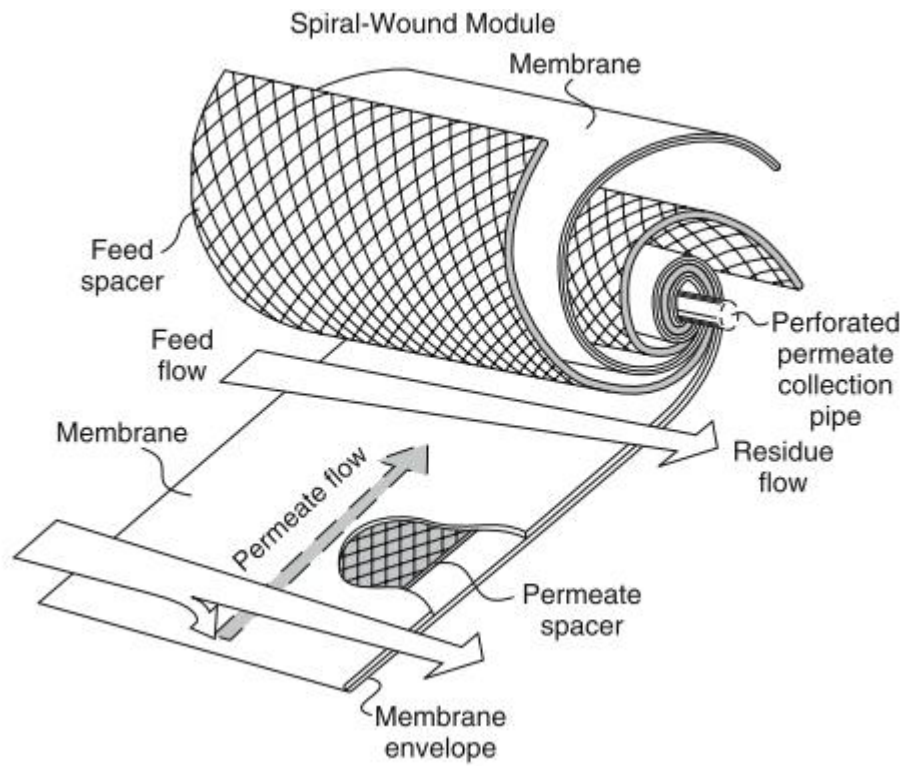


Figure 2-6: Schematic representation of a spiral wound membrane (Baker, 2012)

## 2.7 Membrane types based on pore sizes

### 2.7.1 Microfiltration and Ultrafiltration

Microfiltration (MF) and Ultrafiltration (UF) belong to the pressure driven membrane processes. Concerning operating pressure and molecular separation size, they are characterized between nanofiltration and filtration. The separation mechanisms of the Micro- and Ultrafiltration membranes are analogous and the fields of application strongly overlap. Microfiltration membranes separate suspended particles with diameters between 0.1 and 10 $\mu\text{m}$  (Friedrich & Pinnekamp, 2003; Baker, 2012).

According to the principle of a porous filter, all particles larger than the membrane pores are removed completely. The particles that are retained can develop a covering layer on the membrane surface. This layer then holds back smaller particles which, without a covering layer, would pass through the membrane, hence the process is effected by the covering layer (Friedrich & Pinnekamp, 2003; Baker, 2012).

**Table 2-4: Characteristic features of micro- and ultrafiltration (Friedrich & Pinnekamp, 2003)**

Characteristic features of micro- and ultrafiltration		
	Microfiltration (MF)	Ultrafiltration (UF)
Operation Mode	cross-flow- and dead-end-operation	cross-flow- and dead-end-operation
Operating pressure	0.1-3 bar (transmembrane)	0.5-10 bar (transmembrane)
Separating Mechanism	screening controlled by covering layer, if necessary	screening controlled by covering layer, if necessary
Molecular separation size	solids > 0.1 $\mu\text{m}$	colloids: 20000-200000 Dalton*, solids > 0.005 $\mu\text{m}$
Membrane types	predominantly symmetric polymer or ceramic membranes	asymmetric polymer composite or ceramic membranes
Module types	spiral-wound, hollow-fibre and tube modules, plate or cushion modules	spiral-wound, hollow-fibre and tube modules, plate or cushion modules

\* (Dalton), numerically equivalent to the molecular weight (MW) in [g/mol]

### 2.7.2 Nanofiltration

Nanofiltration (NF) is a pressure-driven membrane process which is the preferred method used for the recycling of aqueous solutions. Concerning operational pressure and separation size, nanofiltration is characterized between reverse osmosis and ultrafiltration. By means of nanofiltration membranes, the retention rate for particles with a molecular mass larger than 200g/mol is high; this corresponds to a molecule diameter of more or less 1nm (Friedrich & Pinnekamp, 2003).

Typical of Nanofiltration membranes is their ion selectivity. The valency of the anion determines the rejection of a dissolved salt. Therefore most salts with monovalent anions (e.g.  $\text{Cl}^{-1}$ ) can pass through the membrane; whereas multivalent anions (e.g.  $\text{SO}_4^{2-}$ ) are removed (Friedrich & Pinnekamp, 2003). On an industrial scale, nanofiltration membranes are used to soften municipal water by extracting sulphates and divalent cations. It is also used as pre-treatment for an ultrapure water treatment plant (Baker, 2012).

**Table 2-5: Characteristic features of nanofiltration (Friedrich & Pinnekamp, 2003)**

Characteristic features of nanofiltration	
	Nanofiltration (NF)
Operation Mode	cross-flow-operation
Operating pressure	2-40 bar (transmembrane)
Separating Mechanism	solubility/diffusion/charge (ion selectivity)
Molecular separation size	dissolved matter: 200-20000 Dalton*, solids > 0.001 mm
Membrane types	asymmetric polymer or composite membranes
Module types	spiral-wound, tube and cushion modules

\* (Dalton), numerically equivalent to the molecular weight (MW) in [g/mol]

### 2.7.3 Reverse Osmosis

Reverse osmosis is a process for removing salts from water using membranes that are water permeable but rejects salt almost completely. It is based on a pressure-driven process, the driving force resulting from the variation of the electrochemical potential on both sides of the membrane. The non-porous reverse osmosis membranes can retain dissolved material with a molecular weight of less than 200 g/mol entirely, so that reverse osmosis obtains higher separation efficiency than nanofiltration. Since dissolved salts are retained to a very high extent,

reverse osmosis has a reputation as a proven membrane procedure, which is already state of the art (Friedrich & Pinnekamp, 2003; Baker, 2012).

**Table 2-6: Characteristic feature of reverse osmosis (Friedrich & Pinnekamp, 2003)**

Characteristic features of reverse osmosis	
	Reverse Osmosis (RO)
Operation Mode	cross-flow-operation
Operating pressure	5-70 bar (transmembrane), in special cases up to 120 bar
Separating Mechanism	solubility/diffusion
Molecular separation size	dissolved matter: <200 Dalton*
Membrane types	asymmetric polymer- or composite membranes
Module types	spiral-wound, tube, plate, cushion on disc tube modules

\* (Dalton), numerically equivalent to the molecular weight (MW) in [g/mol]

## 2.8 Filtration system in the treatment of laundry wastewater

The physical treatments include coarse sand and soil filtration and membrane filtration, followed mostly by a disinfection step. The coarse filter alone has limited effect on the removal of the pollutants present in the grey water (Li et al., 2009).

Šostar-Turk et al. (2005) investigated the use of a UF membrane (0.05  $\mu\text{m}$  pore size) for the treatment of laundry grey water. The UF membrane decreased the BOD from 195 to 86 mg/L corresponding to a removal of 56%. In terms of organic load, the reclaimed greywater obtained by Šostar-Turk et al. (2005) did not meet the non-potable grey water reuse standards proposed in this study. However, the pore sizes of the membranes play an important role on the treatment performance. For example, Green et al. (2004) reported a low strength grey water treatment system with direct Nanofiltration membrane, which was able to achieve an organic removal rate of 93%. Šostar-Turk et al. (2005) also reported that the RO membrane after the UF membrane was able to reduce the BOD from 86 to 2 mg/L corresponding to a removal rate of 98%.

In a study conducted by Ciabattia et al. (2009), a system for purification and reuse of wastewater from an industrial laundry is demonstrated. The use of Granular Activated Carbon (GAC) filtration reduced COD, TSS, Turbidity, Ammonia, Nitrogen, Total Phosphate (TP) and Total surfactants from 602 mg/L; 166 mg/L; 110 NTU; 1.8 mg/L; 1.9 mg/L; 8.78 mg/L to 140 mg/L; 4 mg/L; 1.1 NTU; 0.13 mg/L; 0.45 mg/L; 1.60 mg/L respectively. From the same influent, Ultrafiltration was able to reduce COD, TSS, Turbidity and Total surfactants to 81 mg/L; 2.5 mg/L; 0.8 NTU; 1.00 mg/L.

Guilbaud et al. (2010) explored the feasibility to implement, on board ship, a direct Nanofiltration process in order to treat laundry grey waters and recycle 80% to the inlets of the washing machines. A direct Nanofiltration process (without pre-treatment) on tubular PCI-AFC80 membrane (35 bar, 25 °C, volume reduction- factor 5) allowed them to produce a permeate free of micro-organisms and suspended solids and with only 48mgCOD/L and 7mgTOC/L. However, one shall keep in mind that the higher energy consumption and the membrane fouling are often the key factors limiting the economic viability of membrane systems.

Sumisha et al. (2015) studied the filtration of laundry wastewater using hydrophilic ultrafiltration membranes. The performances of polyvinylpyrrolidone (PVP) modified polyethersulfone (PES) membranes were tested. The influence of operating parameters were also assessed. An increased permeate flux of 55.2 L/m<sup>2</sup>h was achieved for modified PES membrane with high concentration of PVP at transmembrane pressure of 500 kPa and 750 rpm of stirring speed. Results showed that PES membrane with 10% of PVP had increased permeate flux, flux recovery and decrease in fouling when compared with other membranes. High removal

efficiencies were obtained for COD and TDS due to the improved surface property of membranes. It was concluded that modified PES membranes are suitable for the treatment laundry wastewater

Research conducted by Ashfaq et al. (2017) membrane filtration was used to treat hospital laundry wastewater. Two different filtration methods were used. First being “tight” ultrafiltration membrane and the second a combination of “loose” UF followed by nanofiltration membrane. Both approaches met statutory wastewater discharge limit as more than 87% of pollutant was rejected. Results confirmed that the hospital wastewater can be treated effectively at a pressure of 2.5 bar, temperature 25°C and a crossflow rate of 1 L/min.

Nascimento et al. (2019) treated industrial laundry wastewater with a combined coagulation/flocculation/sedimentation process (C/F/S) and membrane separation. In terms of removal efficiencies, 98.4% of the colour, 99.1% of turbidity, 71.7% of the surfactants, and more than 55% of the total dissolved solids, chemical oxygen demand, and total organic carbon (TOC) was removed. It was observed that the combined process was effective in the treatment of industrial laundry wastewater.

**Table 2-7: Summary of previous membrane studies with various pollutant removals**

Reference	Process	TSS		Turbidity		COD		BOD		Pollutant Rejection
		mg/L		NTU		mg/L		mg/L		%
		In	Out	In	Out	In	Out	In	Out	
Šostar-Turk et al. (2005)	UF membrane	35	18	-	-	280	130	195	86	-
	NF membrane	28	0	30	1	226	15	-	-	-
	RO Membrane	18	0	-	-	130	3	86	2	-
Ciabattia et al. (2009)	GAC Filter	166	4	110	1.1	602	140	-	-	-
	UF membrane	166	2.5	110	0.8	602	81	-	-	-
Guilbaud et al. (2010)	NF membrane	78	0	120	-	1340	48	-	-	-

Sumisha et al. (2015)	UF (90% Polyethersulfone, 10% Polyvinylpyrrolidone)	-	-	41.4	0.83	753	90.36	-	-	-
	UF (95% Polyethersulfone, 5% Polyvinylpyrrolidone)	-	-	41.4	1.66	753	112.95	-	-	-
	Commercial UF Polyethersulfone	-	-	41.4	2.9	753	128.01	-	-	-
Manouchehri & Kargari (2017)	MCE MF membrane	240	4.1-10.1	360	1.8-5.6	2538	30.5-675.1	1190	79.7-203.5	-
Ashfaq et al. (2017)	UF 5kDa MWCO	-	-	-	-	-	-	-	-	87
	UF 75 kDa MWCO + NF 200 Da	-	-	-	-	-	-	-	-	
Nascimento et al. (2019)	Coagulation/flocculation/sedimentation + MF/UF	-	-	11.9	0.59	219	54.8	-	-	-



## 2.9 Reverse Osmosis membrane fouling

Malaeb & Ayoub (2011) explain fouling as the build-up of unwanted deposits on the membrane surface or inside the membrane pores which causes a decrease of permeation flux and salt rejection. For most RO applications, water is the operating environment, and it is crucial to understand how water behaves as well as the transport of ions through the RO membrane, which could explain how fouling occurs.

Water permeates through RO membrane via different forms of diffusion. This may be in the form of Brownian diffusion, flush and jump-diffusion (Gao et al., 2015). The structure of the membrane plays a significant role in the intermolecular interactions of water and ions with the membrane surface. For example, if the membrane structure is more compact, more energy will be needed for water to pass through, consequently, particles are more likely to accumulate on the membrane surface, known as surface fouling.

Fouling can be categorised into surface and internal fouling, which is defined based on location on the membrane (Lin et al., 2014). The fouling mechanisms of low-pressure membranes are different from that of high-pressure. MF and UF membranes are more vulnerable to pore adsorption and clogging whereas NF and RO are surface fouling. Fouling is more frequent due to the compact and nonporous nature of these membranes (Greenlee et al., 2009). In comparison with internal fouling, surface fouling can be mitigated more easily by enhancing hydrodynamic conditions of feed water or chemical cleaning (She et al., 2016). As explained by Arkhangelsky et al. (2012) surface fouling is more reversible than internal fouling.

Depending on feed water characteristics and their interactions with a membrane, both surface fouling and internal fouling can be irreversible. Fouling can also be categorized into foulant types, namely biofouling, organic fouling, inorganic scaling and colloidal fouling (Hakizimana et al., 2016). Membrane fouling is typically caused by a combination of different foulants. Membrane autopsy methods are used extensively to examine the origin; degree of membrane fouling and distribution of foulants, because it can provide accurate information about foulant compositions and properties (Gorzalski & Coronell, 2014).

## **2.10 Type of foulants**

Four types of foulants are commonly known: biofouling, organic fouling, Inorganic scaling and colloidal fouling

### **2.10.1 Biofouling**

Biofouling is the process of microorganism adhesion and growth on the membrane surface. A biofilm is formed to an undesirable extent, which could cause huge operational costs. Biofilm formation is important in this process (Creber et al., 2010). According Zhu et al. (2016) biofouling is more intricate compared to other fouling types. Bacteria and the Extracellular Polymeric Substances (EPS) are the two key components of biofilms.

Biofouling is commonly regarded as one of the most hazardous fouling (Al-Juboori & Yusaf, 2012). Membrane biofouling is difficult to remove by pre-treatment methods because microorganisms have a unique ability to cultivate and multiply. Unless pre-treatment can eliminate 100% of the bacteria, the organisms left behind can grow increasingly on the membrane surface and cause fouling.

### **2.10.2 Organic fouling**

Organic fouling is a result of organic matter fouling the membrane surface. Cho et al. (1998) explains that organic matters typically consist of humic elements, polysaccharides, proteins, lipids, nucleic acids and amino acids, organic acids, and cell constituents. In wastewater treatment where RO is used, organic fouling is the main challenge, because the effluent organic matter (EfOM) concentration (10–20 ppm) is much higher compared to standard natural organic matter (NOM) concentration in surface waters (2–5 ppm) (Malaeb & Ayoub, 2011).

Due to the molecular weight and complex structures formed by dissolved organic matters in combination with other substances, organic fouling hinders membrane performance and is difficult to treat (Ding et al., 2016; Teixeira & Sousa, 2013). Moreover, pre-treatment technologies struggle to remove organic matters with a low molecular weight compared to high molecular weight organic matters (Liu et al., 2008).

### **2.10.3 Inorganic scaling**

Inorganic scaling is the build-up of inorganic substances on the membrane surface or inside the membrane pores (Henthorne & Boysen, 2015). Scaling results from the solubility of some inorganic scalants exceeding the equilibrium solubility product and become supersaturated; consequently it deposits on the surface or the pores of the membrane (Shirazi et al., 2010; Antony et al., 2011). Al-Amoudi & Lovitt (2007) explains that the inorganic ions in water, which

exceed the equilibrium solubility product, initially reach the nucleation stage, and then go through homogenous or heterogeneous crystal growth processes. Inorganic precipitation restricts water permeation through the membrane (Elimelech et al., 1997).

#### **2.10.4 Colloidal fouling**

Colloidal fouling refers to fouling of the membrane caused by the colloid or particle build up on the membrane surface (Khayet, 2016). Colloids are very small suspended particles. The size of colloids ranges from a few nanometers to a few micrometres (Al-Amoudi & Lovitt, 2007). The general colloidal foulants can be divided into two types, inorganic foulants and organic macromolecules. Colloidal fouling could be affected by various factors such as the colloids size, shape, charge as well as interactions with ions of the colloids (Town et al., 1995).

## 2.11 Factors affecting Scaling

Numerous operating conditions such as pH, temperature, operating pressure, permeation rate, flow velocity, and presence of other salts or metal ions can influence scale formation. In high-pressure membrane systems, concentration polarization also has a significant effect on scale formation due to the increased salt concentrations near the membrane surface where particles might deposit (Antony et al., 2011).

Concentration polarization is a phenomenon that occurs when there is an increased solute or particle concentration near the membrane surface in comparison to the bulk. The concentration of the salts at the membrane surface becomes supersaturated. Dense and nonporous membranes are most affected by this phenomenon because of the degree of rejection of scale-forming salts. Operating parameters such as flux, water recovery, solution chemistry, temperature, membrane properties, and module geometry influence the severity of concentration polarisation (Antony et al., 2011; Matin et al., 2019).

When modelling RO systems, concentration polarisation is an important factor and should be considered. A study conducted by Lee & Lee (2000) confirmed that concentration polarisation influences surface crystallisation. The degree of surface crystallization, initial flux and the concentration polarization remain low at low operating pressures. As the cross-flow velocity of the fluid is increased, the degree of concentration polarization reduces and results in less surface crystallisation.

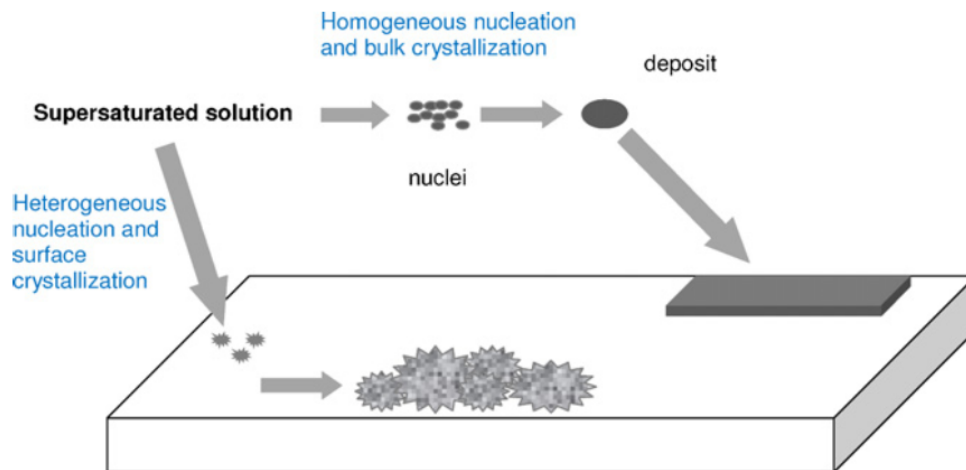


Figure 2-7: Schematic representation of scaling

## **2.12 Scale Control Techniques**

According to Antony et al. (2011) and Matin et al. (2019), scale minimizing techniques can be categorised into three groups:

- i. Miscellaneous pre-treatments,
- ii. Optimizing of operating parameters and system design, and
- iii. Addition of antiscalant.

These methods are dependent on feed water characteristics, membrane compatibility with acid or scale inhibitor and cost.

### **2.12.1 Altering feed water characteristics**

This technique usually involves the use of miscellaneous pre-treatment options to reduce the mineral concentration or alkalinity. The quality of feedwater is altered to decrease scale-forming tendency. The following are examples of common pretreatment methods:

i) Coagulation - Coagulation mainly removes the particulate and colloidal constituents prior to media filtration and low pressure membrane filtration. Dissolved silica and iron content in feed water causes scale, fortunately coagulation is an effective method for minimizing those scale forming constituents (Antony et al., 2011).

ii) Ion-exchange softening - In this pretreatment, magnesium and calcium ions that are concentrated in the RO feed water are exchanged for sodium ions adsorbed on exchange resin. This method is effective in systems intended for operating at high recovery on feeds with significant alkalinity.

Once the calcium and magnesium ions have replaced all the sodium ions, the resin (NaZ) must be regenerated using a brine solution. Ion-exchange softening can reduce the need for continuous feed of either acid or antiscalant, consequently the process is very costly and makes alternative methods more attractive (Antony et al., 2011).

iii) Acidification - Acidification involves reducing the pH of the feed water to 5–7 and increasing the solubility of alkaline scale, especially Calcium carbonate that is a possible scalant in all feed water types. Acid addition shifts the equilibrium to the left and keeps the calcium carbonate in the dissolved form. Sulphuric acid or hydrochloric acid is normally used for pH adjustment. Hydrochloric acid is favoured due to the potential for sulphuric acid to form sulphate scales (Antony et al., 2011).

### **2.12.2 Optimisation of operating parameters and system design**

To keep the scale-forming mineral concentration less than the critical threshold limit or by slowing the kinetics of scale formation, specific changes can be made to the system design or the operating parameters.

- i) Limiting product recovery - With an increased product recovery, the concentration polarization effect becomes more prominent, which increases the potential of membrane scaling. By operating at product recoveries sufficiently low, the brine stream is not concentrated enough to form inorganic scales. However, the operation efficiency of the plant causes economic implications (Greenlee et al., 2009)
- ii) Feed flow reversal - This method aims at reducing the elapsed nucleation time by regularly switching the feed entrance and concentrate exit positions of the RO process before scale formation occurs. By reversing the flow, supersaturated brine at the exit port is replaced with unsaturated brine and vice versa reducing the potential for scale (Uchymiak et al., 2009).
- iii) Intermediate chemical demineralization - This operating method applies scale mitigation for high water recovery in a two-stage RO process and involves chemical demineralization of the concentrate stream after the first stage (Gabelich et al., 2007).
- iv) Rotation filtration - By rotating of the RO module/cell, the centrifugal flow instabilities help to reduce concentration polarization and scale formation. Rotation is expected to favour bulk crystallization over surface scaling, and the high shear forces reduce the ion concentration build up at the membrane surface (Antony et al., 2011).

### 2.12.3 Antiscalant addition

Antiscalant, also known as scale inhibitor, addition is a useful conventional pre-treatment technique used to minimize and control scaling, in so doing, enhance the performance of RO membrane (Asadollahi et al., 2017; Antony et al., 2011; She et al., 2016). Anti-scalants are advantageous because of the low dosage levels needed to better the process. The feed water quality remains almost constant with the substoichiometric amount of antiscalant added. Scale inhibition does not occur by formation or breaking of bonds but by disturbing one or more aspects of the crystallization process (Asadollahi et al., 2017; Antony et al., 2011; She et al., 2016).

Antiscalants impede the nucleation phase of crystallization or delay the growth phase of crystallization; they do not eliminate the scaling constituents or its tendency. Addition of anti-scalants has an economic benefit of achieving higher product recovery by increasing the effective solubility limits of scaling salts. Commercially available anti-scalants can be classified into three major groups: phosphates, phosphonates, and polycarboxylates (Asadollahi et al., 2017; Antony et al., 2011).

Polyphosphates, especially sodium hexametaphosphate (SHMP),  $((\text{NaPO}_3)_6)$ , was the first commercially available antiscalant to the membrane industry. Advantages of antiscalant include operation cost reduction, environmental acceptability, and harmlessness compared to the alternative techniques (Asadollahi et al., 2017; Antony et al., 2011).

Although scale formation can be reduced by using anti-scalants, some of the limitations experienced in RO operation are explained below (Antony et al., 2011):

- i. At high concentrations, anti-scalants can be a foulant.
- ii. It was observed anti-scalants could enhance the biofouling potential in RO systems. Certain anti-scalants can increase biological growth up to 10 times their normal growth rate.
- iii. Chemicals leftover from pre-treatment may react with anti-scalants and form foulants or negatively affect antiscalant efficiency. Cationic flocculants in particular can react with some types of anti-scalants and form sticky foulants.
- iv. Polyacrylates are membrane foulant when iron and other metal ions are present. Similarly, Hydroxyethylidene Diphosphonic acid (HEDP) loses its antiscalant efficiency at high alkalinities and in the presence of chlorine.
- v. Monitoring the presence of anti-scalants in the system is complex.

## 2.13 RO Process parameters

### 2.13.1 Flux

Permeate or water flux ( $J_w$ ) is the volumetric flow rate of permeate per unit surface area of the RO membrane. Water flux is proportional to the net pressure driving force across the membrane. However salt flux ( $J_s$ ) is the amount of salt passing through unit membrane surface area per unit time and is proportional to the concentration gradient across the membrane (Qasim et al., 2019). Hence with an increase in driving pressure, the concentration of solute in the permeate decreases due to constant salt leakage and increased water flux (Kucera, 2011).

The flux can be calculated according to the following formula of (Hu et al., 2016; Aziz & Kasongo, 2019):

$$\mathbf{Flux} = J_v = \frac{Q}{A} \quad \mathbf{Equation\ 2-1}$$

Q, A and  $J_v$  are the volumetric flow rate of permeate (L/hr), the effective area of the membrane ( $m^2$ ) and the permeate water flux respectively.

### 2.13.2 Salt Rejection

Contaminant removal or rejection is defined as the percentage removal of a contaminant from the feed stream by the membrane and may be calculated by using Equation 2. Reverse osmosis systems are used to remove dissolved salts; for that reason, measuring salt rejection is a direct way to monitor the performance.

Contaminant removal may be calculated for any parameter of interest (turbidity, total suspended solids, total organic carbon, etc.); however, consistent units must be maintained throughout the calculation. Rejection depends mainly on two factors, namely the type of feed constituents, their characteristics, and the type of RO membrane. Normally, solutes with high degree of dissociation and hydration, high molecular weight, and low polarity demonstrate high rejection (Kucera, 2011; Qasim et al., 2019; Water Environment Federation, n.d.; Kasongo et al., 2019).

$$\mathbf{R} = \left( 1 - \frac{EC_{permeate}}{EC_{Feed}} \right) * 100 \quad \mathbf{Equation\ 2-2}$$

$EC_{permeate}$  ( $\mu S/cm$ ),  $EC_{feed}$  ( $\mu S/cm$ ) and R (%) are the permeate conductivity, feed conductivity and salt rejection respectively.



### **2.13.3 Pressure**

Reverse osmosis usually operates in the pressure range of 1035 kPa to 10 350 kPa (Geankoplis, 1993). As previously explained, operating pressure has a direct effect on the water flux, while its effect on the salt rejection is indirect.

When feed pressure is increased, the permeation of water molecules through the membrane is increased while solute molecules passage stays more or less unaffected, hence the permeate contains lower concentration of solutes (Geankoplis, 1993).

An increase in pressure drop generally results from a disruption in the flow pattern through the membrane, usually caused by fouling of the membrane (Kucera, 2011).

### **2.13.4 Recovery**

The fraction of the feed water which becomes permeate water is called the percentage recovery. When the recovery rate is increased, there is a decrease in concentrate recycled but rather more collected as permeate. A high recovery rate can also cause soluble salts to precipitate. If the percentage recovery is too high, it may lead to bigger issues due to scaling and fouling (Kucera, 2011).

### **2.13.5 Temperature**

Passage of both solute and solvent (water) increases exponentially with increasing temperature. It has been reported the rejection decreases when increasing feed temperature, while the permeation flux increases significantly (Mohammed et al., 2014). The reason of this effect is due to the decrease of feed solution viscosity which leads to the decrease of fouling on the membrane surface (Mohammed et al., 2014).

### **2.13.6 pH**

The stability of polyamide thin film composite membrane is vulnerable to the pH of the feed solution. However, the Polyamide (PA) Thin Film Composite (TFC) membranes can operate within a pH ranging from 2 to 11. The pH also affects the rejection efficiency of the membrane. Highest rejections of most species are found to be in the pH range of 7 to 7.5. The reason of low salt rejection in the scenario of higher or lower pH operating condition can be attributed to stems from the ionic state of the rejected ions, as well as some changes at a molecular level on the membrane surface. Conversely, the pH barely affects the water flux stays more or less constant over the range of pH (Kucera, 2011).

## **2.14 Membrane Surface Characterization**

### **2.14.1 Fourier Transform Infra-Red Spectroscopy**

Fourier Transform Infra-Red spectroscopy (FTIR) is one of the older and widely used technologies to investigate the chemical functionality of surfaces. FTIR probes the vibrations of molecular bonds, like all infra-red spectroscopy techniques. This is because infra-red (IR) frequencies (approximately 10<sup>12</sup> to 10<sup>14</sup> Hz) overlap with molecular vibration frequencies. The movement of atoms within a molecule, which involve no rotation and do not alter the centre of mass of the molecule, is called a molecular vibration. If the frequency of IR radiation is identical to that of a particular molecular vibration, then it can cause the vibration to shift to a higher energy state. The vibrations may include stretching (both symmetric and asymmetric), and bending (in-plane or out of plane), referred to as 'normal' modes (Smith, 2011; Griffiths & De Haseth, 2007).

FTIR instruments produce results much faster than conventional IR spectrometers. Inside the instrument, a black-body source emits a beam of IR radiation. This beam passes through an interferometer where various beams with different path lengths are joint to create constructive and destructive interference. This interference pattern is called an interferogram. As the beam is passed through the sample and wavelengths of IR light are absorbed in a manner specific to that sample then the interferogram will be in turn characteristic of that sample. This can be plotted as an interferogram of energy versus frequency. Computer software then subtracts a reference (background) signal from the sample interferogram by Fourier transform to produce the sample spectrum (Johnson et al., 2018; Smith, 2011; Griffiths & De Haseth, 2007).

ATR-FTIR is valuable for examining sample surfaces and so is of particular interest for study of chemically modified membrane surfaces. This technique typically requires an add-on module to the FTIR instrument. During ATR-FTIR operation, a beam of IR light is directed onto a high refractive index crystal, which may typically be germanium, zinc selenide, diamond, thallium–bromiodide or silicon, placed in direct contact with the sample. Multiple internal reflections of the IR beam are created, which produces an evanescent wave, which interacts with the material of the sample. Absorption of the evanescent wave by the sample leads to its attenuation, before being reflected back through the crystal and onto the detector (Johnson et al., 2018; Smith, 2011; Griffiths & De Haseth, 2007).

Tang et al. (2007) confirmed that FTIR is an important tool to explore the chemical properties of RO membranes that can probe the functional group present both at surface as well as deep down to few micron meters (i.e., in the range from 200 nm to more than 1  $\mu$ m) depending on the incident wave number and incident angle. Authors, including Tang et al. (2009), further

explained that in the lower wave number range (from 1800-800  $\text{cm}^{-1}$ ), ATR-FTIR offers more depth and samples functional group present both in the top polyamide (PA) active layer and the polysulfone support layer beneath it, however, at higher waver number (2700-3700  $\text{cm}^{-1}$ ) ATR-FTIR focuses on the chemical characteristics of the top layer (<200 nm).

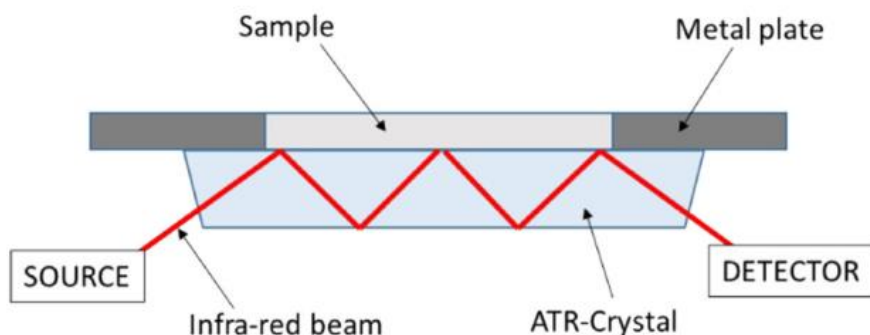


Figure 2-8: Basic operation of an ATR-FTIR system (Johnson et al., 2018)

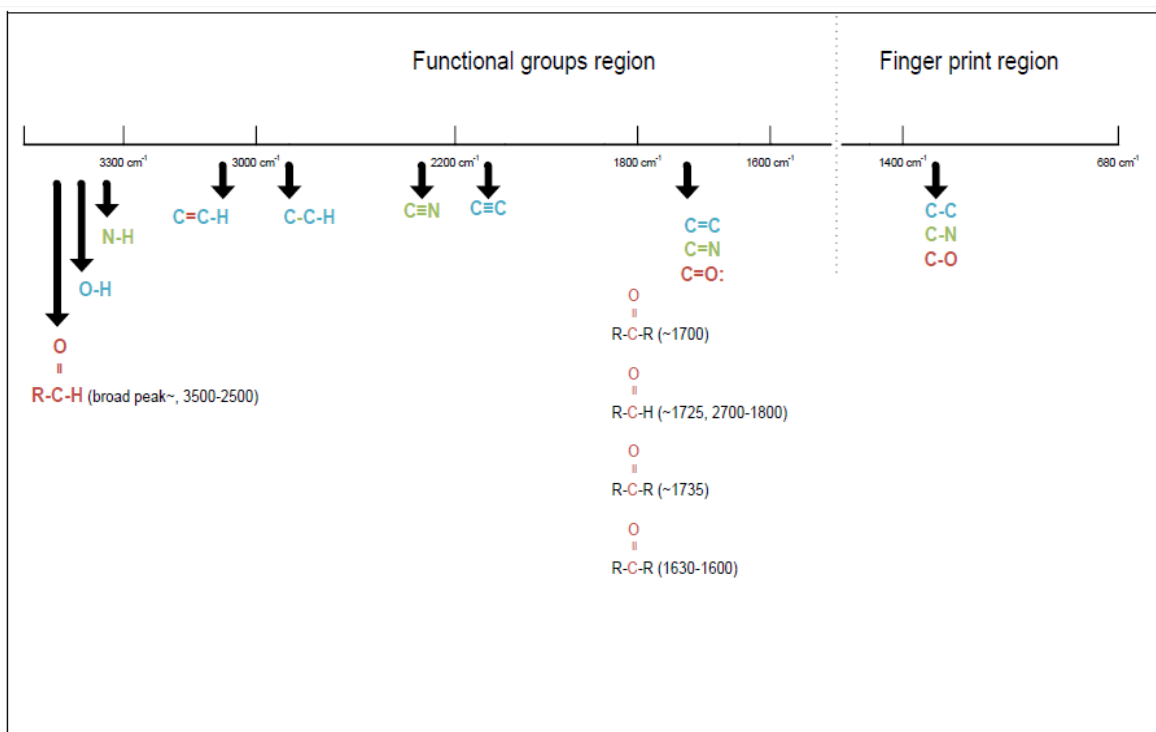


Figure 2-9: Characteristics of functional groups frequencies on FTIR spectra (Coates, 2006)

### **2.14.2 Nuclear Magnetic Resonance Spectroscopy**

Nuclear Magnetic Resonance (NMR) is a technique that can specify some of the biofilm characteristics by using the absorption of radio-labelled substrates existing in the biofilm to the applied radio frequencies in the presence of magnetic field (Serafim et al., 2002). The nuclei of some atoms such as  $^1\text{H}$ ,  $^{19}\text{F}$ ,  $^{23}\text{Na}$  and  $^{31}\text{P}$  and the isotopes like  $^{13}\text{C}$  and  $^{15}\text{N}$  have the property of the magnetic moment. This property refers that the nuclei of the atoms mentioned above and isotopes can be oriented in the presence of magnetic field, and stimulated when exposed to radio frequency radiation. When the nuclei of the energized atoms return to the equilibrium state, they release radio frequency radiation that can be picked up by an NMR probe (Janknecht & Melo, 2003). The captured radio frequency signals can be interpreted to extract some information concerning the examined biofilm. NMR has the advantage of being a non-destructive and non-invasive technique that allows obtaining information pertaining to the metabolic pathways and hydrodynamic and mass transfer phenomena in biofilm structure (Al-Juboori & Yusaf, 2012).

### **2.14.3 X-ray Photon Spectroscopy**

X-ray photon spectroscopy (XPS) is a quantitative surface analytical method, which offers information concerning the elemental composition information. Based on a phenomenon called photo-emission, the surface is bombarded with electromagnetic energy of sufficient energy so that a finite number of the surface atoms will absorb a photon and emit an electron, XPS works on this principle (Carley & Morgan, 2016; Johnson et al., 2018).

Electrons will have a kinetic energy equal to the difference between the energy essential to eject the electron from its orbital (binding energy) and the energy of the absorbed photon. It is these removed electrons and their kinetic energy which is identified by this method. Data is conventionally plotted as binding energy on the x-axis versus the intensity on the y-axis, with the binding energy within the range of 0 to 1200 eV. The binding energy for each peak is normally characteristic for a specific element, even though the chemical state of the emitting atom may have an effect on the binding energy and shape of the peak, producing some information on chemical bonding state (Johnson et al., 2018; Carley & Morgan, 2016).

### **2.14.4 Atomic Force Microscopy**

Atomic Force Microscopy is a microscopic technique also referred to as scanning probe microscopy (SPM). It uses a sharp probe, mounted on a flexible microcantilever arm, which physically interrelates with the sample surface to achieve high-resolution images of surface topography. It can also be used to examine interaction forces between the probe and the

surface, which lead to measurement of nano-mechanical surface properties, adhesion forces and long range interaction forces (Johnson et al., 2012; Al Malek et al., 2012).

Fundamentally, the sharp imaging tip is scanned across the sample surface in three dimensions by use of piezo crystals, which either are connected with the sample holder or probe holder, depending upon the specific instrument. The arrangement of the piezo also differs, with some instruments using a tube shaped piezo crystal, which flexes to produce x, y movement or extends/retracts to produce movement on the z axis. On the other hand, separate piezos may be used for each axis of movement (Johnson et al., 2018).

There are now a great number of imaging modes that exist for a particular application, many of which are exclusive and instrument manufacturer specific, but there are three basic modes most commonly used: contact mode, tapping mode and non-contact mode. The primary data achieved are high-resolution three-dimensional scans of the surface topography. Quantitative information can be obtained which includes deviations to morphology due to fouling or chemical modification and in some cases the diameter of pore openings and porosity (Johnson et al., 2018).

#### **2.14.5 Scanning Electron Microscopy and Energy Dispersive X-ray Spectroscopy**

Scanning Electron Microscopy (SEM) works by scanning a concentrated beam of electrons onto the sample surface. Secondary electrons emitted by the sample, backscattered electrons and X-rays are captured by the suitable detector and then used to make an image of the sample surface or other information.

The interaction between beam electrons and the samples can be elastic or inelastic. If the interaction is inelastic then secondary electrons (SE) are emitted with different energy from the incident electrons. On the other hand, if the interaction is elastic then the electrons are deflected and scattering takes place: any electrons which are deflected at an angle  $\geq 90^\circ$  are termed back-scattered electrons (BSE) and can be captured by a unique detector (Johnson et al., 2018; Goldstein et al., 2017; Zhou et al., 2006).

Interaction of incident electrons with the sample surface may cause the emission of X-ray photons. Collection of this X-ray signal can give significant information about the elemental composition of the surface, using a technique called energy dispersive X-ray (EDX) spectroscopy. EDX spectroscopy is able to detect elements with higher atomic number than boron. Each element has a characteristic X-ray spectrum, the detected spectra will allow elemental analysis of the sample surface (Johnson et al., 2018; Goldstein et al., 2017; Zhou et al., 2006).

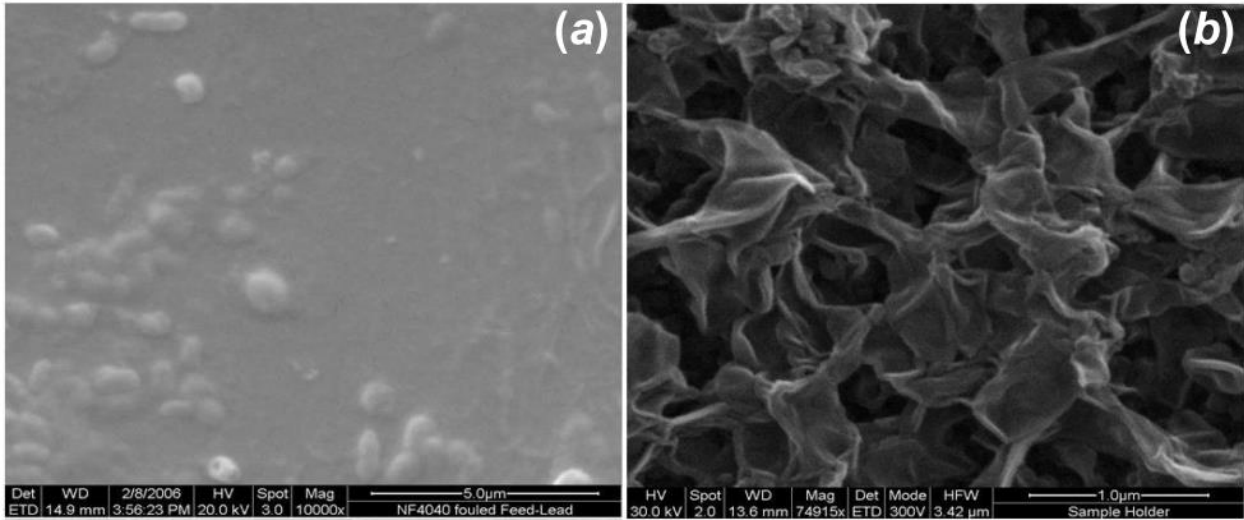


Figure 2-10: SEM images (a) biofouled NF-4040 membrane used for reclaimed water treatment and (b) virgin XLE membrane (Advanced Water Technology Center, 2015)

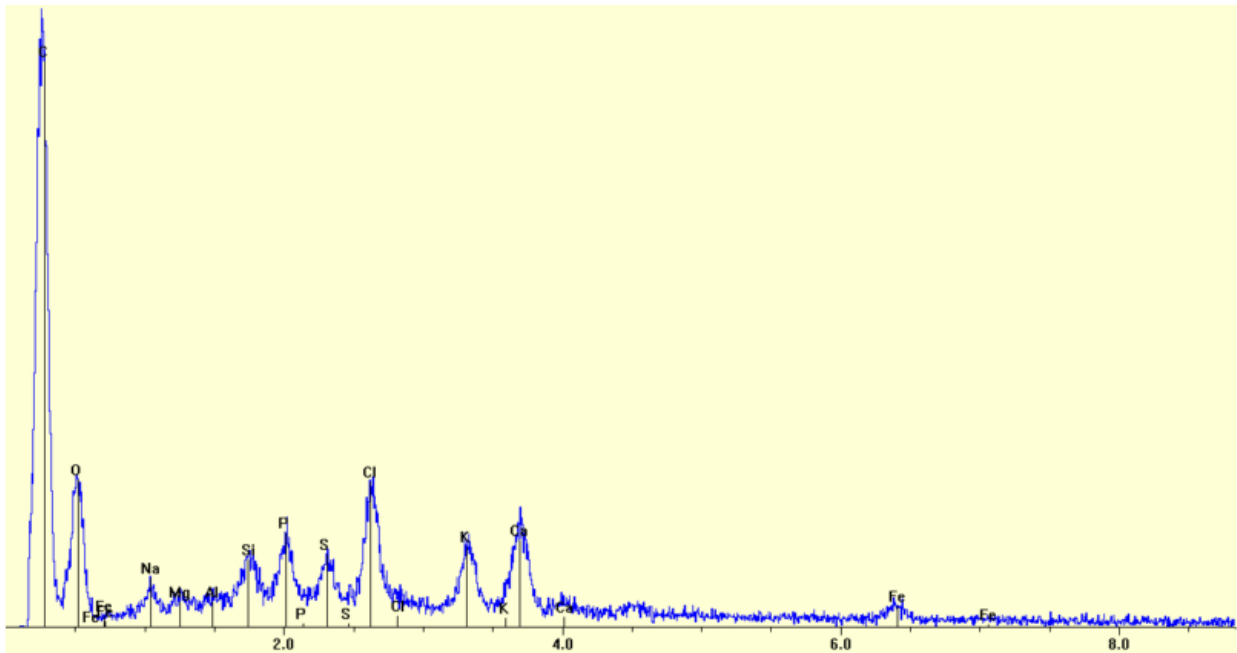


Figure 2-11: EDS spectrum of a fouled MF membrane (Advanced Water Technology Center, 2015)

# **CHAPTER 3**

## **Research Methodology**

### **3 Research Methodology**

#### **3.1 Introduction**

In this chapter, the details are given regarding the use of equipment and materials, as well as experimental procedures followed during all experimental runs conducted. Descriptions of instruments used are also included. During this research, a quantitative experimental approach was used.

This project is divided into two sections namely:

- i. Bench scale reverse osmosis process;
- ii. Scale inhibition using an antiscalant;

All experiments were conducted at the Cape Peninsula University of Technology, Bellville, Chemical Engineering and Chemistry Building in the Environmental Engineering Water Laboratory 1.18.



### 3.2 RO system process description

#### 3.2.1 Experimental Set-up

The research project was conducted on a bench-scale RO Cell (SEPA CF Cell) unit, using a simulated feed containing different concentrations of organics (soaps, detergents, chlorinated and aromatic solvents) and inorganic (metal ions and particles, heavy metals, sand and soil dusts) substances. A low-pressure high flow rate hydra-cell pump was used to pump the feed water through the cell. Permeate was discharged into a holding tank and the brine recycled into the feed tank. The feed velocity was controlled via a flow controller and the pressure around the cell were kept constant. Using the needle valve on the brine outlet, the feed pressure was regulated manually in order to achieve a constant flux and readings were recorded accordingly.



Photo 3-1: RO bench-scale unit in the Environmental Engineering water system laboratory (October 2019)

**Table 3-1: RO system equipment**

Feed Tank	1
Hydra Cell Pump	2
Pipes	3
RO SEPA CF Cell	4
Hydraulic Hand Pump	5

Other equipment used during experiments with the RO system

- Bench-scale RO (cell) unit
- 25L model laundry wastewater as feed
- Hanna analytical equipment and reagents
- Portable EC and pH meters
- Stop watch
- Measuring cylinder

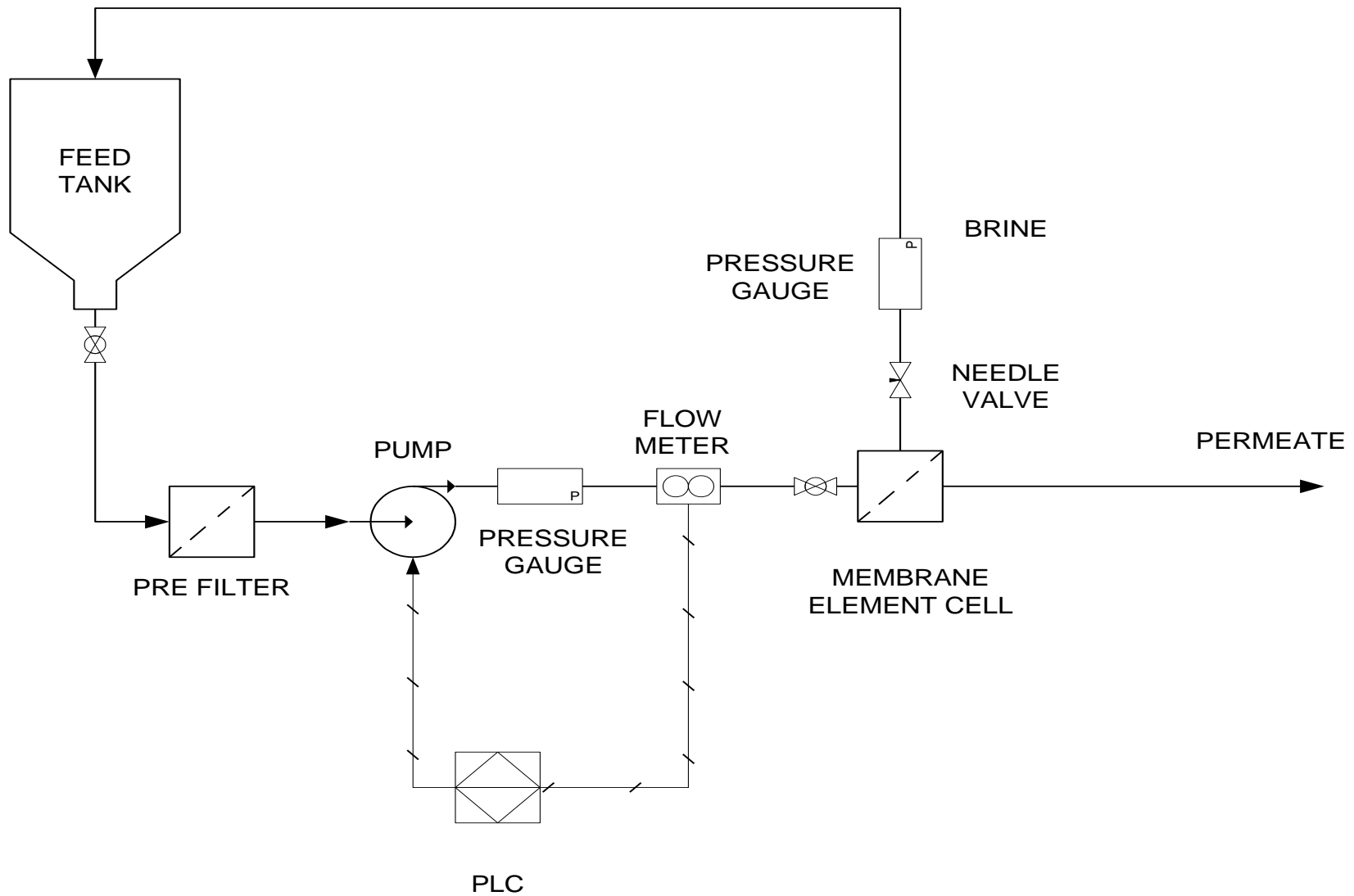


Figure 3-1: Schematic representation of the RO PFD

### 3.2.2 RO System Operation

The operating conditions were manually set-up. Conductivity, TDS and temperatures of the feed, permeate and recycled brine was recorded every 45min for the 19-hour experimental short run and every 5 hours for the 104-hour experimental long run.

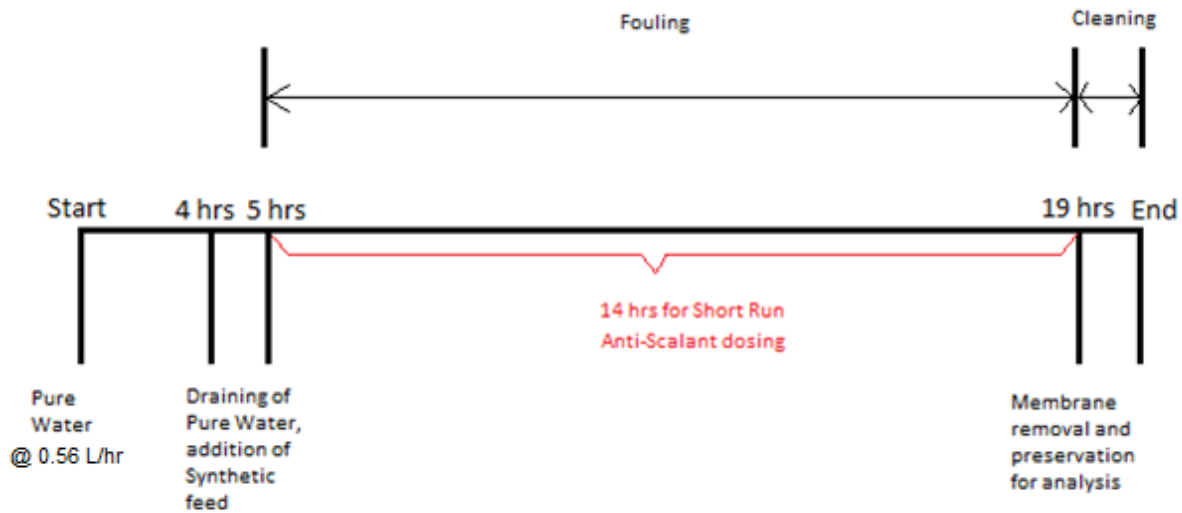
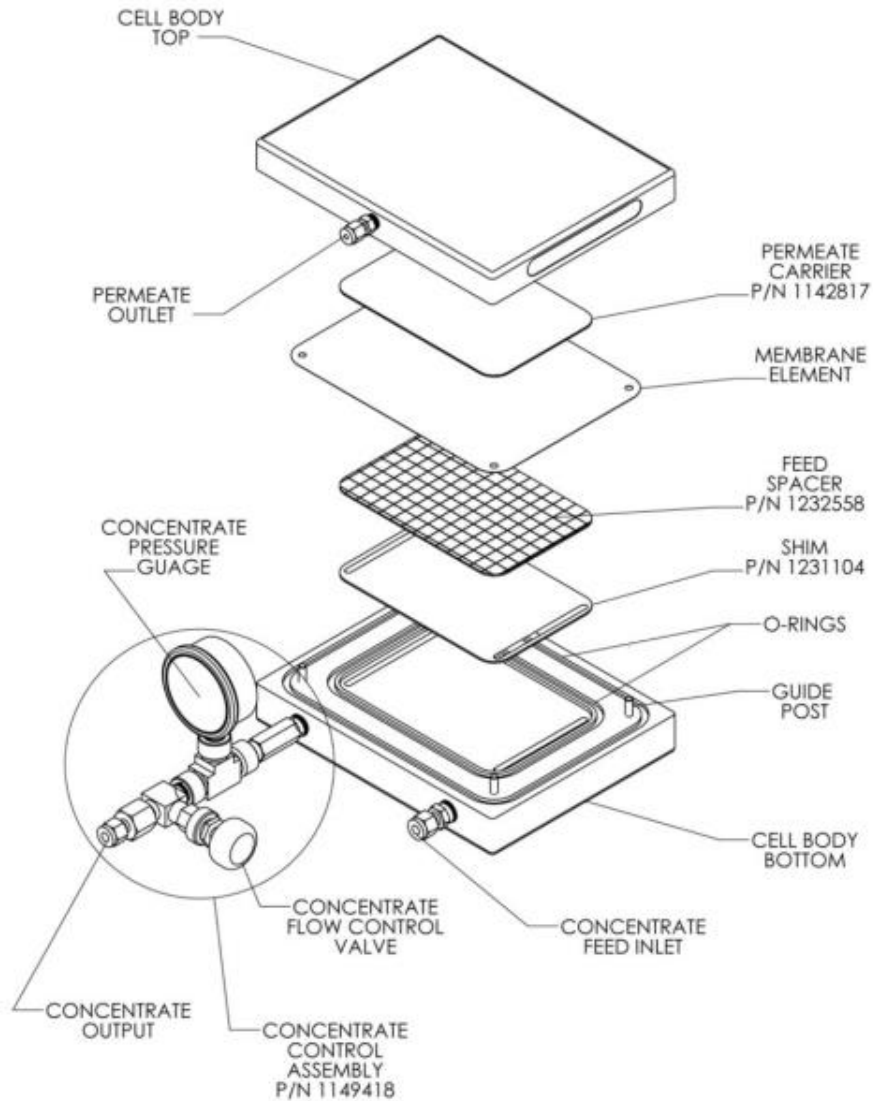


Figure 3-2: Timeline during the fouling experimental runs using the RO cell

### 3.2.3 RO Cell Start up procedure

- A screw driver is used to wedge open the cell module due to hydraulic pressure;
- Two spacers are cut out in the same shape as the membrane active area surface as shown in Figure 3-3: the spacer with bigger holes is placed on the higher pressure side (feed side); the spacer with smaller holes is placed on the low pressure side (permeate side);
- The spacers are then rinsed with deionised water;
- The membrane is cut from an opened spiral wound DOW FILMTEC membrane (XLE-4040) in a rectangular shape with dimensions 14.5cm x 9.5 cm, giving an active surface area of 0.014 m<sup>2</sup>, so that it covers the inner O-Ring in the flat cell. It is significant that the shiny side of the membrane is faced down on the cell;



**Figure 3-3: Typical Sepa CF Cell Body Assembly (Sterlite Corporation, 2015)**

- The cell is closed and placed back in its holder and compressed using the hydraulic pump;
- The hydraulic pump pressure is then set to 12-14 bars. After the cell is secured the pump is switched on and the feed valve is opened;
- Fresh de-ionised (DI) water is then transferred to the feed tank;
- Operating conditions of system was set and controlled manually. The operating conditions and time were pre-set for the experimental runs as follows:

(1) Starting time: 30sec

(2) Shutdown time: 30sec

(3) Experimental run time: 14-hour short run and 100-hour long run

(4) Feed pressure: 10 bar;

- The system was started and the feed flowrate was increased slowly from zero to 0.56 L/hr;
- Once the standard conditions were achieved it was allowed to reach steady state by recording the flux in 30 min intervals until the flux remained constant. Once a steady flux was achieved (mostly after 4 hours), the de-ionised water was drained and replaced with the synthetic feed;
- After the system reached stability again at the required system conditions, the conductivity, TDS and temperature of the feed, brine and permeate were recorded every 45 minutes throughout the experimental short run.

#### **3.2.4 Membrane cleaning**

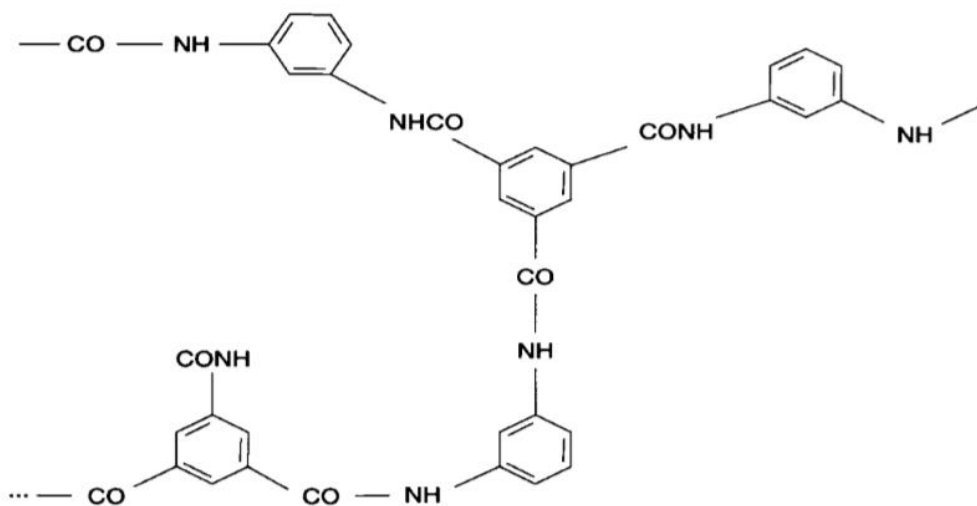
- Before membranes are used for experiments they were soaked in de-ionised water for at least 24 hours;
- The system was flushed before experimental runs with de-ionised water. The conductivity of the water used to flush the system had an electro-conductivity of  $7\mu\text{S}\cdot\text{cm}^{-1}$ . Each experimental run started with a new membrane.
- After experimental runs were complete, the system was shut down and the membrane was removed and preserved for analysis. The cell was then closed and pressurized for cleaning for 30 minutes with DI water at a flowrate of 0.7 L/hr.

#### **3.2.5 Membrane replacement**

The membrane cell is opened and rinsed with DI water. Both spacers are removed and soaked in DI water to ensure all contaminants are washed away. The spacers are placed back into the cell together with a new membrane, closed up and ready for the next experimental run.

**Table 3-2: Operating limits of the Filmtec XLE-4040 PA TFC membrane (Lenntech, n.d.)**

Membrane Type	Polyamide Thin-Film Composite
Maximum Operating Temperature	45°C
Maximum Operating Pressure	41 bar
Maximum Feed Flow Rate	3.2 (m <sup>3</sup> /hr)
Maximum Pressure Drop	0.9 bar
pH Range, Continuous Operation	2 to 11
pH Range, Short-Term Cleaning (30 min)	1 to 13
Maximum Feed Silt Density Index (SDI)	SDI 5
Free Chlorine Tolerance	<0.1 ppm



**Figure 3-4: Chemical structure of a polyamide composite RO membrane composition (Kucera, 2015)**

**Table 3-3: RO system operating conditions**

Initial Conditions	Feed Solution
Flux: 40 L/m <sup>2</sup> .hr	simulated Laundry wastewater
Pressure: 10 bar	
Flowrate: 0.56 L/hr	
Temperature: Ambient	

### 3.2.6 Equipment used during RO operation

- A 50mL graduated glass cylinder and stopwatch were used to manually measure the flow rates of the streams (feed, brine and permeate)



**Figure 3-5: Cylindrical beaker (Left) and stop watch (right)**

- The conductivity meter used in this project simultaneously measured conductivity from which the salt rejection (%) was calculated; the total dissolved solids (mg/L) and the temperature (°C).



**Figure 3-6: YSI Eco Sense EC300 conductivity meter model use during the experiments**

- The HI96769 Anionic Surfactant Portable Photometer (Hanna Instruments) combines accuracy and ease of use in an ergonomic, portable design. A user can accurately



determine the concentration of anionic surfactants as Sodium dodecylbenzenesulfonate within a 0.00 to 3.50 mg/L (ppm) range using the HI95769-01 ready-made reagents.



**Figure 3-7: Anionic Surfactant Portable Photometer (left) and reagents (right)**

### 3.2.7 COD and surfactant analysis

COD and surfactant analyses were used to characterize the membrane performance before and after filtration. Both analyses were done externally.

**Table 3-4: Experiment summary**

Experiment	Run	Experiment	Run
1	No Anti Scalant_Std Laundry Det Conc (13.2ml)	14	Duplicate of Run 9_Anti Scalant_4ppm_std Laundry Det Conc (13.2ml)
2	No Anti Scalant_2xLaundry Det Conc (26.4ml)	15	Anti Scalant_8ppm_std Laundry Det Conc (13.2ml)
3	Anti Scalant 4ppm_4xLaundry Det Conc (52.8ml)	16	Duplicate of Run 15_Anti Scalant_8ppm_std Laundry Det Conc (13.2ml)
4	No Anti Scalant_4xLaundry Det Conc (52.8ml)	17	Anti Scalant_4ppm_1.5x Laundry Det Conc (19.8ml)
5	No Anti Scalant_4xLaundry Det Conc (52.8ml)	18	Duplicate of Run 17_Anti Scalant_4ppm_1.5x Laundry Det Conc (19.8ml)
6	Duplicate of Run 5_No Anti Scalant_4xLaundry Det Conc (52.8ml)	19	Anti Scalant_8ppm_1.5x Laundry Det Conc (19.8ml)
7	Duplicate of Run 1_No Anti Scalant_Std Laundry Det Conc (13.2ml)	20	Duplicate of Run 19_Anti Scalant_8ppm_1.5x Laundry Det Conc (19.8ml)
8	Duplicate of Run 2_No Anti Scalant_2xLaundry Det Conc (26.4ml)	21	Anti Scalant_4ppm_2x Laundry Det Conc (26.4ml)
9	Anti Scalant_4ppm_std Laundry Det Conc (13.2ml)	22	Duplicate of Run 21_Anti Scalant_4ppm_2x Laundry Det Conc (26.4ml)
10	No Anti Scalant_3xLaundry Det Conc (39.6ml)	23	Anti Scalant_8ppm_2x Laundry Det Conc (26.4ml)
11	No Anti Scalant_1.5xLaundry Det Conc (19.8ml)	24	Duplicate of Run 23_Anti Scalant_8ppm_2x Laundry Det Conc (26.4ml)
12	No Anti Scalant_2.5xLaundry Det Conc (33ml)	25	Long Run 1_No Scalant_Std Laundry Det Conc (13.2ml)
13	Duplicate of Run 11_No Anti Scalant_1.5xLaundry Det Conc (19.8ml)	26	Long Run 2_Anti Scalant_8ppm_Std Laundry Det Conc (13.2ml)

Std= Standard, Det= Detergent, Conc= Concentration

### 3.2.8 Make-up of the simulated feed

Synthetic (simulated) feed make-up were measured in terms of chemical mass, weighed on an analytical scale. Thereafter it was mixed in a volumetric flask to be diluted with 1L of water. This was done individually for each chemical. As the chemicals dissolved, the solution were mixed in the into the feed tank. The tank was filled with water to make a total feed volume of 25L synthetic feed. The liquid detergent amount was varied to observe the effect it has on the reverse osmosis operation.

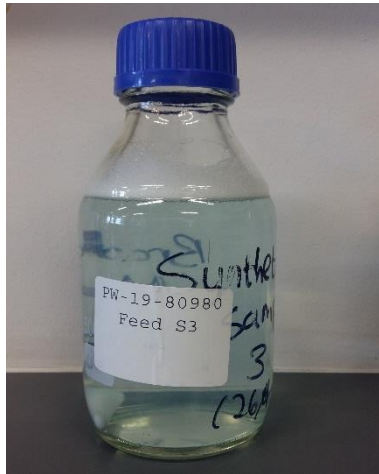


Photo 3-2: Synthetic laundry wastewater

Table 3-5: Synthetic feed solution composition

Chemical	Amount/ 25 Litre Deionised Water
Liquid detergent	13.2 mL
Fabric Softener	7 mL
Test Dust	10 g
Na <sub>2</sub> SO <sub>4</sub>	1.33 g
NaHCO <sub>3</sub>	0.667 g
Na <sub>2</sub> HPO <sub>4</sub>	1.33 g

### 3.3 Antiscalant Addition

Vitec 3000® is a powerful, broad spectrum, liquid antiscalant and dispersant that is compatible with organic coagulants. It is highly effective at low dose rates and in a wide range of feed waters (Lenntech, 2015).

This product is a multi-component antiscalant that prevents scale precipitation and disperses colloidal particles in cellulose acetate and polyamide membrane systems. It is compatible with organic coagulants that may be indirectly present in municipal feed waters Vitec 3000 has been approved for use in systems producing drinking water in the United Kingdom, conforming to the German Institute for Standardisation (DIN) 15040, and by National Sanitation Foundation (NSF) International under NSF/ American National Standards Institute (ANSI) Standard 60 (Lenntech, 2015).



**Figure 3-8: Vitec 3000 23kg pail (Left) and Pipette (Right)**

Specifications: Appearance: Clear, amber liquid; pH:10.7-11.8; Specific gravity (@25°C):1.2-1.3  
A typical Vitec 3000 dose ranges from 2-5 mg/L. For the experiments, an antiscalant dose of 0, 4 and 8 mg/L were used. By using a 5mL pipette, antiscalant were added to the feed tank every 45 min for short runs and every 5 hours for the long runs.

### **3.4 Membrane Surface Characterization**

A qualitative analysis (SEM-EDS) and semi-quantitative analysis (ATR-FTIR) were used to characterize the membrane before and after modifications. Both analyses were done externally.

#### **3.4.1 ATR-FTIR Analysis**

The Nicolet iS10 FTIR equipment was regarded as essential with regard to the characterization of materials, and in particular with regard to following degradation reactions of polymers. As part of fundamental research the FTIR spectrophotometer is a way of simply identifying subtle morphological changes.

ATR-FTIR analysis was conducted using OMNIC software to observe the chemical change after treating laundry wastewater with antiscalant versus no antiscalant. The ATR-FTIR spectra were recorded at a resolution of  $8\text{ cm}^{-1}$  during 64 scans at a nominal incident angle of  $45^\circ$  with wave numbers ranging between  $4000$  and  $400\text{ cm}^{-1}$ .

#### **3.4.2 SEM-EDS Analysis**

The Nova NanoSEM is a high resolution Field Emission SEM, combining low kV imaging and analytical capabilities with unique low vacuum performance.

The scanning electron microscope was used to observe changes in membrane morphology after modification of the membrane surface. Top view images were scanned at 10000x and 40000x magnifications and 5.00 kV landing electron for all samples, while cross-section images were at a 500x and 200x magnification and 20.00 kV landing electron.

# **CHAPTER 4**

## **Results and Discussion**

## 4 Results and Discussion

Results presented under this chapter are divided into three sections:

- i. Membrane surface characteristics
- ii. RO process with scale inhibition
- iii. Development of Flux model

### 4.1 Membrane Surface Characterisation

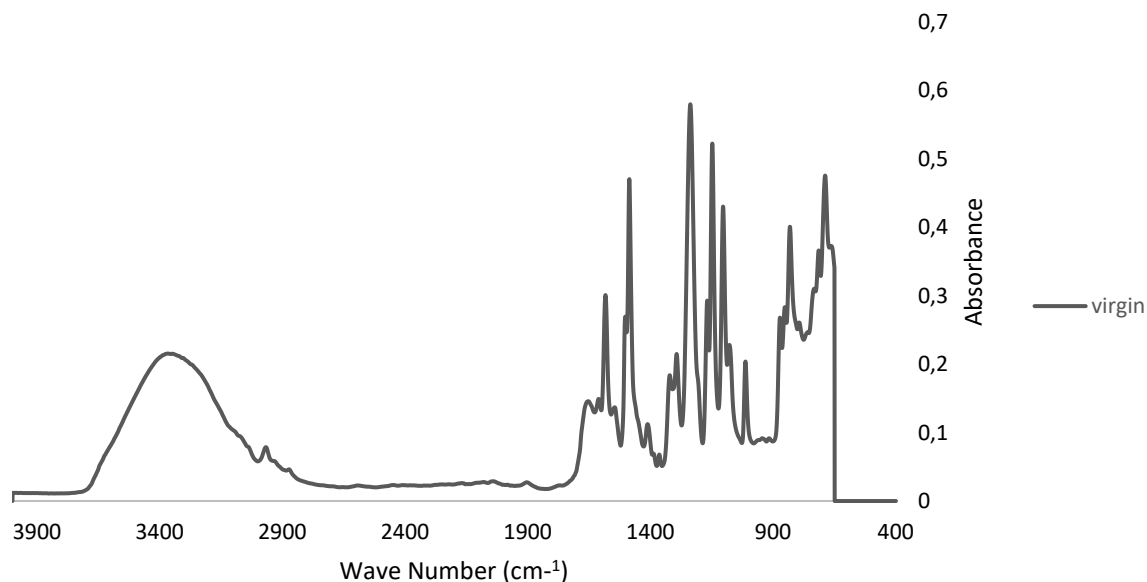
Many of the properties exhibited by separation membranes are due to interactions at the interface with their environment, including flux, rejection of solutes and surface fouling. As such, when trying to understand how such interactions affect their function and when developing novel membranes with improved properties, a thorough understanding of their surface properties is essential (Johnson et al., 2018). ATR-FTIR and SEM-EDX analyses were used to characterise the membrane surface in this study.

#### 4.1.1 ATR-FTIR Analysis

ATR-FTIR analysis was used to examine the effect of antiscalant on the TFC membrane surface before and after fouling. The analysis delivered a suitable method of identifying different chemical groups on the surface of the membrane.

The ATR-FTIR spectra were recorded at a resolution of  $8\text{ cm}^{-1}$  during 64 scans at a nominal incident angle of  $45^\circ$  with wave numbers ranging between  $4000$  and  $400\text{ cm}^{-1}$ . To capture certain functionalities in both the clean and fouled membrane samples, spectra were zoomed in to a region of  $2000\text{-}600\text{ cm}^{-1}$ .

The wavenumber intensities were normalised to allow accurate representations and easy comparisons between spectra. The identification of the functional groups at different peaks are presented in Figure 2-9 in Chapter 2.

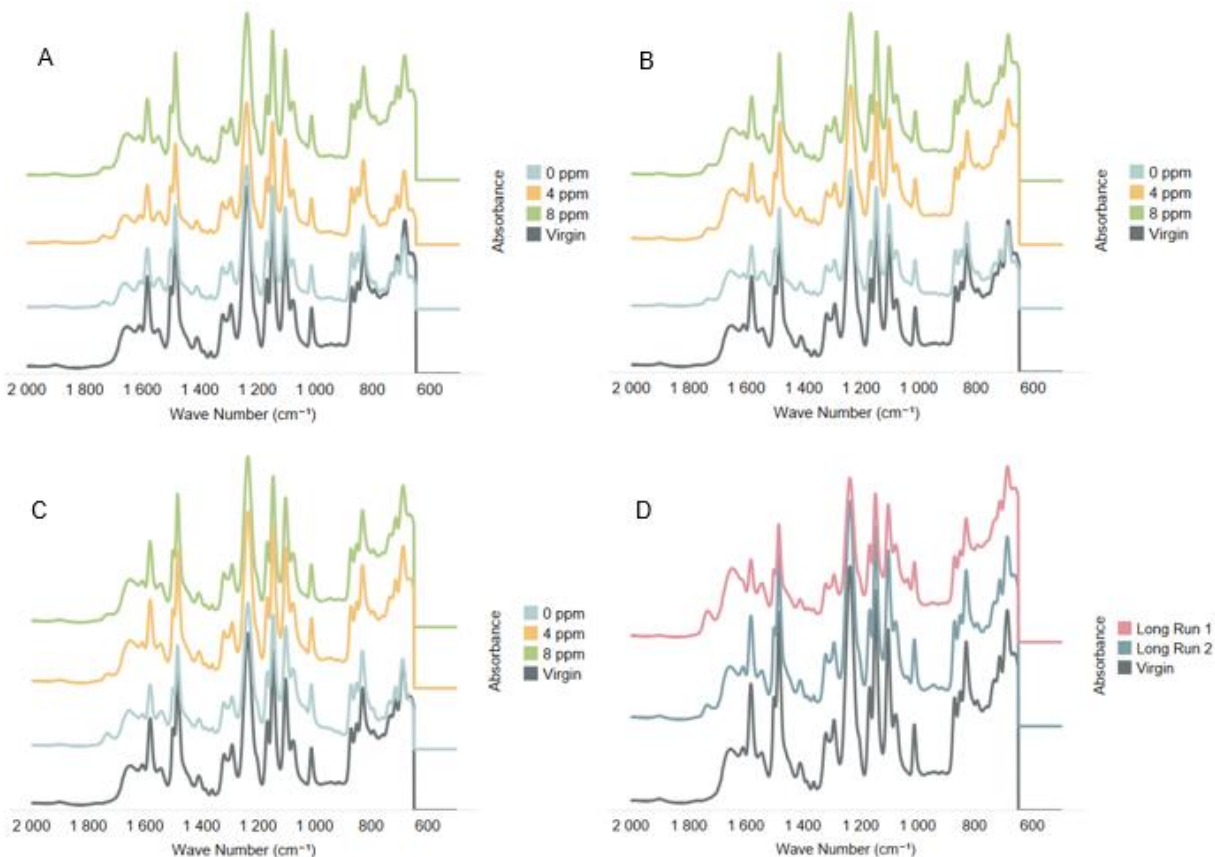


**Figure 4-1: Full ATR-FTIR Spectra for Virgin membrane**

In Figure 4-1, all the characteristic peaks can be seen in a virgin XLE polyamide (PA) thin film composite (TFC) membrane in its clean state. The broad peak at 3300 cm<sup>-1</sup> is a complex band due to the N–H and –COOH stretching present in the PA active layer (Shafi et al., 2017). Similarly, the sharp peak at ~3000 cm<sup>-1</sup> with a nearby shoulder at ~2900 cm<sup>-1</sup> is a characteristic peak of aliphatic stretching arising from C–H bonds present in the active PA layer (Shafi et al., 2017). Peaks at ~1666 and 1486 cm<sup>-1</sup> are characteristics of the carbonyl (C=O) functional group.

According to Socrates (1980), C–H symmetric deformation vibration of > C(CH<sub>2</sub>)<sub>2</sub> and aromatic in-plane ring bend stretching vibration are present in PA layer. The peak at ~1239 cm<sup>-1</sup> is a characteristic of C–O–C asymmetric stretching vibration of the aryl-O-aryl group in a polysulfone support layer (Shafi et al., 2017). However, the peak at ~1000 cm<sup>-1</sup> may either be assigned to the sulfonic group (Qiu et al., 2007), or it could be due to symmetric SO<sub>2</sub> stretching vibrations present in the polysulfone layer.





**Figure 4-2: Zoomed in ATR-FTIR Spectra for varying concentrations of laundry detergent. A: 13.2 mL; B: 19.8 mL; C: 26.4 mL & D: Long Run 1 (0 ppm anti-scalant) and long run 2 (8 ppm anti-scalant)**

Spectra of both the fouled and virgin membranes at varying antiscalant concentrations seemed similar. This could arguably be due to better comparison of any chemical change that may have occurred under these conditions where the ATR-FTIR spectra were zoomed into in the region of 2000-600  $\text{cm}^{-1}$ . This region probes the chemical characteristics deeper in the membranes, up to a few microns.

Investigating the zoomed spectra in the region of 2000-600  $\text{cm}^{-1}$  (Figure 4-2) reveals that the peak at  $\sim 1600 \text{ cm}^{-1}$  is diminished for the experimental runs without any antiscalant dosing when compared to their virgin states. This could be due to the carbonyl group present in the PA layer, which is being masked by the foulant layer. For the membranes dosed with antiscalant, a similar trend can be observed in all the graphs at those peaks, thus corresponding to their virgin states, indicating less scaling on the membrane surface.

When examining the long experimental run the ATR-FTIR Spectra data (graph D), has a similar detection. The long experimental run 1 (with antiscalant dosing) has less intense peaks (at 1600

cm<sup>-1</sup>; 1420 cm<sup>-1</sup> and 1000 cm<sup>-1</sup>) compared to the virgin membrane which indicates a scalant layer masking the PA layer (Shafi et al., 2017). However, more noticeably is the difference in the intensities of the peaks in long experimental run 2 (dosed with 8 ppm). The intensity of the peaks across the spectra is almost exact to the virgin membrane and this is an evidence of the fact that less scale is deposited on the surface of the membranes compared to long experimental run 1.

#### 4.1.2 SEM-EDX Analysis

SEM was used to qualitatively observe the structures of the membranes before and after fouling at different antiscalant dosages. SEM photographs of the top surface layer are shown in Figures 4-3 to 4-6. The SEM analysis was conducted with a magnification of 40,000 for all samples.

The accumulation of foulant on RO membranes strongly depends on foulant-surface interaction and as mentioned in the literature (Asadollahi et al., 2017), feed pressure plays a critical role toward foulant accumulation and adhesion on the membrane surface in the NF and RO desalination processes (Shafi et al., 2017).

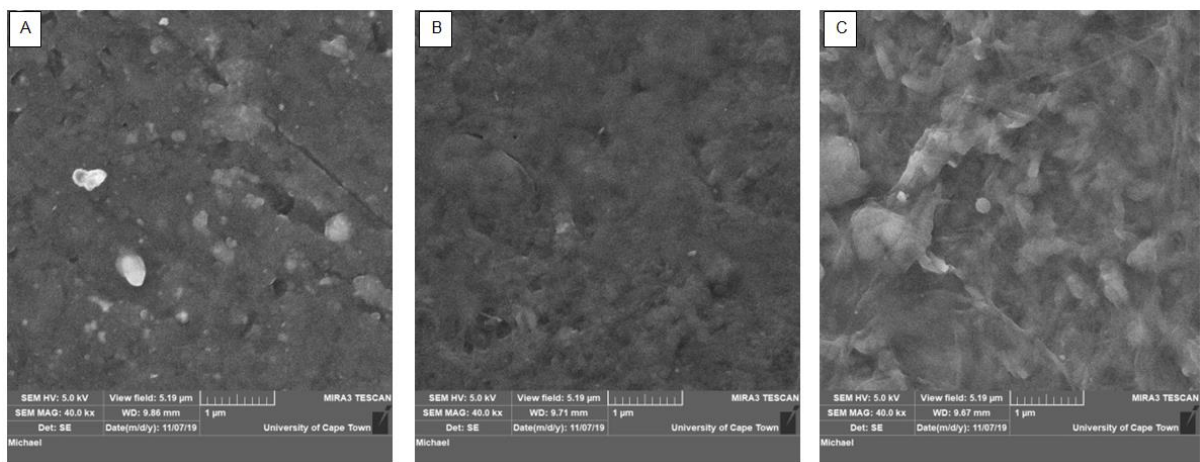


Figure 4-3: Membranes with 13.2 mL Laundry Detergent at various antiscalant dosages- A: 0 ppm; B: 4 ppm & C: 8 ppm

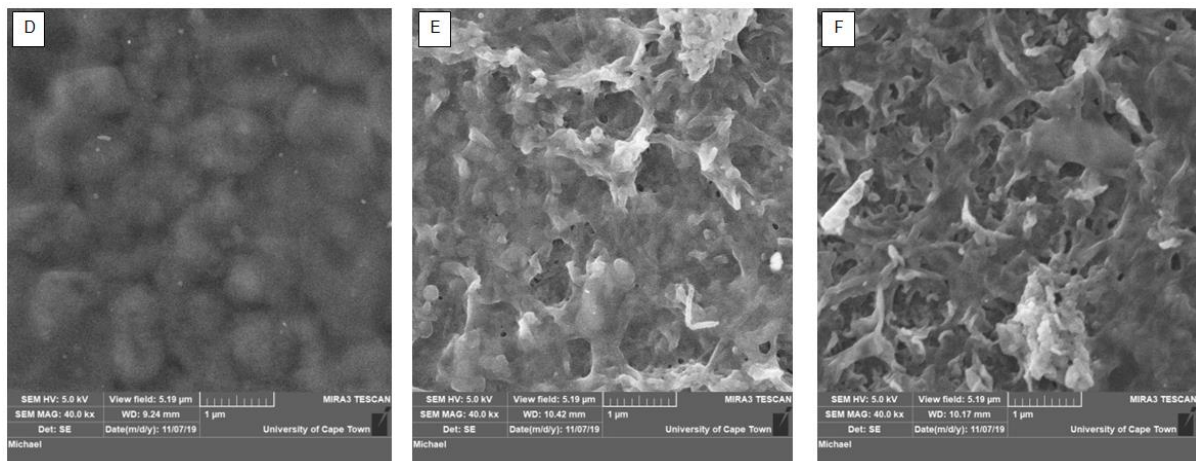
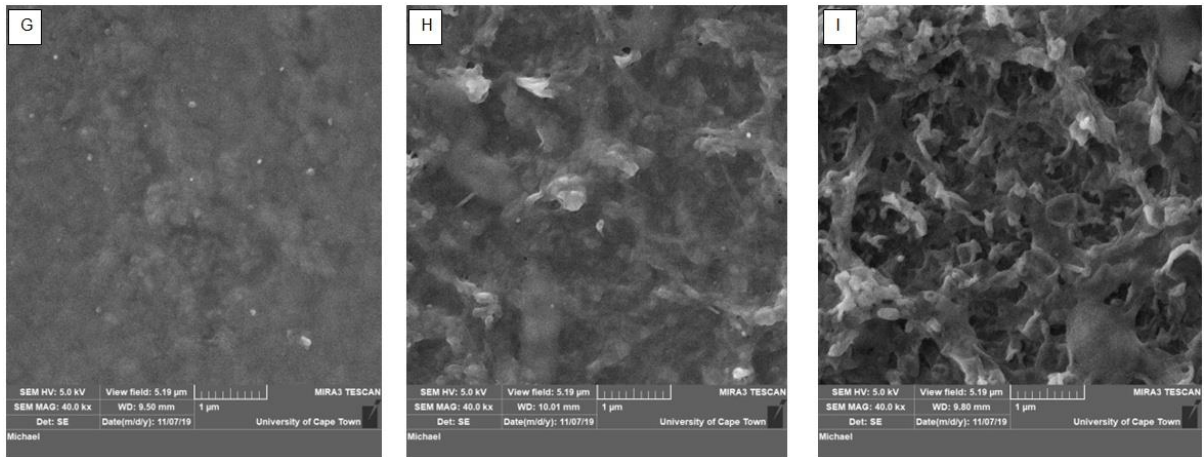
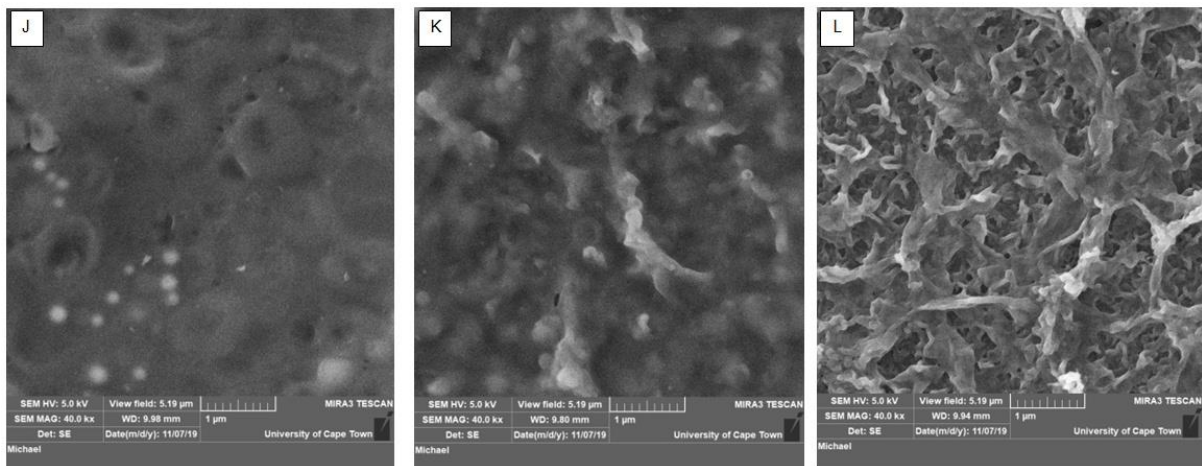


Figure 4-4: Membranes with 19.8 mL Laundry Detergent at various anti-scalant dosages- D: 0 ppm; E: 4 ppm & F: 8 ppm



**Figure 4-5: Membranes with 26.4 mL Laundry Detergent at various anti-scalant dosages- G: 0 ppm; H: 4 ppm & I: 8 ppm**



**Figure 4-6: Long Run 1 (No anti-scalant); K: Long Run 2 (Anti-scalant- 8 ppm) & L: Virgin membrane**

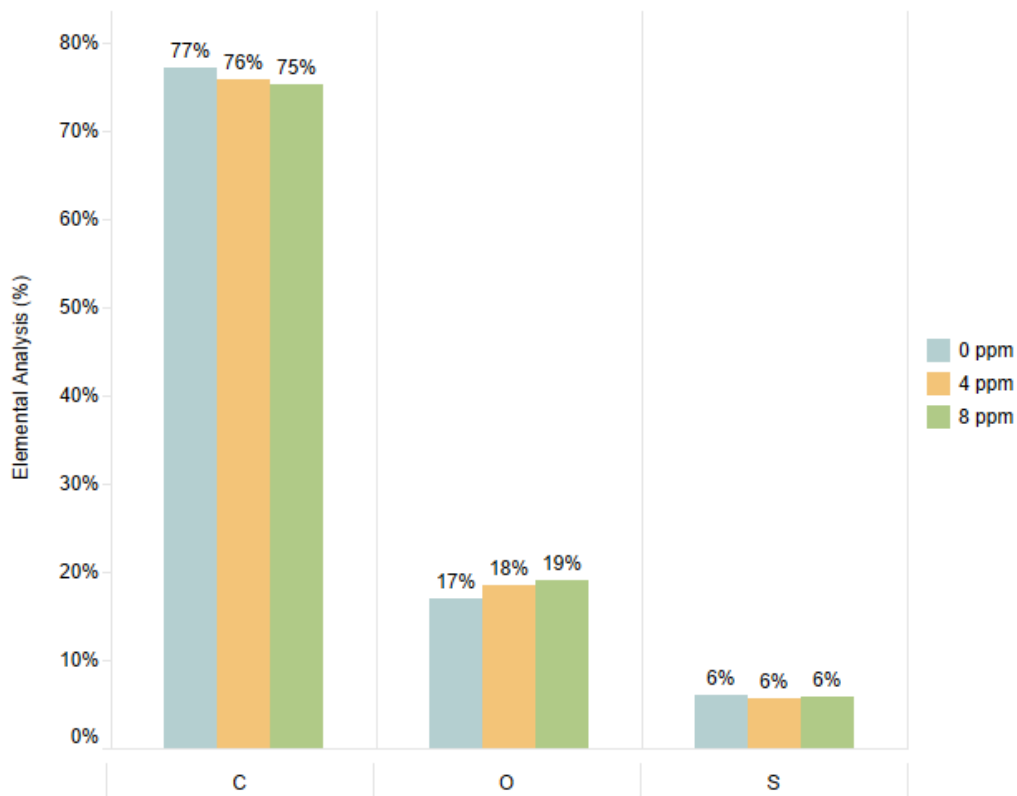
Matin et al. (2014) reported that before any fouling or scaling occurred, virgin membranes display a leaf-like surface morphology. This morphology is clearly evident according to the virgin membranes in Figure 4-6 (L). It can be seen that the deposited scalant fully and significantly covers the surface of fouled membranes and this is accounted for by SEM images A, D, G, and J.

In contrast to the fouled membranes, membranes B, E, H and K are only sparsely covered with the scalant layer. The underlying leaf-like surface morphology reveals itself under the thin and sporadically deposited foulant layer. The sparsely spread scalant layer on the surface of the membrane provides clear evidence of the effectiveness of antiscalant dosing in improving the fouling resistance of the RO membranes. Membranes C, F and I confirm the effectiveness of antiscalant dosing as they reveal a more distinctive leaf-like surface

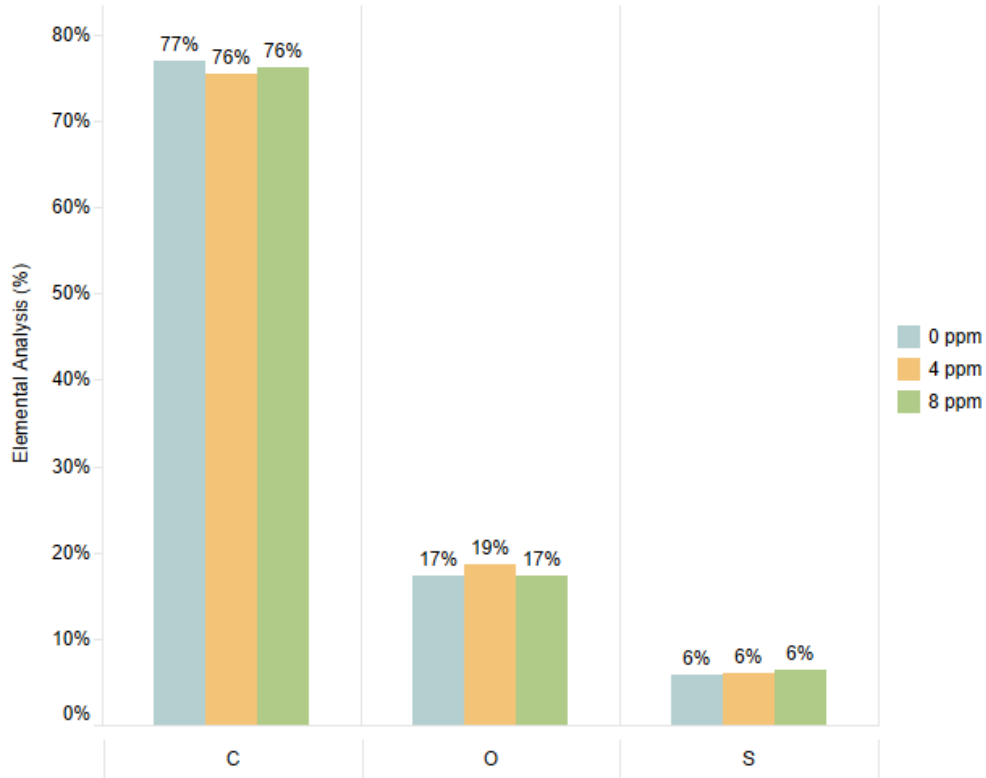
morphology under a thinner deposit of scalant layer. Similar observations were obtained by Aziz & Kasongo (2019) when using a commercial antiscalant to treat brackish water.

When comparing figures of the same detergent concentration, it can be seen that the ridge and valley structure of the membranes becomes clearer as the antiscalant concentration is increased from 0 to 8 ppm. These results provide clear evidence that the correct dosing of antiscalant significantly disrupts and hinders the foulant adhesion on the surface of the membranes. This hindered attachment of scalant on the surface of the membranes results in a much lower rate of flux decline when compared to membranes with no antiscalant addition.

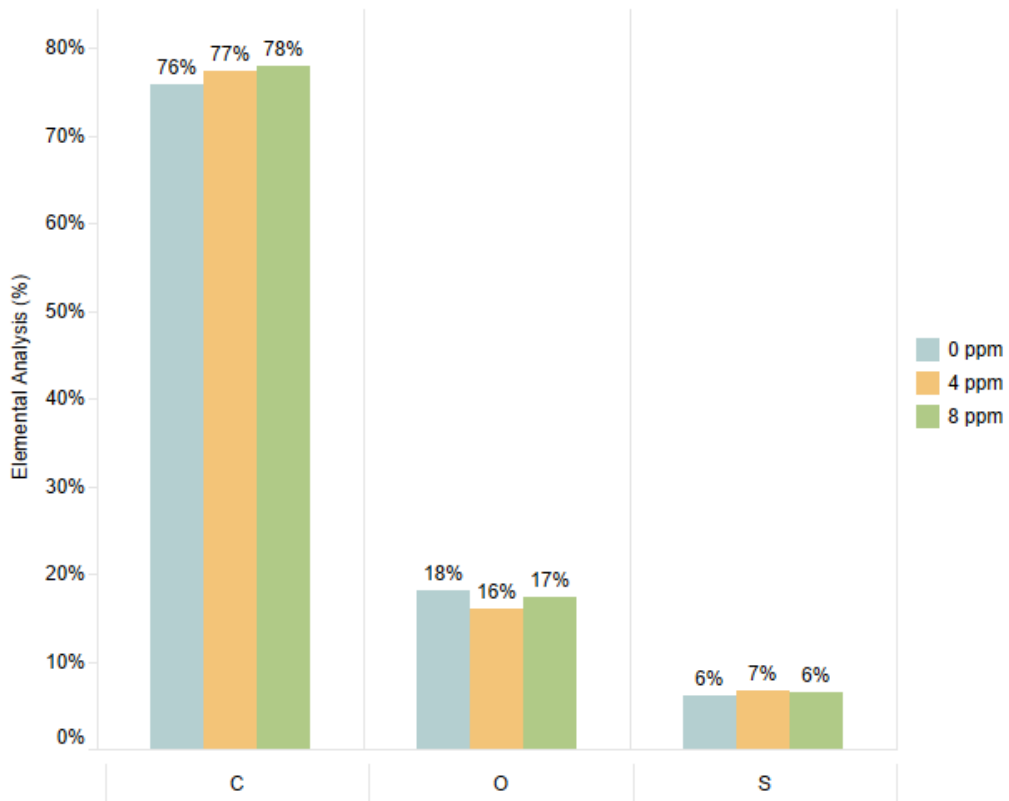
Energy dispersive X-ray (EDX) analysis was performed on the specimens in conjunction with the SEM. Figures 4-7 to 4-10 shows the results of EDX for both the virgin membrane and membranes after being scaled at different antiscalant dosages. EDX results of the virgin membrane (Figure 4-10) confirm the presence of the following elements in descending order C (77%) O (17%), S (6%), respectively.



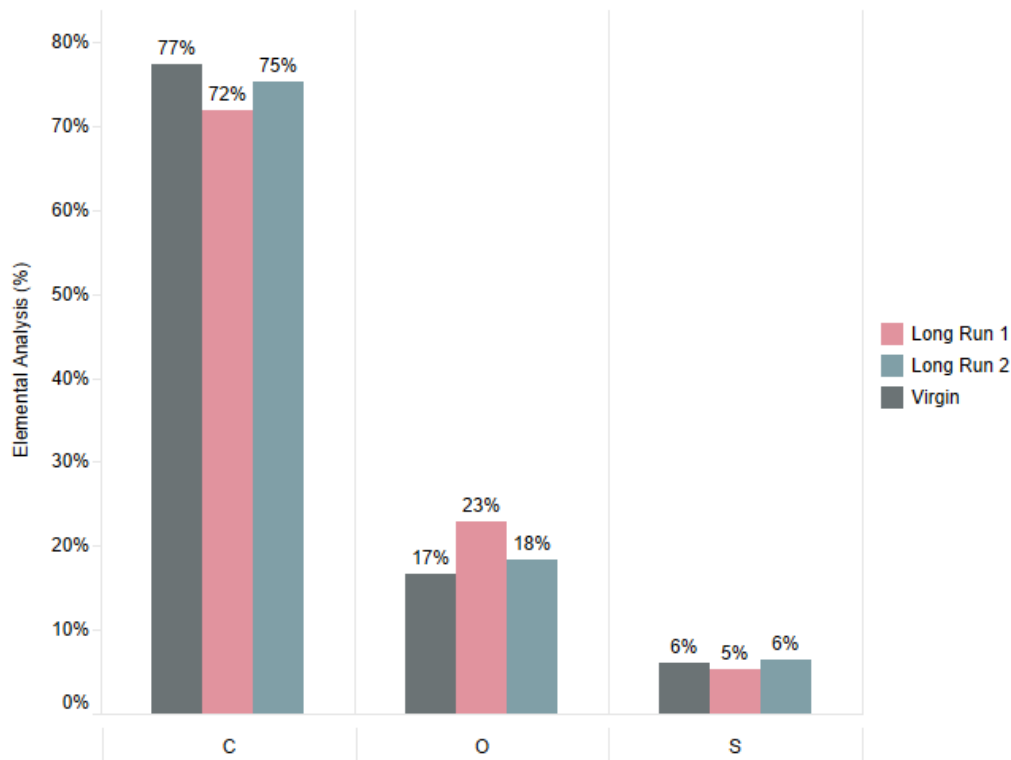
**Figure 4-7: EDX analysis of membrane: 13.2 mL Laundry Detergent**



**Figure 4-8: EDX analysis of membrane: 19.8 mL Laundry Detergent**



**Figure 4-9: EDX analysis of membrane: 26.4 mL Laundry Detergent**



**Figure 4-10: EDX analysis of Virgin membrane; Long run 1 (0 ppm anti-scalant) and Long run 2 (8 ppm anti-scalant)**

There is not much difference between the membrane samples for the experimental short runs, concerning the relative ratios of the constituent elements (Figure 4-7 to 4-9). Given the fact that the depth of analysis in EDX is a couple of microns, it seems likely that in each condition, the EDX involves the analysis of the virgin membrane material. Hence for the short experimental runs, there is only a thin layer of scalant on the membrane surface. A similar observation was reported by Shafi et al., (2017).

When examining long experimental run 1 and 2 (Figure 4-10), a major difference in the relative ratios can be seen. The experimental long run 2 (with 8ppm antiscalant addition) demonstrated relative ratios closer to that of the virgin membranes in comparison with experimental long run 1, which indicated that less scaling had occurred during experimental long run 2. This proves again that the antiscalant dosing to be effective.

When examining the carbon content of the experimental runs with no antiscalant dosing, it was observed that the amount of carbon decreased with an increase in laundry detergent concentration. This could be due to the carbonyl group present in the PA layer which were masked by the foulant layer. This is in agreement with the ATR-FTIR spectra previously explained. The presence of the sulfonate groups in the surfactant molecule resulted in an

increase in the overall oxygen and sulphur content of the surface, has been demonstrated by the EDX data.



## 4.2 RO Process performance

Several studies reported on the influence of the PA active layer and the PSF support on the performance and properties of the RO membranes. It is said that the membrane selectivity and flux are mainly controlled by the PA active layer with the porous PSF support assuming a minor influence (Roh, 2002; Hirose et al., 1996). In RO plants, system automation and reliability are important factors where plants are vulnerable to a valve or pump failure and membrane fouling and sensor data loss (McFall et al., 2007). To assess membrane performance accurately, water permeation and salt rejection properties are key indicators (Zhang et al., 2016). In this section the permeate flux decline and rejection performance of the membrane were investigated.

### 4.2.1 The flux performances during the fouling test

The figures (4-11 to 4-14) below present the permeate flux profile of the membranes during the filtration of laundry feed wastewater and antiscalant addition. The initial permeate flux of all experimental runs was kept constant. All experimental runs were duplicated and the average values used to plot the data graphs.

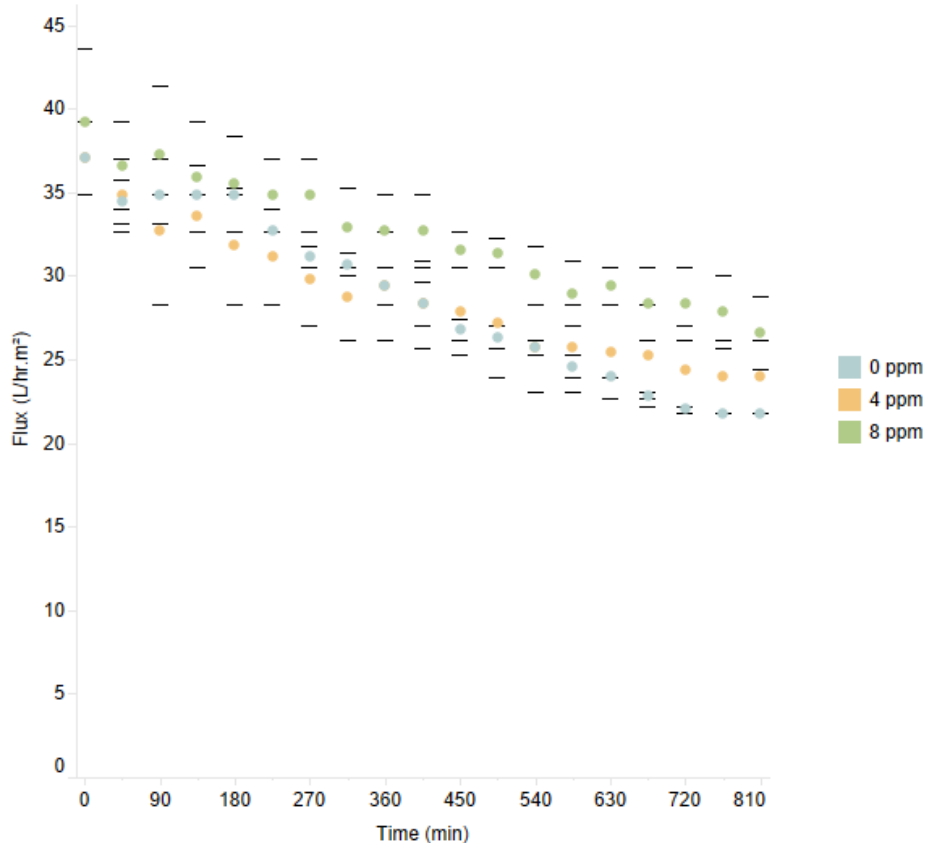
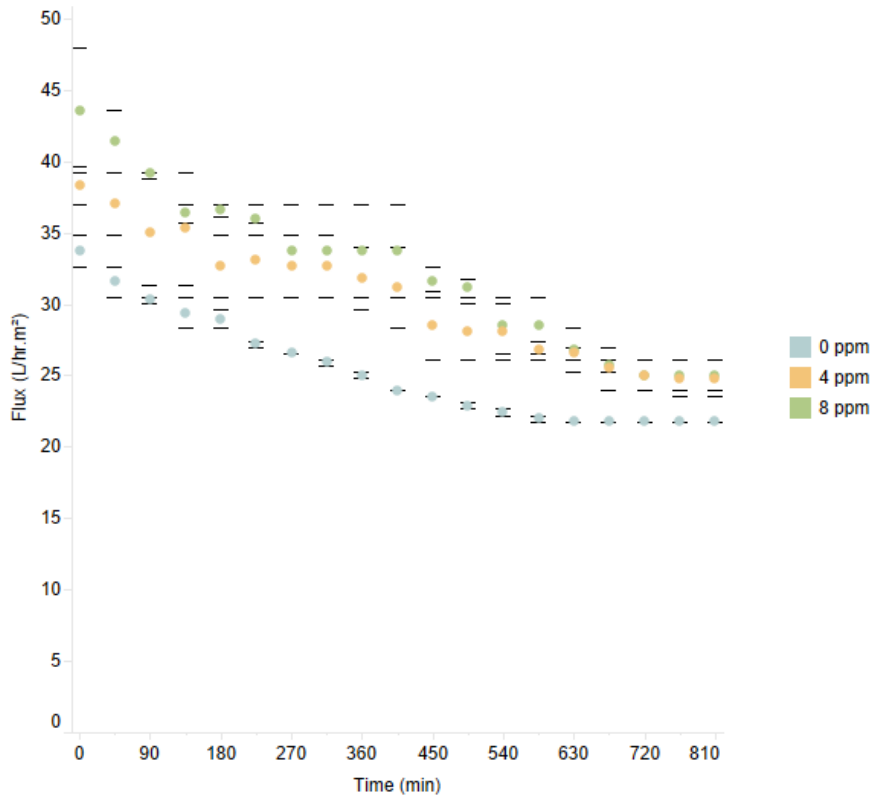
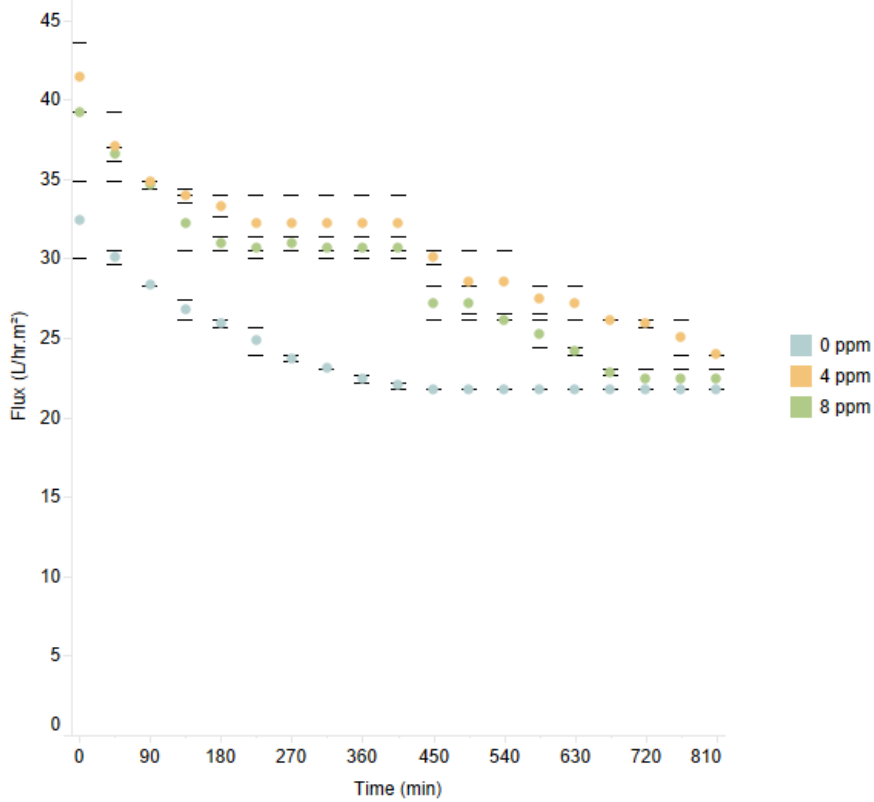


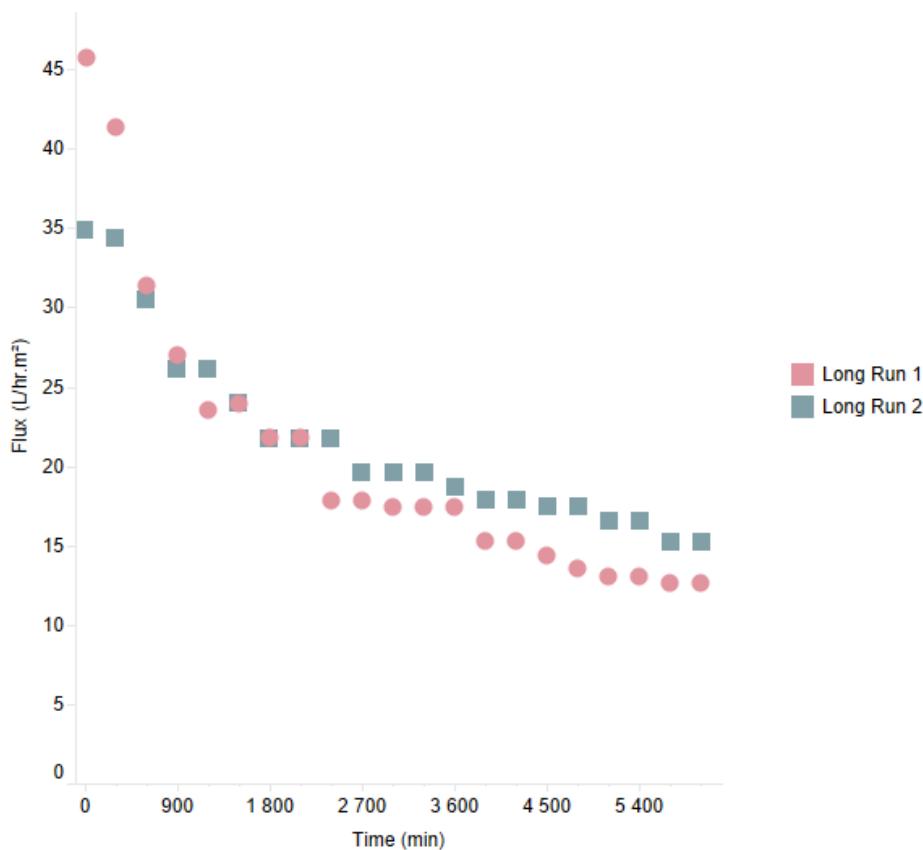
Figure 4-11: Time dependent average permeate flux of membrane: 13.2 mL Laundry Detergent



**Figure 4-12: Time dependent average permeate flux of membrane: 19.8 mL Laundry Detergent**



**Figure 4-13: Time dependent average permeate flux of membrane: 26.4 mL Laundry Detergent**



**Figure 4-14: Time dependent average permeate flux of membranes for Long Run 1 and Long Run 2**

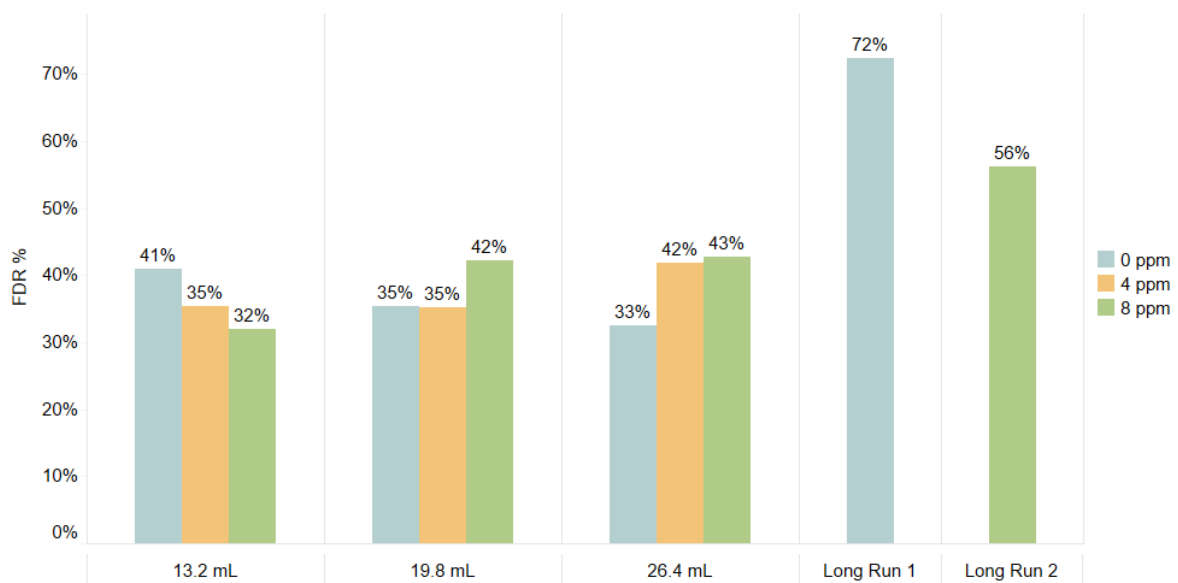
It could be seen that there is a persistent flux decline, for all four graphs in Figures 4-11 to 4-14, which proved the presence of fouling, more specifically scaling, as confirmed by Guilbaud et al. (2010) and Sumisha et al. (2015). The membrane pore size and hydrophilicity are the two major factors influencing the pure water flux performance of membranes (Sumisha et al., 2015). In the first few minutes of filtration, the scaling seems not to be that significant. However, over time the flux decline is more noticeable, and the flux difference between the membranes with antiscalant increased. The flux decline was associated with the fouling phenomena caused by the accumulation of anionic surfactant molecules on the membrane surface, with a build-up of a concentration polarisation layer or entrapment in the polyamide layer. As the concentration of laundry detergent increases, a greater flux decline was observed. This was demonstrated by the experimental short-run data with no antiscalant addition (Figures 4-11 to 4-13).

At 13.2 mL Laundry detergent, the flux only reaches a steady flux after 800 minutes, whereas at 26.4 mL Laundry detergent, the flux reaches a steady flux after 450 min. Although the graphs reveal that a gradual decrease of the flux could not be totally eliminated, the accumulation of fouling matter on the membranes with antiscalant addition was significantly lesser than membranes with no antiscalant addition. As the antiscalant dosage increased, the decrease in flux was less significant and this was observed for all four graphs. In Figure 4-14 the membrane, with antiscalant addition (Long Run 2), flux after 100

hours or 6000 minutes was higher than that of the membrane with no antiscalant addition (Long Run 1), this observation was to be expected, as the anti-scalant minimized scaling in Long Run 2. A similar observation was made by Aziz & Kasongo (2019).

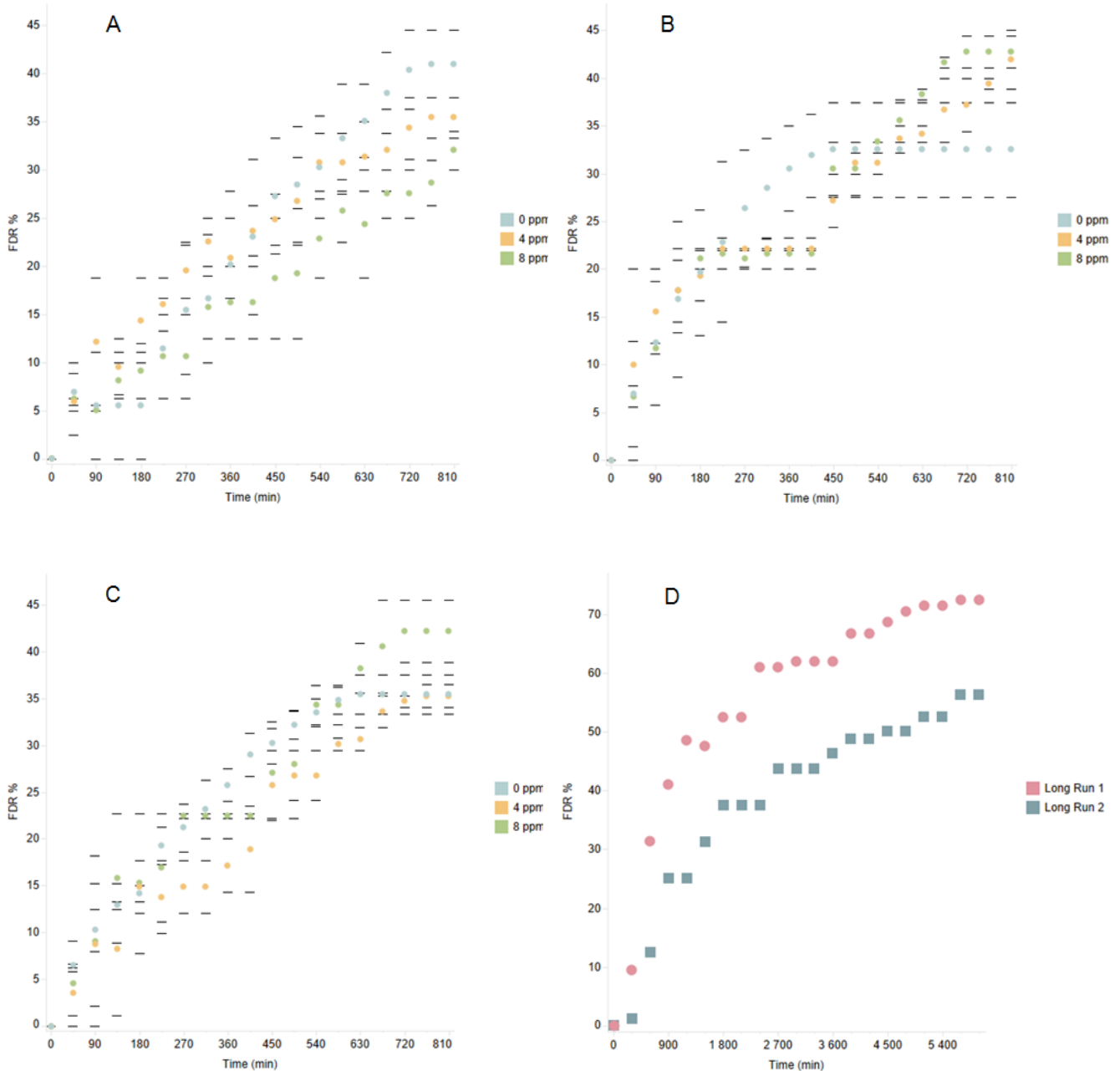
#### 4.2.2 Flux Decline Ratio

Figure 4-15 depicted the Flux Decline Ratio (FDR) of the membranes at varying antiscalant dosages. FDR is another key indicator of fouling of the membrane surface. The lower the FDR, the higher the flux due to less fouling of the membrane surface (Shafi et al., 2017).



**Figure 4-15: Flux decline Ratio at the end of the experiment**

From the graphs in Figure 4-16, it was observed that there are no significant differences for the first few minutes of operation, however, over a time period the difference is more noticeable. The average FDR percentage for each condition was as follows: 22.37% (13.2 mL, 0 ppm); 22.44% (13.2 mL, 4 ppm); 17.09% (13.2 mL, 8 ppm); 24.74% (19.8 mL, 0 ppm); 20.72% (19.8 mL, 4 ppm); 25.28% (19.8 mL, 8 ppm); 25.72% (26.4 mL, 0 ppm); 25.56% (26.4 mL, 4 ppm); 26.5% (26.4 mL, 8 ppm); 54.78% (Long run 1) and 38.09% (Long run 2).



**Figure 4-16: Flux Decline Ratio over time of membranes- A: 13.2 mL Laundry detergent; B: 19.8 mL Laundry detergent; C: 26.4 mL Laundry detergent & D: Long Runs**

From graph A and D (13.2 mL Laundry detergent concentration and Long Runs respectively), significantly lower values of FDR were observed for the case of 8ppm antiscalant dosage, thus revealing that the membrane resisted the scaling phenomenon better than the membranes with 0 and 4 ppm antiscalant dosages. It can be concluded that the 8ppm concentration antiscalant doing performed better against the surfactant dosing. This striking difference of performances of resistance to fouling and permeate flux decline were directly linked to the varying antiscalant dosing.

### 4.2.3 Salt rejection & Surfactant and COD removal

As explained by Baker (2012), the higher salt rejections and relatively lower flux decline is because of the higher feed pressure that allowed more passage of solvent (water) through the membranes, leaving behind more solute (salts), which resulted in an increase of salt rejection. This phenomenon is also determined by the membrane pore size and Donnan exclusion effects.

Figure 4-17 showed the percentage salt rejection trend observed during the RO fouling test. where the salt rejection is significantly high. However, it was observed that membranes with no antiscalant addition performed slightly better than membranes with antiscalant dosing. At equimolar amounts of antiscalant and scale-forming ions, the anti-scalants can act as a chelating agents. Antiscalant could also produce soluble complex molecules with particular metal ions, inactivating the ions so that they cannot react with other elements or ions to produce precipitates or scale (Antony et al., 2011).

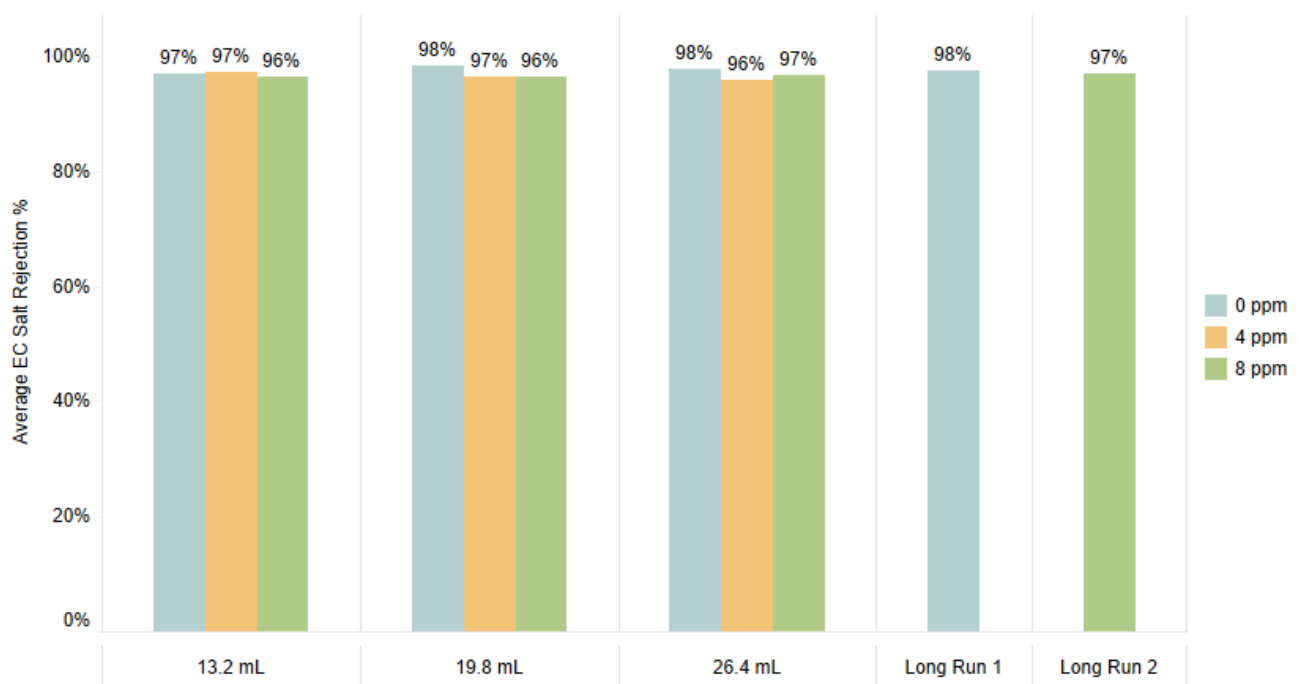
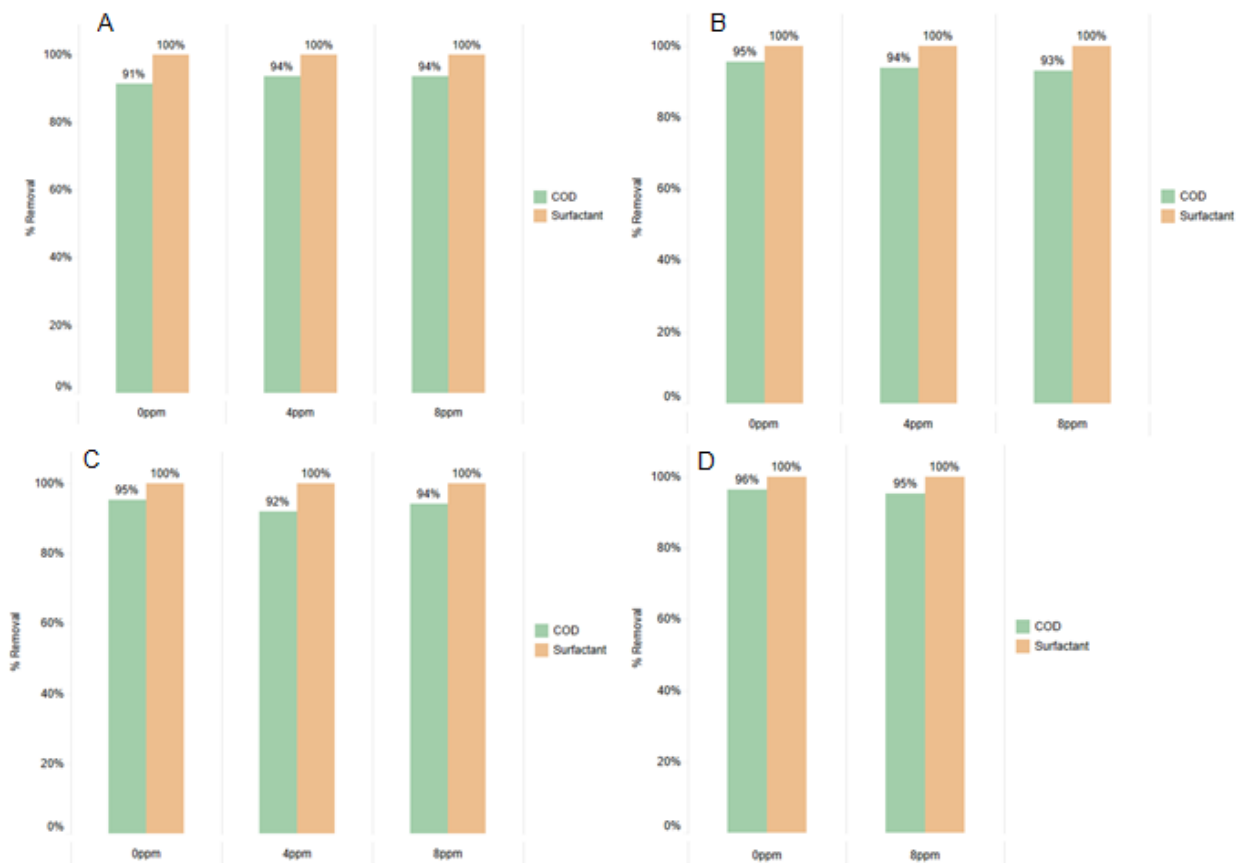


Figure 4-17: Average EC Salt Rejection for all experiments

Antony et al. (2011) also go on to explain that a good antiscalant should retain the initial flux, extend the product recovery, and produce a salt rejection curve that does not involve a significant decline in salt rejection over time. It is important to mention that fouling of membranes by organic molecules or microbes is a serious impediment of membranes-based filtration processes.



**Figure 4-18: COD and Surfactant removal percentages at varying dosages of anti-scalant- A: 13.2 mL Laundry Detergent; B: 19.8 mL Laundry Detergent; C: 26.4 mL Laundry Detergent & D: Long Runs**

To clarify the fouling phenomena of RO membranes, it was necessary to quantify the amount of surfactant before and after treatment. Quantities of surfactants adsorbed on the RO membrane surface or in the bulk, during the RO process has been reported in previous approaches (Baudequin et al., 2014a; Boussu et al., 2007; Hinke et al., 1988). According to the concentration polarisation (CP) theory, the concentration of SDS in the vicinity of the RO membrane surface is much higher than that of the feed solution during filtration which is confirmed with work by Mai et al. (2016).

In a surfactant-membrane system, the actions of surfactants at the membrane surface depends on several chemical and physical factors, including feed fluid composition (e.g. surfactant structure, concentration, pH, ionic strength, temperature), membrane properties

(e.g. chemical composition inducing charge and hydrophobicity, roughness), and hydrodynamic conditions as explained by Mai et al. (2016). These authors go on to explain that active layers made of aromatic thin-film polyamide or cellulose esters; which most RO and NF membranes; have a global negative charge at pH above 5.

From Figure 4-18, the surfactant rejection exceeded 99.8% in almost all the experimental runs over the various range of feed concentrations. The high rejection of anionic surfactant was also found in a previous study during a RO process by Baudequin et al. (2014) and can be explained by two rejection mechanisms for organic molecules: electrostatic repulsion and size exclusion.

However, a small percentage of surfactant was analytically found in the permeate, indicating that some surfactant molecules were still able to pass through the RO membrane. An equilibrium between surfactants in solution and on the RO membrane occurs through hydrophobic interactions, and adsorbed surfactant molecules can undergo chain folding, by which they penetrated the active polyamide layer of the membrane, and subsequently diffuse or are adsorbed in the active layer and in the support layer. This is reported in a previous study with perfluoro-octane sulfonates (PFOS) (Tang et al., 2006).

Another indication of membrane performance was the removal of COD before and after filtration. From the COD removal shown in Figure 4-18, a similar trend was observed when compared to the average electro conductivity (EC) calculating the salt rejection in Figure 4-16. The removal was significantly high. Though it was observed that membranes with no antiscalant addition performed slightly better than membranes with antiscalant dosing.



### **4.3 Development of Permeate Flux Decline Model**

Design-Expert 11 software was used to analyse the measured response of permeate flux. The significance test for the regression models and the significance test of individual model coefficients were determined by the same statistical software package, ANOVA, for all responses. The resulting ANOVA shown in Table 4-1 for the Flux Cubic model outlines the analysis of variance for this response and shows the significant model terms affecting the flux decline. This table also demonstrated additional adequacy measures, for example,  $R^2$  and adjusted  $R^2$ . The  $R^2$  value indicates the degree of fit and is defined as the ratio of the explained variation to the total variation. It was suggested that a good model fit should be for a  $R^2$  of at least 0.8. In this study the adjusted  $R^2$  was found to be 0.8617 as shown in Table 4-1, suggesting that this Cubic model was a good fit for these data. The model was significant as indicated by the very low probability value of less than 0.05. A p-value that is lower than 0.05 suggested that the model is statistically significant at the 5% level of significance.

**Table 4-1: ANOVA Response for Cubic model**

**Response 1: Flux**

Source	Sum of Squares	df	Mean Square	F-value	p-value	
Model	2364.03	16	147.75	21.64	< 0.0001	Significant
A-Time	400.04	1	400.04	58.60	< 0.0001	
B-Laundry	9.28	1	9.28	1.36	0.2510	
Detergent Amount						
C-Anti-Scalant	167.62	1	167.62	24.55	< 0.0001	
Concentration						
AB	2.54	1	2.54	0.3723	0.5455	
AC	16.72	1	16.72	2.45	0.1261	
BC	3.82	1	3.82	0.5601	0.4589	
A <sup>2</sup>	28.81	1	28.81	4.22	0.0471	
B <sup>2</sup>	4.73	1	4.73	0.6933	0.4104	
C <sup>2</sup>	25.69	1	25.69	3.76	0.0601	
ABC	18.94	1	18.94	2.77	0.1042	
A <sup>2</sup> B	1.07	1	1.07	0.1565	0.6947	
A <sup>2</sup> C	18.57	1	18.57	2.72	0.1075	
AB <sup>2</sup>	0.2652	1	0.2652	0.0389	0.8448	
AC <sup>2</sup>	0.2652	1	0.2652	0.0389	0.8448	
B <sup>2</sup> C	18.54	1	18.54	2.72	0.1078	
BC <sup>2</sup>	62.53	1	62.53	9.16	0.0045	
A <sup>3</sup>	0.0000	0				
B <sup>3</sup>	0.0000	0				
C <sup>3</sup>	0.0000	0				
Residual	252.60	37	6.83			
Lack of Fit	34.46	10	3.45	0.4266	0.9208	Not significant
Pure Error	218.14	27	8.08			
Cor Total	2616.63	53				
Source	Sequential p-value	Lack of Fit p-value	Adjusted R <sup>2</sup>	Predicted R <sup>2</sup>		
Cubic	0.0321	0.9208	0.8617	0.7896		

A represents the Time, B represents the Laundry Detergent Amount, and C represents the Anti-scalant dosage. The final model in terms of coded factors are represented in Equation 4.1

$$\text{Flux} = 30.63 - 7.45 A + 1.14 B + 4.83 C - 0.3254 AB - 0.8346 AC + 0.3992 BC + 1.55A^2 - 0.6281B^2 - 1.46 C^2 - 1.09 ABC + 0.3654A^2B - 1.52 A^2C + 0.1821AB^2 + 0.1821AC^2 - 1.52B^2C - 2.80BC^2 + 0.0000A^3 + 0.0000B^3 + 0.0000C^3 \quad \dots\text{Equation 4-1}$$

The coded equation (Equation 4-1) was useful for identifying the relative impact of the factors by comparing the factor coefficients. This equation should not be used to determine

the relative impact of each factor because the coefficients were scaled to accommodate the units of each factor and the intercept was not at the centre of the design space.

### 4.3.1 Permeate Flux Decline Model Validation

Model validation was important to obtain an adequate model. The permeate flux model validation was evaluated by plotting a normal probability (%) against the externally studentised residuals as shown in Figure 4-19. It can be observed the relationship between normal probability and externally studentised residuals fits fairly well linearly. The linear fit means that no response transform was necessary and that there was no specious problem with the normality of the data.

Design-Expert® Software

Flux

Color points by value of Flux:

21.78  47.91

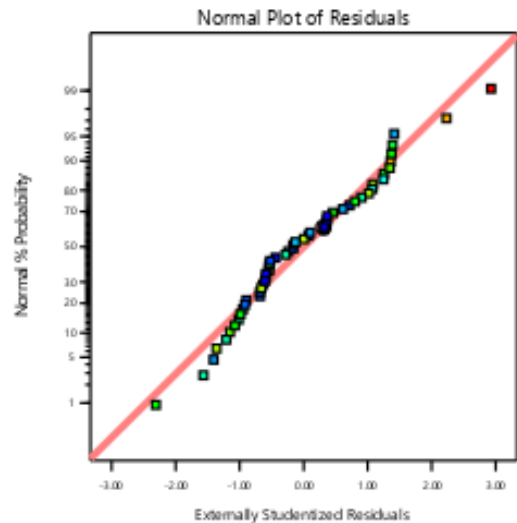


Figure 4-19: Normal plot of residuals for flux model

The validation of the permeate flux model was evaluated by the relationship between the actual and the predicted values as shown in Figure 4-20. This figure indicates that the developed model was adequate for the prediction of flux since the predicted values were relatively close to the observed experimental flux values.

Design-Expert® Software

Flux

Color points by value of Flux:

21.78  47.91

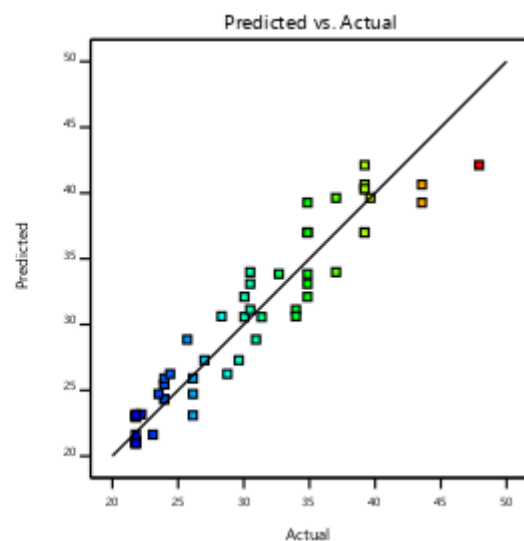


Figure 4-20: Predicted values vs Actual values

### 4.3.2 Effect of process parameters on Permeate Flux Decline

The permeate flux decline during filtration via reverse osmosis membrane of laundry wastewater was directly related to the process parameters investigated, either as a main or as a part of an interaction effect. The reason for predicting the permeate flux was to develop a model, to aid in the selection of an appropriate range for process optimisation.

The primary factor affecting COD removal most, appears to be the time of operation. The model indicated that if the time decreases with 1 coded unit, the flux decreases with 5 units, which in this case was permeate flux decline. Anti-scalant dosage and amount of laundry detergent also played a significant role in permeate flux decline. When the laundry detergent amount (concentration) was changed by 1 coded unit the flux was increased slightly. When the antiscalant dosage was changed by 1 coded unit then the flux was increased by approximately 4 units. Figure 4-21 showed a perturbation plot highlighting the effect of Time, laundry detergent amount and antiscalant dosage on permeate flux decline. Comparisons of the effect of factors could be made at a certain point in the design space using a perturbation plot. It does however not show the effect of interactions of the factors.

Design-Expert® Software  
Factor Coding: Actual

Flux (L/hr.m<sup>2</sup>)

Actual Factors

A: Time = 405  
B: Laundry Detergent Amount = 19.8  
C: Anti-Scalant Concentration = 4.08

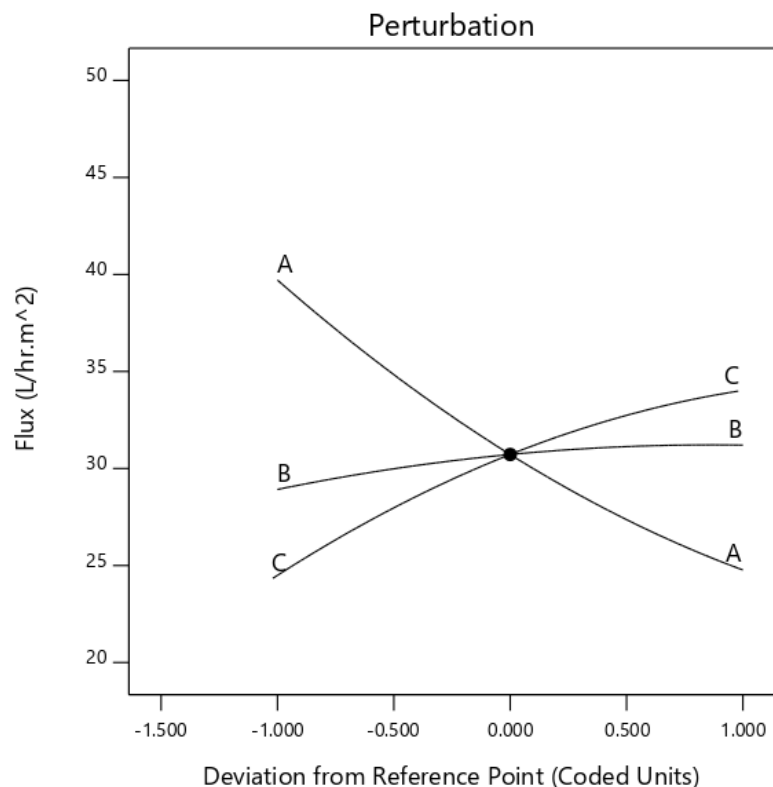


Figure 4-21: Perturbation graph of factor interaction

Figure 4-21 showed the interaction of laundry detergent amount, antiscalant dosage and time as well as its effects on permeate flux decline, within the design space. A 2-D contour and 3-D surface plot is shown in Figure 4-23 and Figure 4-24, respectively. These plots showed the influence of increasing time as well as the effects of changes in laundry

detergent amount and antiscalant dosage. Figure 4-24 showed that an increase in time beyond 270 minutes' resulted in significant permeate flux decline depending on the antiscalant dosage. However, the Laundry detergent amount had minimal impact on flux with antiscalant addition. The experimental results verified these indications. The model thus successfully described the permeate flux decline of laundry wastewater using RO membrane within the design space of the model.

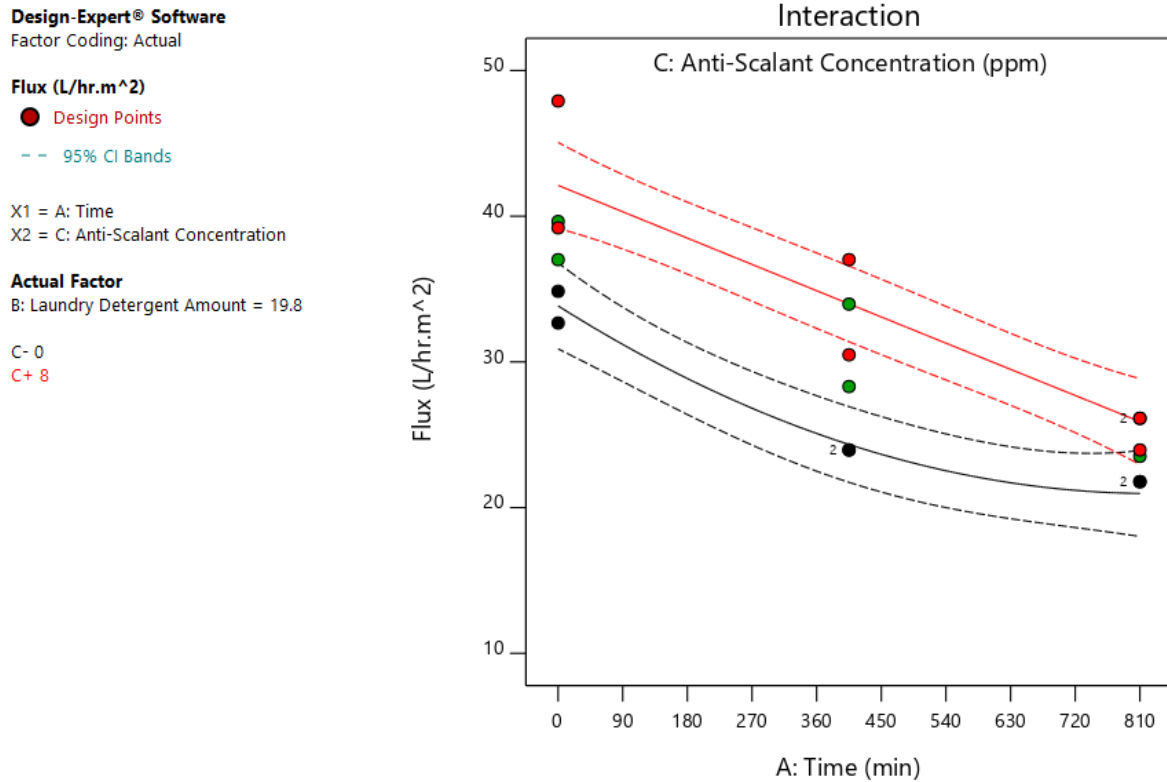



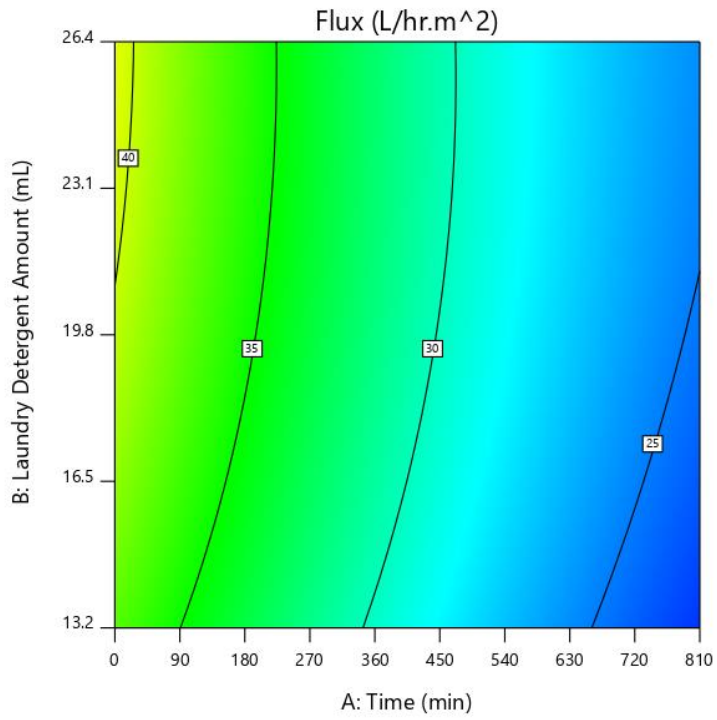
Figure 4-22: Interaction graph between the different factors and permeate flux decline

Design-Expert® Software  
Factor Coding: Actual

Flux (L/hr.m<sup>2</sup>)  
21.78  47.91

X1 = A: Time  
X2 = B: Laundry Detergent Amount

Actual Factor  
C: Anti-Scalant Concentration = 4.08

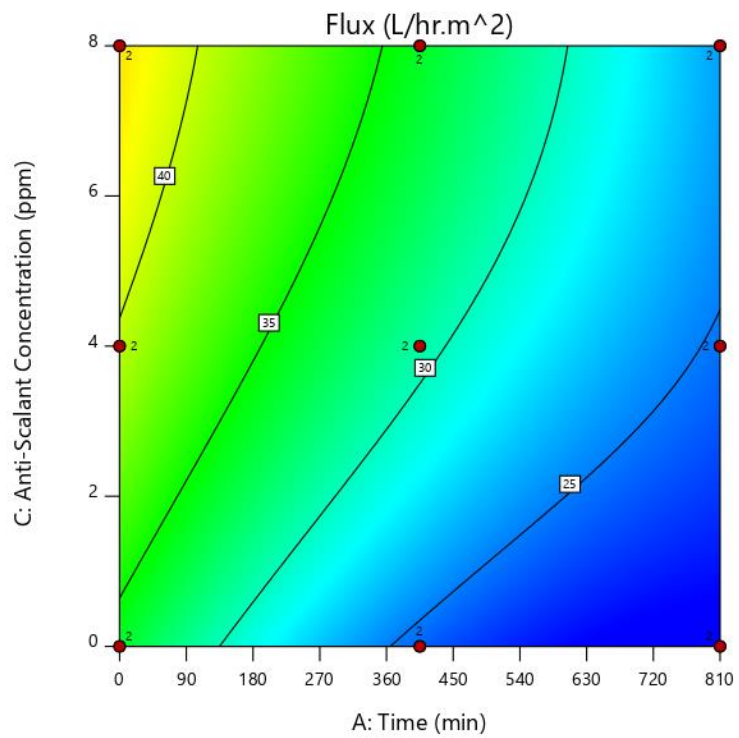


Design-Expert® Software  
Factor Coding: Actual

Flux (L/hr.m<sup>2</sup>)  
 Design Points  
21.78  47.91

X1 = A: Time  
X2 = C: Anti-Scalant Concentration

Actual Factor  
B: Laundry Detergent Amount = 19.8



Design-Expert® Software  
Factor Coding: Actual

Flux (L/hr.m<sup>2</sup>)  
21.78 47.91

X1 = B: Laundry Detergent Amount  
X2 = C: Anti-Scalant Concentration

Actual Factor  
A: Time = 396.9

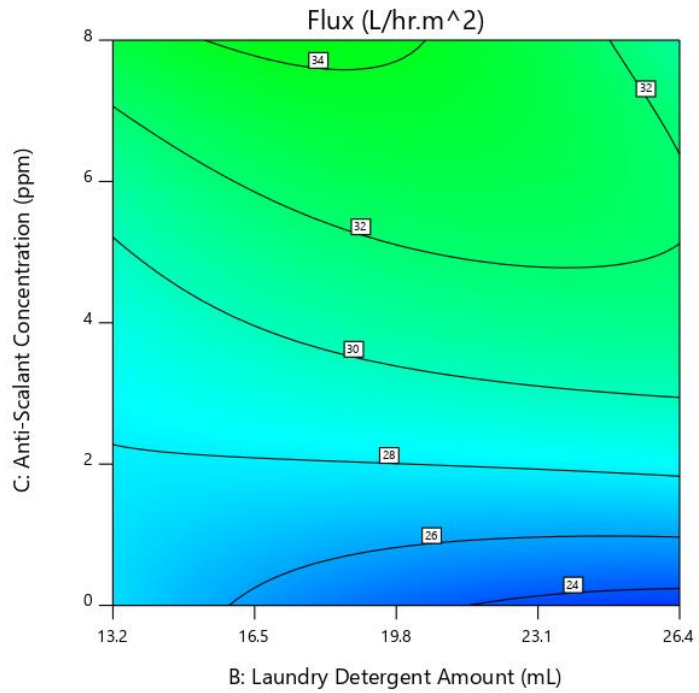


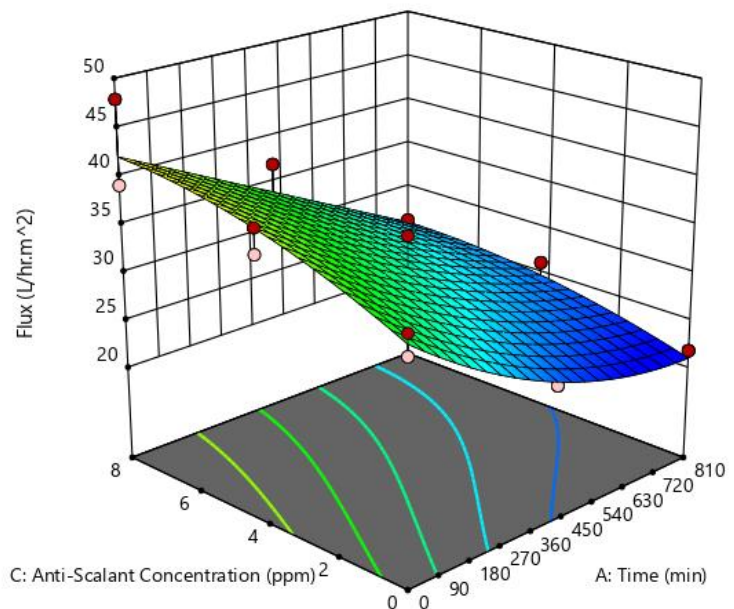
Figure 4-23: 2D contour plots showing the influence of increasing time as well as the effects of changes in laundry detergent amount and anti-scalant dosage

Design-Expert® Software  
Factor Coding: Actual

Flux (L/hr.m<sup>2</sup>)  
● Design points above predicted value  
○ Design points below predicted value  
21.78 47.91


X1 = A: Time  
X2 = C: Anti-Scalant Concentration

Actual Factor  
B: Laundry Detergent Amount = 19.8



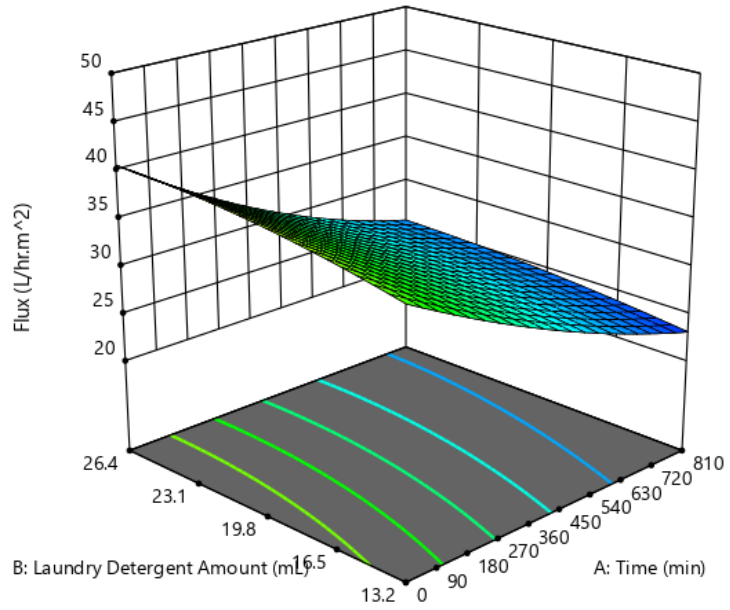


Design-Expert® Software  
Factor Coding: Actual




Flux (L/hr.m<sup>2</sup>)  
21.78  47.91

X1 = A: Time  
X2 = B: Laundry Detergent Amount

Actual Factor  
C: Anti-Scalant Concentration = 4.08



Design-Expert® Software  
Factor Coding: Actual

Flux (L/hr.m<sup>2</sup>)  
 Design points above predicted value  
 Design points below predicted value  
21.78  47.91

X1 = B: Laundry Detergent Amount  
X2 = C: Anti-Scalant Concentration

Actual Factor  
A: Time = 405

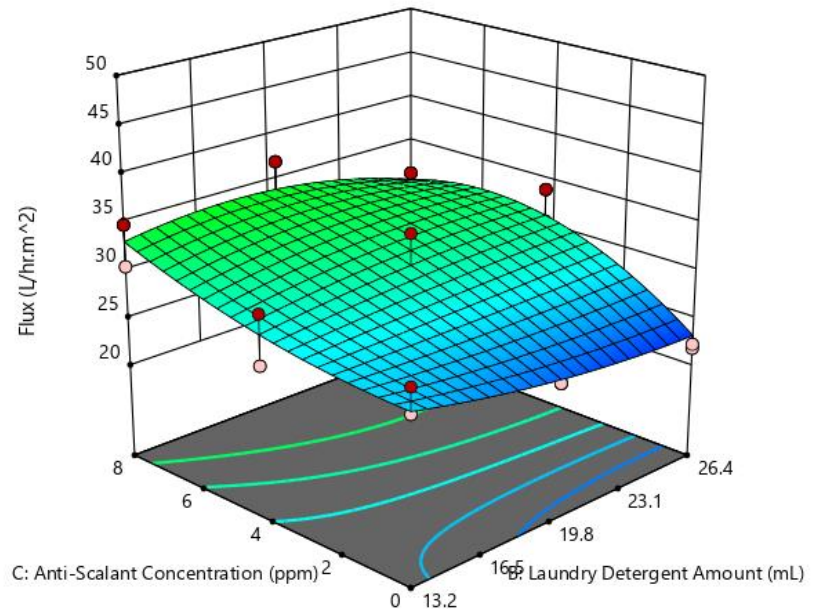


Figure 4-24: 3D contour plots showing the influence of increasing time as well as the effects of changes in laundry detergent amount and anti-scalant dosage

# **CHAPTER 5**

## **Conclusion and Recommendations**

## 5 Conclusion and Recommendations

### 5.1 Conclusion

The decrease in membrane performance over extended periods in the treatment of wastewater is a major problem which is caused by fouling. Fouling mechanisms are related to membrane surface characteristics and the interaction between the membrane surface and wastewater constituents.

The removal of anionic surfactants and COD in laundry wastewater by low pressure, extra low energy RO membranes municipal discharge and possible reuse application were investigated. The effects of laundry detergent concentration on the permeate flux and rejection characteristics of the membrane were examined. Removal efficiencies for LAS and COD concentrations were measured to quantify membrane performances.

The effect of using a commercial anti-scalant to minimise scaling and improve membrane performance was also evaluated. Detailed selected quantitative analysis of fouling were investigated on membrane surface characteristics using Scanning Electron Microscopy (SEM); Attenuated Total Reflection-Fourier Transform Infrared Spectroscopy (ATR-FTIR) and Energy Dispersive X-Ray Spectroscopy (EDX), before and after antiscalant addition.

During the ATR-FTIR analysis, all the characteristic peaks of a virgin XLE PA TFC membrane can be seen in its clean state. It was observed that more foulant was deposited onto the surface with lower or no antiscalant dosage compared to the higher antiscalant dosed membranes.

A morphological change of the membranes surface was observed using SEM analysis. It was evident that the correct dosing of antiscalant significantly disrupted and hindered the foulant adhesion on the surface. This hindered attachment of scalant on the surface resulted in a much lower flux decline rate when compared to membranes with no antiscalant addition. EDX revealed that the amount of carbon decreased with an increase in laundry detergent concentration. This was due to the carbonyl group present in the PA layer being masked by the foulant layer.

The average FDR percentage for each condition was as followed: 22.37% (13.2 mL, 0 ppm); 22.44% (13.2 mL, 4 ppm); 17.09% (13.2 mL, 8 ppm); 24.74% (19.8 mL, 0 ppm); 20.72% (19.8 mL, 4 ppm); 25.28% (19.8 mL, 8 ppm); 25.72% (26.4 mL, 0 ppm); 25.56% (26.4 mL, 4 ppm); 26.5% (26.4 mL, 8 ppm); 54.78% (Long run 1) and 38.09% (Long run 2). The flux decline could be associated with the fouling phenomenon caused by the accumulation of anionic surfactant molecules on the membrane surface, where the build-up of a concentration polarisation layer and the entrapment in the polyamide layer.

Surfactant rejection exceeded 99.8% in almost all the experimental runs over a range of varied feed concentrations. The integrity of the RO membrane was upheld throughout all the

experimental runs indicated by the overall salt rejection for a bench-scale unit, with a consistent EC removal between 97-98%, as stipulated by the manufacturers. An average COD removal throughout was between 91-96%, respectively. It must be noted that the COD removal during the membranes with no anti-scalant addition performed slightly better than membranes with anti-scalant dosing.

Using Design Expert 11, it was observed the predictive model successfully described the permeate flux decline of laundry wastewater using RO membrane within the design space of the model. It can be confirmed that the membrane performance with model laundry wastewater improved when using commercial antiscalant.

Finally, anionic surfactant and COD removal using the RO bench-scale unit at the predetermined process variables were successful for municipal discharge and potential future reuse application.

## **5.2 Recommendations**

Future studies should investigate a direct measurement and analysis on the fouling layer formed during the filtration of the effluent to acquire a characteristics of the layer composition using AFM and XPS to assist with remediation action. Commercial and model laundry wastewater feed should be compared to assist in design solutions for possible scale-up to pilot plant level. Lastly a cost and feasibility study for possible full-scale implementation.

# References

## References

- Advanced Water Technology Center. 2015. Membrane Characterization and Autopsy and Water Quality Analysis : Analytical Capabilities and Techniques.
- Al-Amoudi, A. & Lovitt, R.W. 2007. Fouling strategies and the cleaning system of NF membranes and factors affecting cleaning efficiency. *Journal of Membrane Science*, 303(1–2): 4–28.
- Al-Juboori, R.A. & Yusaf, T. 2012. Biofouling in RO system: Mechanisms, monitoring and controlling. *Desalination*, 302: 1–23. <http://dx.doi.org/10.1016/j.desal.2012.06.016>.
- Andersen, M., Kristensen, G.H., Brynjolf, M. & Grüttner, H. 2002. Pilot-scale testing membrane bioreactor for wastewater reclamation in industrial laundry. *Water science and technology*, 46(4–5): 67–76.
- Antony, A., How, J., Gray, S., Childress, A.E., Le-clech, P. & Leslie, G. 2011. Scale formation and control in high pressure membrane water treatment systems : A review. *Journal of Membrane Science*, 383(1–2): 1–16. <http://dx.doi.org/10.1016/j.memsci.2011.08.054>.
- Arkhangelsky, E., Wicaksana, F., Tang, C., Al-Rabiah, A.A., Al-Zahrani, S.M. & Wang, R. 2012. Combined organic-inorganic fouling of forward osmosis hollow fiber membranes. *Water Research*, 46(19): 6329–6338. <http://dx.doi.org/10.1016/j.watres.2012.09.003>.
- Asadollahi, M., Bastani, D. & Musavi, S.A. 2017. Enhancement of surface properties and performance of reverse osmosis membranes after surface modification : A review. *Desalination*, 420(June): 330–383. <http://dx.doi.org/10.1016/j.desal.2017.05.027>.
- Ashfaq, M.Y., Wang, T., Qiblawey, H., Reesh, I.A. & Judd, S. 2017. Recycling of hospital laundry wastewater using membrane technology. , 60: 5004.
- Aziz, M. & Kasongo, G. 2019. Scaling prevention of thin film composite polyamide Reverse Osmosis membranes by Zn ions. *Desalination*, 464(April): 76–83. <https://doi.org/10.1016/j.desal.2019.04.021>.
- Baker, R.W. 2012. *Membrane Technology and Applications 3rd Edition*. John Wiley and Sons Ltd.
- Baudequin, C., Mai, Z., Rakib, M., Deguerry, I., Severac, R., Pabon, M. & Couallier, E. 2014a.

- Removal of fluorinated surfactants by reverse osmosis – Role of surfactants in membrane fouling. *Journal of Membrane Science*, 458: 111–119. <http://dx.doi.org/10.1016/j.memsci.2014.01.063>.
- Baudequin, C., Mai, Z., Rakib, M., Deguerry, I., Severac, R., Pabon, M. & Couallier, E. 2014b. Removal of fluorinated surfactants by reverse osmosis--role of surfactants in membrane fouling. *Journal of membrane science*, 458: 111–119.
- Berk, Z. 2018. *Food process engineering and technology*. Academic Press.
- Bhattacharyya, D., Jumawan, A.B., Grieves, R.B. & Witherup, S.O. 1978. Ultrafiltration of Complex Wastewaters: Recycling for Nonpotable Use. *Journal (Water Pollution Control Federation)*, 50(5): 846–861. <http://www.jstor.org/stable/25039649>.
- Boddu, V.M., Paul, T., Page, M.A., Byl, C., Ward, L. & Ruan, J. 2016. Gray water recycle: Effect of pretreatment technologies on low pressure reverse osmosis treatment. *Journal of Environmental Chemical Engineering*, 4(4): 4435–4443. <http://dx.doi.org/10.1016/j.jece.2016.09.031>.
- Boussu, K., Kindts, C., Vandecasteele, C. & der Bruggen, B. 2007. Surfactant fouling of nanofiltration membranes: measurements and mechanisms. *ChemPhysChem*, 8(12): 1836–1845.
- Braga, J.K. & Varesche, M.B. a. 2014. Commercial Laundry Water Characterisation. *American Journal of Analytical Chemistry*, (January): 8–16.
- Carley, A.F. & Morgan, D.J. 2016. Surface analysis: X-ray photoelectron spectroscopy.
- Cho, J., Amy, G., Pellegrino, J. & Yoon, Y. 1998. Characterization of clean and natural organic matter (NOM) fouled NF and UF membranes, and foulants characterization. *Desalination*, 118(1–3): 101–108.
- Ciabattia, I., Cesaro, F., Faralli, L., Fatarella, E. & Tognotti, F. 2009. Demonstration of a treatment system for purification and reuse of laundry wastewater. *Desalination*, 245(1–3): 451–459.
- Coates, J. 2006. Interpretation of infrared spectra, a practical approach. *Encyclopedia of analytical chemistry: applications, theory and instrumentation*.



- Creber, S.A., Vrouwenvelder, J.S., van Loosdrecht, M.C.M. & Johns, M.L. 2010. Chemical cleaning of biofouling in reverse osmosis membranes evaluated using magnetic resonance imaging. *Journal of Membrane Science*, 362(1–2): 202–210. <http://dx.doi.org/10.1016/j.memsci.2010.06.052>.
- Ding, S., Yang, Y., Li, C., Huang, H. & Hou, L.A. 2016. The effects of organic fouling on the removal of radionuclides by reverse osmosis membranes. *Water Research*, 95: 174–184. <http://dx.doi.org/10.1016/j.watres.2016.03.028>.
- Donnenfeld, Z., Crookes, C. & Hedden, S. 2018. A delicate balance Water scarcity in South Africa. , (March).
- Elimelech, M., Zhu, X., Childress, A.E. & Hong, S. 1997. Rapid communication Role of membrane surface morphology in colloidal fouling of cellulose acetate and composite aromatic polyamide reverse osmosis membranes. , 127: 101–109.
- Forstmeier, M., Goers, B. & Wozny, G. 2005. Water network optimisation in the process industry d case study of a liquid detergent plant. , 13: 495–498.
- Friedrich, H. & Pinnekamp, J. 2003. *Membrane Technology for Waste Water Treatment*. Germany: Ministry for Environment and Nature Conservation, Agriculture and Consumer Protection of the federal state North Rhine- Westphalia.
- Gabelich, C.J., Williams, M.D., Rahardianto, A., Franklin, J.C. & Cohen, Y. 2007. High-recovery reverse osmosis desalination using intermediate chemical demineralization. *Journal of Membrane Science*, 301(1–2): 131–141.
- Gao, W., She, F., Zhang, J., Dumée, L.F., He, L., Hodgson, P.D. & Kong, L. 2015. Understanding water and ion transport behaviour and permeability through poly(amide) thin film composite membrane. *Journal of Membrane Science*, 487: 32–39.
- Geankoplis, C.J. 1993. Transport Processes and Unit Operations. *Prentice-Hall International*: 1–937. <http://books.google.com/books?id=i9-TQgAACAAJ&pgis=1>.
- Giagnorio, M., Amelio, A., Grüttner, H. & Tiraferri, A. 2017. Environmental impacts of detergents and benefits of their recovery in the laundering industry. *Journal of Cleaner Production*, 154: 593–601. <http://dx.doi.org/10.1016/j.jclepro.2017.04.012>.
- Goldstein, J.I., Newbury, D.E., Michael, J.R., Ritchie, N.W.M., Scott, J.H.J. & Joy, D.C. 2017.

*Scanning electron microscopy and X-ray microanalysis*. Springer.

- Gorzalski, A.S. & Coronell, O. 2014. Fouling of nanofiltration membranes in full- and bench-scale systems treating groundwater containing silica. *Journal of Membrane Science*, 468: 349–359. <http://dx.doi.org/10.1016/j.memsci.2014.06.013>.
- Green, M., Semiap, R. & Dosoretz, C. 2004. Low strength graywater characterization and treatment by direct membrane filtration. , 170: 241–250.
- Greenlee, L.F., Lawler, D.F., Freeman, B.D., Marrot, B. & Moulin, P. 2009. Reverse osmosis desalination: Water sources, technology, and today's challenges. *Water Research*, 43(9): 2317–2348. <http://dx.doi.org/10.1016/j.watres.2009.03.010>.
- Griffiths, P.R. & De Haseth, J.A. 2007. *Fourier transform infrared spectrometry*. John Wiley & Sons.
- Guilbaud, J., Massé, A., Andrs, Y., Combe, F. & Jaouen, P. 2010. Laundry water recycling in ship by direct nanofiltration with tubular membranes. *Resources, Conservation and Recycling*, 55(2): 148–154.
- Guppy, L. & Anderson, K. 2017. Global Water Crisis : the Facts. : 1–3. <http://inweh.unu.edu>.
- Hakizimana, J.N., Gourich, B., Vial, C., Drogui, P., Oumani, A., Naja, J. & Hilali, L. 2016. Assessment of hardness, microorganism and organic matter removal from seawater by electrocoagulation as a pretreatment of desalination by reverse osmosis. *Desalination*, 393: 90–101. <http://dx.doi.org/10.1016/j.desal.2015.12.025>.
- Henthorne, L. & Boysen, B. 2015. State-of-the-art of reverse osmosis desalination pretreatment. *Desalination*, 356: 129–139. <http://dx.doi.org/10.1016/j.desal.2014.10.039>.
- Hinke, E., Laslop, D. & Staude, E. 1988. The influence of charged surfactants upon reverse osmosis. In *Dispersed Systems*. Springer: 94–99.
- Hirose, M., Ito, H. & Kamiyama, Y. 1996. Effect of skin layer surface structures on the flux behaviour of RO membranes. *Journal of Membrane Science*, 121(2): 209–215.
- Hu, Y., Lu, K., Yan, F., Shi, Y., Yu, P., Yu, S., Li, S. & Gao, C. 2016. Enhancing the performance of aromatic polyamide reverse osmosis membrane by surface modification via covalent attachment of polyvinyl alcohol (PVA). *Journal of Membrane Science*, 501: 209–

219. <http://dx.doi.org/10.1016/j.memsci.2015.12.003>.
- Janknecht, P. & Melo, L.F. 2003. Online biofilm monitoring. *Reviews in Environmental Science and Biotechnology*, 2(2–4): 269–283.
- Johnson, D.J., Al Malek, S.A., Al-Rashdi, B.A.M. & Hilal, N. 2012. Atomic force microscopy of nanofiltration membranes: effect of imaging mode and environment. *Journal of membrane science*, 389: 486–498.
- Johnson, D.J., Oatley-Radcliffe, D.L. & Hilal, N. 2018. State of the art review on membrane surface characterisation: Visualisation, verification and quantification of membrane properties. *Desalination*, 434: 12–36.
- Judd, S. 2010. *The MBR book: principles and applications of membrane bioreactors for water and wastewater treatment*. Elsevier.
- Kasongo, G., Steenberg, C., Morris, B., Kapenda, G., Jacobs, N. & Aziz, M. 2019. Surface grafting of polyvinyl alcohol (PVA) cross-linked with glutaraldehyde (GA) to improve resistance to fouling of aromatic polyamide thin film composite reverse osmosis membranes using municipal membrane bioreactor effluent. *Water Practice & Technology*, 14(3): 614–624.
- Khayet, M. 2016. Fouling and Scaling in Desalination. *Desalination*, 393: 1. <http://dx.doi.org/10.1016/j.desal.2016.05.005>.
- Kucera, J. 2011. *Reverse Osmosis: Industrial applications and processes*. Wiley.
- Kucera, J. 2015. *Reverse Osmosis: Industrial Processes and Applications*.
- Lee, S. & Lee, C.H. 2000. Effect of operating conditions on CaSO<sub>4</sub> scale formation mechanism in nanofiltration for water softening. *Water Research*, 34(15): 3854–3866.
- Lenntech. 2015. Avista - PDS - Vitec - 3000. : 1.
- Lenntech. FILMTEC™ XLE-4040 Membranes.
- Li, F., Wichmann, K. & Otterpohl, R. 2009. Review of the technological approaches for grey water treatment and reuses. *Science of the Total Environment*, 407(11): 3439–3449. <http://dx.doi.org/10.1016/j.scitotenv.2009.02.004>.

- Lin, T., Shen, B., Chen, W. & Zhang, X.B. 2014. Interaction mechanisms associated with organic colloid fouling of ultrafiltration membrane in a drinking water treatment system. *Desalination*, 332(1): 100–108. <http://dx.doi.org/10.1016/j.desal.2013.11.001>.
- Liu, S., Lim, M., Fabris, R., Chow, C., Chiang, K., Drikas, M. & Amal, R. 2008. Removal of humic acid using TiO<sub>2</sub> photocatalytic process - Fractionation and molecular weight characterisation studies. *Chemosphere*, 72(2): 263–271.
- Mai, Z., Butin, V., Rakib, M., Zhu, H., Rabiller-baudry, M. & Couallier, E. 2016. Influence of bulk concentration on the organisation of molecules at a membrane surface and flux decline during reverse osmosis of an anionic surfactant. *Journal of Membrane Science*, 499: 257–268. <http://dx.doi.org/10.1016/j.memsci.2015.10.012>.
- Malaeb, L. & Ayoub, G.M. 2011. Reverse osmosis technology for water treatment: State of the art review. *Desalination*, 267(1): 1–8. <http://dx.doi.org/10.1016/j.desal.2010.09.001>.
- Al Malek, S.A., Seman, M.N.A., Johnson, D. & Hilal, N. 2012. Formation and characterization of polyethersulfone membranes using different concentrations of polyvinylpyrrolidone. *Desalination*, 288: 31–39.
- Manouchehri, M. & Kargari, A. 2017. Water recovery from laundry wastewater by the cross flow microfiltration process: A strategy for water recycling in residential buildings. *Journal of Cleaner Production*, 168: 227–238. <http://dx.doi.org/10.1016/j.jclepro.2017.08.211>.
- Matin, A., Rahman, F., Shafi, H.Z. & Zubair, S.M. 2019. Scaling of reverse osmosis membranes used in water desalination: Phenomena, impact, and control; future directions. *Desalination*, 455(December 2018): 135–157.
- Matin, A., Shafi, H.Z., Khan, Z., Khaled, M., Yang, R., Gleason, K. & Rehman, F. 2014. Surface modification of seawater desalination reverse osmosis membranes: characterization studies & performance evaluation. *Desalination*, 343: 128–139.
- McFall, C.W., Christofides, P.D., Cohen, Y. & Davis, J.F. 2007. Fault-tolerant control of a reverse osmosis desalination process. *IFAC Proceedings Volumes*, 40(5): 161–166.
- Mohammed, S.A., Abbas, A.D. & Sabri, L.S. 2014. Effect of Operating Conditions on Reverse Osmosis ( RO ) Membrane Performance Effect of Operating Conditions on Reverse Osmosis ( RO ) Membrane Performance. *Journal of Engineering*, 20(12): 61–70.

- Myburgh, D.P., Aziz, M., Roman, F., Jardim, J. & Chakawa, S. 2019. Removal of COD from Industrial Biodiesel Wastewater Using an Integrated Process: Electrochemical-Oxidation with IrO<sub>2</sub>-Ta<sub>2</sub>O<sub>5</sub>/Ti Anodes and Chitosan Powder as an Adsorbent. *Environmental Processes*, 6(4): 819–840.
- Nascimento, C.O.C., Veit, T., Pal, S.M. & Gonçalves, G.C. 2019. Combined Application of Coagulation / Flocculation / Sedimentation and Membrane Separation for the Treatment of Laundry Wastewater. , 2019.
- Puretec. *Basics of Reverse Osmosis*.
- Qasim, M., Badrelzaman, M., Darwish, N.N. & Darwish, N.A. 2019. Reverse osmosis desalination : A state-of-the-art review. , 459(March): 59–104.
- Qiu, C., Nguyen, Q.T. & Ping, Z. 2007. Surface modification of cardo polyetherketone ultrafiltration membrane by photo-grafted copolymers to obtain nanofiltration membranes. *Journal of membrane science*, 295(1–2): 88–94.
- Ramcharan, T. & Bissessur, A. 2017. Electrocoagulative and Biological Treatment of Laundry Wastewater. *Biological Wastewater Treatment and Resource Recovery*. <http://www.intechopen.com/books/global-warming-impacts-and-future-perspectives/alternative-resources-for-renewable-energy-piezoelectric-and-photovoltaic-smart-structures%0Ahttp://www.intechopen.com/books/biological-wastewater-treatment-and-resource-recove>.
- Roh, I.J. 2002. Influence of rupture strength of interfacially polymerized thin-film structure on the performance of polyamide composite membranes. *Journal of membrane science*, 198(1): 63–74.
- Saqib, J. & Aljundi, I.H. 2016. Membrane fouling and modification using surface treatment and layer-by-layer assembly of polyelectrolytes: State-of-the-art review. *Journal of Water Process Engineering*, 11: 68–87. <http://dx.doi.org/10.1016/j.jwpe.2016.03.009>.
- Serafim, L.S., Lemos, P.C., Levantesi, C., Tandoi, V., Santos, H. & Reis, M.A.M. 2002. Methods for detection and visualization of intracellular polymers stored by polyphosphate-accumulating microorganisms. *Journal of Microbiological Methods*, 51(1): 1–18.
- Shafi, H.Z., Matin, A., Akhtar, S., Gleason, K.K., Zubair, S.M. & Khan, Z. 2017. Organic fouling

- in surface modified reverse osmosis membranes: Filtration studies and subsequent morphological and compositional characterization. *Journal of Membrane Science*, 527(January): 152–163.
- She, Q., Wang, R., Fane, A.G. & Tang, C.Y. 2016. Membrane fouling in osmotically driven membrane processes: A review. *Journal of Membrane Science*, 499: 201–233. <http://dx.doi.org/10.1016/j.memsci.2015.10.040>.
- Shirazi, S., Lin, C.J. & Chen, D. 2010. Inorganic fouling of pressure-driven membrane processes - A critical review. *Desalination*, 250(1): 236–248. <http://dx.doi.org/10.1016/j.desal.2009.02.056>.
- Singh, R.P., Gupta, N., Singh, S., Singh, A., Suman, R. & Annie, K. 2002. Toxicity of ionic and nonionic surfactants to six macrobes found in agra, India. *Bulletin of Environmental Contamination and Toxicology*, 69(2): 265–270.
- Smith, B.C. 2011. *Fundamentals of Fourier transform infrared spectroscopy*. CRC press.
- Socrates, G. 1980. *"Infrared Characteristic Group Frequencies"*. Chichester: Wiley-Interscience.
- Šostar-Turk, S., Petrinić, I. & Simonič, M. 2005. Laundry wastewater treatment using coagulation and membrane filtration. *Resources, Conservation and Recycling*, 44(2): 185–196.
- Sterlite Corporation. 2015. SEPA CF Cell Assembly and Operation Manual. : 24.
- Sumisha, A., Arthanareeswaran, G., Thuyavan, Y.L., Ismail, A.F. & Chakraborty, S. 2015. Treatment of laundry wastewater using polyethersulfone / polyvinylpyrrolidone ultra filtration membranes. *Ecotoxicology and Environmental Safety*, 121: 174–179. <http://dx.doi.org/10.1016/j.ecoenv.2015.04.004>.
- Tang, C.Y., Chong, T.H. & Fane, A.G. 2011. Colloidal interactions and fouling of NF and RO membranes: A review. *Advances in Colloid and Interface Science*, 164(1–2): 126–143. <http://dx.doi.org/10.1016/j.cis.2010.10.007>.
- Tang, C.Y., Fu, Q.S., Robertson, A.P., Criddle, C.S. & Leckie, J.O. 2006. Use of reverse osmosis membranes to remove perfluorooctane sulfonate (PFOS) from semiconductor wastewater. *Environmental science & technology*, 40(23): 7343–7349.

- Tang, C.Y., Kwon, Y.N. & Leckie, J.O. 2009. Effect of membrane chemistry and coating layer on physiochemical properties of thin film composite polyamide RO and NF membranes. I. FTIR and XPS characterization of polyamide and coating layer chemistry. *Desalination*, 242(1–3): 149–167.
- Tang, C.Y., Kwon, Y.N. & Leckie, J.O. 2007. Probing the nano- and micro-scales of reverse osmosis membranes-A comprehensive characterization of physiochemical properties of uncoated and coated membranes by XPS, TEM, ATR-FTIR, and streaming potential measurements. *Journal of Membrane Science*, 287(1): 146–156.
- Teixeira, M.R. & Sousa, V.S. 2013. Fouling of nanofiltration membrane: Effects of NOM molecular weight and microcystins. *Desalination*, 315: 149–155. <http://dx.doi.org/10.1016/j.desal.2012.03.012>.
- Town, R.M., Tercier, M. Lou, Parthasarathy, N., Bujard, F., Rodak, S., Bernard, C. & Buffle, J. 1995. A versatile macro- to micro-size stationary mercury drop electrode. *Analytica Chimica Acta*, 302(1): 1–8.
- Uchymiak, M., Bartman, A.R., Daltrophe, N., Weissman, M., Gilron, J., Christofides, P.D., Kaiser, W.J. & Cohen, Y. 2009. Brackish water reverse osmosis (BWRO) operation in feed flow reversal mode using an ex situ scale observation detector (EXSOD). *Journal of Membrane Science*, 341(1–2): 60–66.
- UNESCO. 2003. 2003 Unesco Water For people.pdf.
- Water Environment Federation. Membrane Systems for Wastewater Treatment. : 241–250.
- Welz, P.J. & Muanda, C. 2018. *NATSURV 8: Water and wastewater management in the laundry industry*.
- Wu, B. 2019. Science of the Total Environment Membrane-based technology in greywater reclamation: A review. *Science of the Total Environment*, 656: 184–200. <https://doi.org/10.1016/j.scitotenv.2018.11.347>.
- Zhang, Q., Zhang, C., Xu, J., Nie, Y., Li, S. & Zhang, S. 2016. Effect of poly(vinyl alcohol) coating process conditions on the properties and performance of polyamide reverse osmosis membranes. *Desalination*, 379: 42–52. <http://dx.doi.org/10.1016/j.desal.2015.10.012>.

Zhou, W., Apkarian, R., Wang, Z.L. & Joy, D. 2006. Fundamentals of scanning electron microscopy (SEM). In *Scanning microscopy for nanotechnology*. Springer: 1–40.

Zhu, X.Z., Zhang, F., Li, W.W., Li, J., Li, L.L., Yu, H.Q., Huang, M.S. & Huang, T.Y. 2016. Insights into enhanced current generation of an osmotic microbial fuel cell under membrane fouling condition. *Journal of Membrane Science*, 504: 40–46. <http://dx.doi.org/10.1016/j.memsci.2015.12.050>.



# Appendices

# Appendix A

Data from batch experiments

**RO cell experimental runs with 13.2 mL Laundry Detergent and  
variable anti-scalant dosage concentration  
(0, 4, and 8 ppm)**

## **Appendix A.1**

Data from batch experiments

**RO cell experimental runs with 13.2 mL Laundry Detergent and 0  
ppm anti-scalant**

Kinetic data for the RO cell experimental runs with 13.2 mL Laundry Detergent and 0 ppm anti-scalant, measuring operation parameters in the feed, brine and permeate.

Below in Table A.1-1 the operating conditions is illustrated for the RO process and included are the membrane specification:

**Table A.1-1: Membrane specification and initial operating conditions of experimental run.**

Dimensions	14.5 cm x 9.5 cm
Active Area	0.013775 m <sup>2</sup>
Nomination	XLE-4040
Feed Pressure:	10 bar
Piston Pressure:	14 bar
Feed flow rate:	0.56 L/hr
Brine Pressure:	10 bar

**Table A.1-2: Experimental run**

Time (min)	Feed			Brine		Permeate						
	EC F (µS)	TDS F (g/L)	Temperature F (°C)	EC (µS)	TDS (g/L)	EC P (µS)	TDS P (g/L)	Temperature (°C)	Time (min)	Volume (L)	Flow Rate (l/h)	Flux (L/h m <sup>2</sup> )
0	231,2	0,1717	18,5	236,5	0,173	2,7	0,002	19	0	0,009	0,54	39,20145191
45	237,8	0,1739	19,1	241,7	0,1755	2,1	0,0015	18,9	45	0,0082	0,492	35,7168784
90	244,2	0,1776	19,4	240,3	0,1736	2,7	0,002	19,2	90	0,008	0,48	34,84573503
135	242,6	0,1785	19,8	253,7	0,1819	1,9	0,0021	19,2	135	0,008	0,48	34,84573503
180	254,9	0,183	20	258,4	0,184	1,8	0,0014	19	180	0,008	0,48	34,84573503
225	258,8	0,1855	20,1	262,3	0,1814	1,8	0,0013	19,2	225	0,0075	0,45	32,66787659
270	263,2	0,1879	20,2	257,8	0,184	1,7	0,0012	19	270	0,007	0,42	30,49001815
315	267,2	0,1913	20,2	269,7	0,1925	2	0,0015	18,8	315	0,0069	0,414	30,05444646
360	270,1	0,1932	20,2	274,8	0,1959	2,2	0,0016	19,2	360	0,0065	0,39	28,31215971
405	274,3	0,1968	20,1	277,2	0,1981	2,4	0,0018	18,5	405	0,0062	0,372	27,00544465
450	277,8	0,1996	20,1	280,5	0,2011	2,4	0,0018	18,4	450	0,006	0,36	26,13430127
495	281,6	0,2023	20	283,2	0,2036	2,3	0,0017	18,3	495	0,0059	0,354	25,69872958
540	283,6	0,2044	19,9	286,4	0,2061	2,1	0,0016	18	540	0,0058	0,348	25,26315789
585	287,1	0,2074	19,7	289,5	0,209	2,2	0,0017	17,9	585	0,0055	0,33	23,95644283
630	289,6	0,2102	19,5	291	0,211	2	0,0015	17,9	630	0,0055	0,33	23,95644283
675	292	0,2125	19,4	293,4	0,2135	4,6	0,0035	17,6	675	0,0052	0,312	22,64972777
720	293,9	0,2152	19,2	295,8	0,2164	2,3	0,0017	17,2	720	0,005	0,3	21,77858439
765	295,5	0,2175	19	297,5	0,2187	1,5	0,0012	17	765	0,005	0,3	21,77858439
810	298,2	0,2202	18,8	300,4	0,2215	1,2	0,0009	16,9	810	0,005	0,3	21,77858439

**Table A.1-3: Experimental run duplicate**

Time (min)	Feed			Brine		Permeate						
	EC F (µS)	TDS F (g/L)	Temperature F (°C)	EC (µS)	TDS (g/L)	EC P (µS)	TDS P (g/L)	Temperature (°C)	Time (min)	Volume (L)	Flow Rate (l/h)	Flux (L/h m <sup>2</sup> )
0	236,3	0,1735	18,9	238,4	0,1736	11,2	0,0082	18,9	0	0,008	0,48	34,84573503
45	239,9	0,1749	19,3	242,3	0,1758	11,6	0,0085	19,3	45	0,0076	0,456	33,10344828
90	244,3	0,1766	19,7	246,9	0,1775	9,5	0,0071	19,3	90	0,008	0,48	34,84573503
135	249,2	0,1789	20	243,3	0,1742	14,1	0,0103	19,4	135	0,008	0,48	34,84573503
180	253,7	0,1811	20,3	255	0,1814	15	0,0107	19,7	180	0,008	0,48	34,84573503
225	258,9	0,1831	20,6	260,2	0,1843	17	0,0123	19,7	225	0,0075	0,45	32,66787659
270	264	0,1866	20,7	266,8	0,1887	15,4	0,0111	19,9	270	0,0073	0,438	31,79673321
315	267,2	0,1885	20,8	270,2	0,1909	16	0,0116	19,8	315	0,0072	0,432	31,36116152
360	271,7	0,192	20,9	273,6	0,1931	15,8	0,0114	19,8	360	0,007	0,42	30,49001815
405	274,3	0,1947	20,9	277,9	0,1956	15,5	0,0111	19,8	405	0,0068	0,408	29,61887477
450	279,9	0,1972	20,9	282	0,1988	15,6	0,0112	19,8	450	0,0063	0,378	27,44101633
495	284,8	0,2009	21	287,2	0,2023	15,3	0,0109	19,7	495	0,0062	0,372	27,00544465
540	289,5	0,2039	21	291,6	0,2055	16,4	0,0114	19,7	540	0,006	0,36	26,13430127
585	294,4	0,2072	21	296,7	0,2082	16,1	0,0116	19,7	585	0,0058	0,348	25,26315789
630	297,6	0,2095	21	300,8	0,2121	17,2	0,0125	19,7	630	0,0055	0,33	23,95644283
675	302,2	0,2135	21	304,7	0,2145	15,8	0,0113	19,6	675	0,0053	0,318	23,08529946
720	306,2	0,2155	20,9	308,5	0,2177	14,4	0,0104	19,4	720	0,0051	0,306	22,21415608
765	309,8	0,219	20,8	311,9	0,2205	15,2	0,0109	19,4	765	0,005	0,3	21,77858439
810	312,8	0,2216	20,8	315,3	0,223	16,2	0,0117	19,1	810	0,005	0,3	21,77858439

## Data analysis report on the two ranges of data of unmodified membranes

Data analysis using Microsoft Excel was performed to assess the significance of data of an experimental run and the 'duplicate run' has a significant difference or not.

### F-Test Two-Sample for Variances

	<i>Variable</i> 1	<i>Variable</i> 2
Mean	28,79358	28,47263
Variance	23,41799	30,46547
Observations	19	19
df	18	18
F	0,768673	
P(F<=f) one-tail	0,291289	
F Critical one-tail	0,45102	

### t-Test: Two-Sample Assuming Unequal Variances

	<i>Variable</i> 1	<i>Variable</i> 2
Mean	28,79358	28,47263
Variance	23,41799	30,46547
Observations	19	19
Hypothesized Mean Difference	0	
df	35	
t Stat	0,190583	
P(T<=t) one-tail	0,424977	
t Critical one-tail	1,689572	
P(T<=t) two-tail	0,849954	
t Critical two-tail	2,030108	

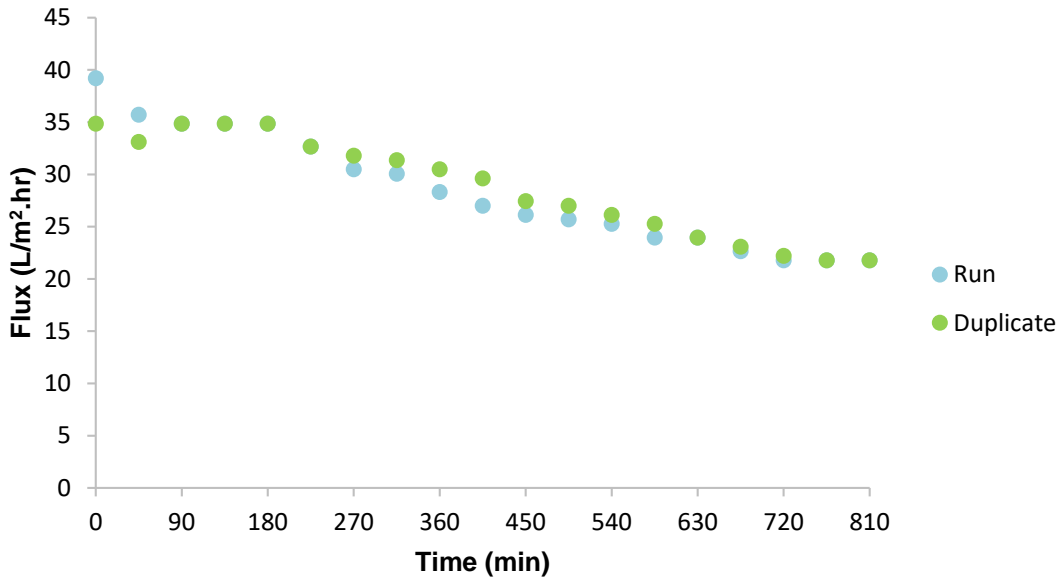


Figure A.1-1: Permeate flux decline of experimental run and duplication

Table A.1-4: Average experimental flux and FDR

Experimental Run 1			Average	Experimental Run 2		
Time (min)	Flux (L/m <sup>2</sup> .hr)	FDR (%)	Flux (L/m <sup>2</sup> .hr)	Time (min)	Flux (L/m <sup>2</sup> .hr)	FDR (%)
0	39.20	0.00	37.02	0	34.85	0.00
45	35.72	8.89	34.41	45	33.10	5.00
90	34.85	11.11	34.85	90	34.85	0.00
135	34.85	11.11	34.85	135	34.85	0.00
180	34.85	11.11	34.85	180	34.85	0.00
225	32.67	16.67	32.67	225	32.67	6.25
270	30.49	22.22	31.14	270	31.80	8.75
315	30.05	23.33	30.71	315	31.36	10.00
360	28.31	27.78	29.40	360	30.49	12.50
405	27.01	31.11	28.31	405	29.62	15.00
450	26.13	33.33	26.79	450	27.44	21.25
495	25.70	34.44	26.35	495	27.01	22.50
540	25.26	35.56	25.70	540	26.13	25.00
585	23.96	38.89	24.61	585	25.26	27.50
630	23.96	38.89	23.96	630	23.96	31.25
675	22.65	42.22	22.87	675	23.09	33.75
720	21.78	44.44	22.00	720	22.21	36.25
765	21.78	44.44	21.78	765	21.78	37.50
810	21.78	44.44	21.78	810	21.78	37.50



## **Appendix A.2**

Data from batch experiments

**RO cell experimental runs with 13.2 mL Laundry Detergent and 4 ppm  
anti-scalant**

Kinetic data for the RO cell experimental runs with 13.2 mL Laundry Detergent and 4 ppm anti-scalant, measuring operation parameters in the feed, brine and permeate.

Below in Table A.2-1 the operating conditions is illustrated for the RO process and included are the membrane specification:

**Table A.2-1: Membrane specification and initial operating conditions of experimental run.**

Dimensions	14.5 cm x 9.5 cm
Active Area	0.013775 m <sup>2</sup>
Nomination	XLE-4040
Feed Pressure:	10 bar
Piston Pressure:	14 bar
Feed flow rate:	0.56 L/hr
Brine Pressure:	10 bar

**Table A.2-2: Experimental run**

Time (min)	Feed			Brine		Permeate						
	EC F (µS)	TDS F (g/L)	Temperature F (°C)	EC (µS)	TDS (g/L)	EC P (µS)	TDS P (g/L)	Temperature (°C)	Time (min)	Volume (L)	Flow Rate (l/h)	Flux (L/h m <sup>2</sup> )
0	238.1	0.1782	18.1	242.2	0.1791	11.3	0.0083	18.8	0	0.008	0.48	34.84573503
45	244.6	0.1805	18.8	248.2	0.1817	10.3	0.0074	18.8	45	0.0075	0.45	32.66787659
90	251.4	0.1837	19.2	255	0.1848	10.1	0.0075	19.2	90	0.0065	0.39	28.31215971
135	257.1	0.1867	19.7	261.7	0.1879	14	0.0102	19.4	135	0.007	0.42	30.49001815
180	264.2	0.1908	19.9	266.4	0.1907	10.8	0.0078	19.3	180	0.0065	0.39	28.31215971
225	270.5	0.1939	20.2	273.3	0.1949	11.2	0.008	19.5	225	0.0065	0.39	28.31215971
270	276.6	0.1972	20.4	277.8	0.1977	10.7	0.0078	19.5	270	0.0062	0.372	27.00544465
315	282.5	0.2011	20.5	284.1	0.2016	10.5	0.0076	19.3	315	0.006	0.36	26.13430127
360	287.2	0.2041	20.6	289	0.205	11.3	0.0083	19.2	360	0.006	0.36	26.13430127
405	292.2	0.2078	20.6	294.4	0.2095	13.6	0.0099	19.1	405	0.0059	0.354	25.69872958
450	298.6	0.2119	20.6	299.3	0.2123	12.1	0.0089	19	450	0.0058	0.348	25.26315789
495	302.2	0.2152	20.6	304	0.216	12.7	0.0093	18.9	495	0.0055	0.33	23.95644283
540	307.3	0.2188	20.5	309.9	0.2203	11.8	0.0087	18.8	540	0.0053	0.318	23.08529946
585	311.4	0.2215	20.5	313.6	0.2238	12.9	0.0096	18.6	585	0.0053	0.318	23.08529946
630	316.3	0.2258	20.4	318.8	0.2272	11.8	0.0088	18.8	630	0.0052	0.312	22.64972777
675	323.6	0.2308	20.4	325.4	0.2317	14.8	0.0102	18.7	675	0.0051	0.306	22.21415608
720	326.3	0.2326	20.4	330.8	0.2361	13.7	0.0101	18.7	720	0.005	0.3	21.77858439
765	333.1	0.238	20.4	335.7	0.2397	12.4	0.0092	18.7	765	0.005	0.3	21.77858439
810	338.7	0.2422	20.4	341.3	0.2435	12.2	0.0089	18.6	810	0.005	0.3	21.77858439

**Table A.2-3: Experimental run duplicate**

Time (min)	Feed			Brine		Permeate						
	EC F (µS)	TDS F (g/L)	Temperature F (°C)	EC (µS)	TDS (g/L)	EC P (µS)	TDS P (g/L)	Temperature (°C)	Time (min)	Volume (L)	Flow Rate (l/h)	Flux (L/h m <sup>2</sup> )
0	265.7	0.1785	23.3	268.7	0.1794	4.3	0.0029	23.3	0	0.009	0.54	39.20145191
45	272.3	0.1824	23.7	276.3	0.1835	4.2	0.0028	23.4	45	0.0085	0.51	37.02359347
90	280.7	0.186	24	284.6	0.1878	6	0.004	23.8	90	0.0085	0.51	37.02359347
135	286.3	0.1894	24.2	291.3	0.1919	8	0.0055	23.9	135	0.0084	0.504	36.58802178
180	293.7	0.1932	24.4	298.5	0.1956	7.4	0.005	24.1	180	0.0081	0.486	35.28130672
225	301.4	0.1973	24.6	305.1	0.1989	5.7	0.0037	24.2	225	0.0078	0.468	33.97459165
270	308.6	0.2014	24.8	312.5	0.203	5.6	0.0037	24.4	270	0.0075	0.45	32.66787659
315	315.4	0.2051	25	320.3	0.207	6.5	0.0043	24.3	315	0.0072	0.432	31.36116152
360	325.4	0.2103	25.3	328.4	0.2113	7.3	0.0049	24.4	360	0.0075	0.45	32.66787659
405	331.9	0.2146	25.4	335.9	0.2162	7.4	0.0048	24.3	405	0.0071	0.426	30.92558984
450	339.1	0.219	25.4	343.4	0.2207	8.2	0.0054	24	450	0.007	0.42	30.49001815
495	344.8	0.2228	25.4	350.7	0.2256	8.9	0.0056	24.3	495	0.007	0.42	30.49001815
540	354.3	0.2283	25.5	357.6	0.2304	9.1	0.006	24.3	540	0.0065	0.39	28.31215971
585	361.1	0.233	25.5	366.2	0.2355	6.7	0.0044	24.4	585	0.0065	0.39	28.31215971
630	369.2	0.238	25.5	373.9	0.2406	5.5	0.0037	24.1	630	0.0065	0.39	28.31215971
675	376.9	0.2432	25.5	381.7	0.2455	6.1	0.004	24.2	675	0.0065	0.39	28.31215971
720	384.8	0.2481	25.5	389.8	0.2502	7.1	0.0047	24	720	0.0062	0.372	27.00544465
765	392.6	0.2535	25.4	398.2	0.256	6.3	0.0042	24.1	765	0.006	0.36	26.13430127
810	400.6	0.2589	25.4	406.2	0.2614	5.5	0.0036	23.9	810	0.006	0.36	26.13430127

## Data analysis report on the two ranges of data of unmodified membranes

Data analysis using Microsoft Excel was performed to assess the significance of data of an experimental run and the 'duplicate run' has a significant difference or not.

### F-Test Two-Sample for Variances

	<i>Variable</i> 1	<i>Variable</i> 2
Mean	25.97383	31.59041
Variance	14.4866	16.11312
Observations	19	19
df	18	18
F	0.899057	
P(F<=f) one-tail	0.411937	
F Critical one-tail	0.45102	

### t-Test: Two-Sample Assuming Unequal Variances

	<i>Variable 1</i>	<i>Variable 2</i>
Mean	25.97382749	31.59040978
Variance	14.4866037	16.11311523
Observations	19	19
Hypothesized Mean Difference	0	
df	36	
t Stat	4.425783937	
P(T<=t) one-tail	4.27636E-05	
t Critical one-tail	1.688297694	
P(T<=t) two-tail	8.55271E-05	
t Critical two-tail	2.028093987	

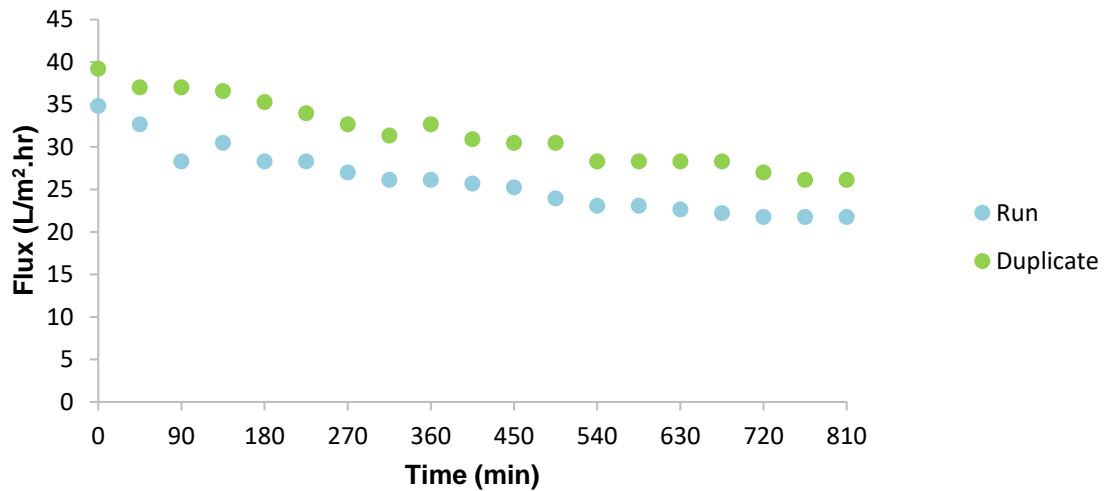


Figure A.2-1: Permeate flux decline of experimental run and duplication

Table A.2-4: Average experimental flux and FDR

Experimental Run 1			Average	Experimental Run 2		
Time (min)	Flux (L/m <sup>2</sup> .hr)	FDR (%)	Flux (L/m <sup>2</sup> .hr)	Time (min)	Flux (L/m <sup>2</sup> .hr)	FDR (%)
0	34.85	0.00	37.02	0	39.20	0.00
45	32.67	6.25	34.85	45	37.02	5.56
90	28.31	18.75	32.67	90	37.02	5.56
135	30.49	12.50	33.54	135	36.59	6.67
180	28.31	18.75	31.80	180	35.28	10.00
225	28.31	18.75	31.14	225	33.97	13.33
270	27.01	22.50	29.84	270	32.67	16.67
315	26.13	25.00	28.75	315	31.36	20.00
360	26.13	25.00	29.40	360	32.67	16.67
405	25.70	26.25	28.31	405	30.93	21.11
450	25.26	27.50	27.88	450	30.49	22.22
495	23.96	31.25	27.22	495	30.49	22.22
540	23.09	33.75	25.70	540	28.31	27.78
585	23.09	33.75	25.70	585	28.31	27.78
630	22.65	35.00	25.48	630	28.31	27.78
675	22.21	36.25	25.26	675	28.31	27.78
720	21.78	37.50	24.39	720	27.01	31.11
765	21.78	37.50	23.96	765	26.13	33.33
810	21.78	37.50	23.96	810	26.13	33.33

## **Appendix A.3**

Data from batch experiments

**RO cell experimental runs with 13.2 mL Laundry Detergent and 8 ppm  
anti-scalant**

Kinetic data for the RO cell experimental runs with 13.2 mL Laundry Detergent and 8 ppm anti-scalant, measuring operation parameters in the feed, brine and permeate.

Below in Table A.3-1 the operating conditions is illustrated for the RO process and included are the membrane specification:

**Table A.3-1: Membrane specification and initial operating conditions of experimental run.**

Dimensions	14.5 cm x 9.5 cm
Active Area	0.013775 m <sup>2</sup>
Nomination	XLE-4040
Feed Pressure:	10 bar
Piston Pressure:	14 bar
Feed flow rate:	0.56 L/hr
Brine Pressure:	10 bar



**Table A.3-2: Experimental run**

Time (min)	Feed			Brine		Permeate					
	EC F (µS)	TDS F (g/L)	Temperature F (°C)	EC (µS)	TDS (g/L)	EC P (µS)	TDS P (g/L)	Temperature (°C)	Volume (L)	Flow Rate (l/h)	Flux (L/h m <sup>2</sup> )
0	285	0.1808	26.3	289.2	0.182	18.5	0.0118	25.9	0.01	0.6	43.55716878
45	293.8	0.1857	26.5	297.6	0.1871	14.4	0.0094	25.9	0.009	0.54	39.20145191
90	301.7	0.1904	26.6	304.1	0.1915	11.4	0.0073	26	0.0095	0.57	41.37931034
135	310.8	0.1954	26.8	314.9	0.1971	10.2	0.0065	26.4	0.009	0.54	39.20145191
180	318.3	0.1999	26.9	323.9	0.2019	11.2	0.007	26.3	0.0088	0.528	38.33030853
225	326.6	0.2046	27	331.8	0.2073	15	0.0095	26.5	0.0085	0.51	37.02359347
270	337.2	0.2106	27.1	339.7	0.2113	15.8	0.0106	26.3	0.0085	0.51	37.02359347
315	346.8	0.2165	27.2	348.9	0.2171	14.7	0.0094	25.9	0.0081	0.486	35.28130672
360	356.1	0.2223	27.1	357.8	0.2231	15.2	0.0097	25.8	0.008	0.48	34.84573503
405	364.5	0.2285	27.1	367.3	0.2293	13.7	0.0088	25.7	0.008	0.48	34.84573503
450	374.4	0.2346	27	377.2	0.2366	15.6	0.01	25.5	0.0075	0.45	32.66787659
495	383.5	0.2408	26.9	385.9	0.2434	14	0.0091	25.3	0.0074	0.444	32.2323049
540	391.2	0.2466	26.8	396.9	0.2495	13.6	0.0087	25.4	0.0073	0.438	31.79673321
585	404.7	0.2545	26.7	407.8	0.2566	13	0.0084	25.5	0.0071	0.426	30.92558984
630	413.8	0.2606	26.7	418.5	0.2636	12.1	0.0078	25.5	0.007	0.42	30.49001815
675	325.4	0.2675	26.8	430	0.2704	12.3	0.0079	25.6	0.007	0.42	30.49001815
720	436.3	0.2741	26.8	442.4	0.2773	11.6	0.0074	25.8	0.007	0.42	30.49001815
765	451.8	0.2832	26.9	455.8	0.2857	12.9	0.0083	25.8	0.0069	0.414	30.05444646
810	461.5	0.2896	27	469	0.2932	11.1	0.0072	25.6	0.0066	0.396	28.7477314

**Table A.3-3: Experimental run duplicate**

Time (min)	Feed			Brine		Permeate					
	EC F (µS)	TDS F (g/L)	Temperature F (°C)	EC (µS)	TDS (g/L)	EC P (µS)	TDS P (g/L)	Temperature (°C)	Volume (L)	Flow Rate (l/h)	Flux (L/h m <sup>2</sup> )
0	259.2	0.1799	21.6	263.6	0.1812	7	0.0049	22	0.008	0.48	34.84573503
45	267.9	0.1843	22.2	273.4	0.1861	9.8	0.0067	22.4	0.0078	0.468	33.97459165
90	276.9	0.1884	22.6	281	0.1898	8.5	0.0058	22.5	0.0076	0.456	33.10344828
135	285.5	0.193	23.1	289.1	0.1946	7.6	0.005	22.8	0.0075	0.45	32.66787659
180	294.6	0.1974	23.3	298.2	0.199	8	0.0054	22.8	0.0075	0.45	32.66787659
225	301.6	0.202	23.5	305.9	0.2033	8.5	0.0058	22.9	0.0075	0.45	32.66787659
270	309.6	0.2068	23.7	313.5	0.2081	11	0.0075	22.7	0.0075	0.45	32.66787659
315	317.8	0.2114	23.8	319.6	0.2121	10.3	0.0073	22.7	0.007	0.42	30.49001815
360	325.9	0.2165	23.9	327.4	0.2167	10.8	0.008	22.7	0.007	0.42	30.49001815
405	332.5	0.2212	23.8	334.2	0.2219	9.6	0.0087	22.5	0.007	0.42	30.49001815
450	340.4	0.2267	23.7	342.3	0.2278	11.7	0.0091	22.4	0.007	0.42	30.49001815
495	347.9	0.2322	23.8	350.7	0.2326	12.1	0.0098	22.6	0.007	0.42	30.49001815
540	356.9	0.2376	23.8	360	0.2397	13.8	0.0104	22.6	0.0065	0.39	28.31215971
585	362.5	0.2423	23.8	368.6	0.245	14.7	0.01	22.5	0.0062	0.372	27.00544465
630	372.8	0.2498	23.8	377.5	0.251	18.3	0.0125	22.6	0.0065	0.39	28.31215971
675	382.7	0.2555	23.7	385.3	0.2567	17.5	0.0119	22.5	0.006	0.36	26.13430127
720	389.2	0.2598	23.7	394.4	0.263	15.8	0.0108	22.4	0.006	0.36	26.13430127
765	394.7	0.2646	23.6	402	0.2686	15	0.0103	22.2	0.0059	0.354	25.69872958
810	402.4	0.2694	23.5	411.3	0.2745	15.5	0.0106	22.2	0.0056	0.336	24.39201452

## Data analysis report on the two ranges of data of unmodified membranes

Data analysis using Microsoft Excel was performed to assess the significance of data of an experimental run and the 'duplicate run' has a significant difference or not.

### F-Test Two-Sample for Variances

	<i>Variable 1</i>	<i>Variable 2</i>
Mean	34.66233642	30.05444646
Variance	18.38867808	9.612616564
Observations	19	19
df	18	18
F	1.912973222	
P(F<=f) one-tail	0.089217934	
F Critical one-tail	2.217197134	

### t-Test: Two-Sample Assuming Unequal Variances

	<i>Variable 1</i>	<i>Variable 2</i>
Mean	34.66233642	30.05444646
Variance	18.38867808	9.612616564
Observations	19	19
Hypothesized Mean Difference	0	
df	33	
t Stat	3.795682207	
P(T<=t) one-tail	0.00029927	
t Critical one-tail	1.692360258	
P(T<=t) two-tail	0.000598539	
t Critical two-tail	2.034515287	

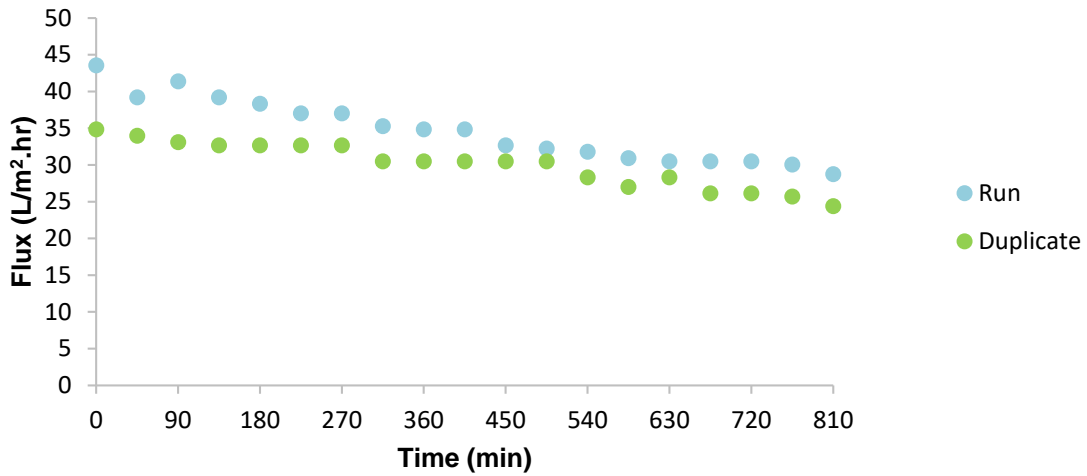


Figure A.3-1: Permeate flux decline of experimental run and duplication

Table A.3-4: Average experimental flux and FDR

Experimental Run 1			Average	Experimental Run 2		
Time (min)	Flux (L/m <sup>2</sup> .hr)	FDR (%)	Flux (L/m <sup>2</sup> .hr)	Time (min)	Flux (L/m <sup>2</sup> .hr)	FDR (%)
0	43.56	0.00	39.20	0	34.85	0.00
45	39.20	10.00	36.59	45	33.97	2.50
90	41.38	5.00	37.24	90	33.10	5.00
135	39.20	10.00	35.93	135	32.67	6.25
180	38.33	12.00	35.50	180	32.67	6.25
225	37.02	15.00	34.85	225	32.67	6.25
270	37.02	15.00	34.85	270	32.67	6.25
315	35.28	19.00	32.89	315	30.49	12.50
360	34.85	20.00	32.67	360	30.49	12.50
405	34.85	20.00	32.67	405	30.49	12.50
450	32.67	25.00	31.58	450	30.49	12.50
495	32.23	26.00	31.36	495	30.49	12.50
540	31.80	27.00	30.05	540	28.31	18.75
585	30.93	29.00	28.97	585	27.01	22.50
630	30.49	30.00	29.40	630	28.31	18.75
675	30.49	30.00	28.31	675	26.13	25.00
720	30.49	30.00	28.31	720	26.13	25.00
765	30.05	31.00	27.88	765	25.70	26.25
810	28.75	34.00	26.57	810	24.39	30.00

# Appendix B

Data from batch experiments

**RO cell experimental runs with 19.8 mL Laundry Detergent and  
variable anti-scalant dosage concentration  
(0, 4, and 8 ppm)**

## **Appendix B.1**

Data from batch experiments

**RO cell experimental runs with 19.8 mL Laundry Detergent and 0 ppm  
anti-scalant**

Kinetic data for the RO cell experimental runs with 19.8 mL Laundry Detergent and 0 ppm anti-scalant, measuring operation parameters in the feed, brine and permeate.

Below in Table B.1-1 the operating conditions is illustrated for the RO process and included are the membrane specification:

**Table B.1-1: Membrane specification and initial operating conditions of experimental run.**

Dimensions	14.5 cm x 9.5 cm
Active Area	0.013775 m <sup>2</sup>
Nomination	XLE-4040
Feed Pressure:	10 bar
Piston Pressure:	14 bar
Feed flow rate:	0.56 L/hr
Brine Pressure:	10 bar

**Table B.1-2: Experimental run**

Time (min)	Feed			Brine		Permeate						
	EC F (μS)	TDS F (g/L)	Temperature F (°C)	EC (μS)	TDS (g/L)	EC P (μS)	TDS P (g/L)	Temperature (°C)	Time (min)	Volume (L)	Flow Rate (l/h)	Flux (L/h m <sup>2</sup> )
0	278.7	0.1965	20.9	268.8	0.1872	10.9	0.0077	21.4	0	0.0075	0.45	32.66787659
45	285.2	0.1986	21.5	289.1	0.1997	10.6	0.0072	21.8	45	0.007	0.42	30.49001815
90	290.2	0.2005	21.9	294.1	0.2011	9	0.006	22	90	0.0069	0.414	30.05444646
135	295.7	0.2026	22.1	299.1	0.2035	7.1	0.0049	22.1	135	0.0065	0.39	28.31215971
180	300.3	0.2048	22.5	301.9	0.2047	8.8	0.0061	22.3	180	0.0065	0.39	28.31215971
225	304.2	0.2063	22.8	307.9	0.2079	7.8	0.0054	22.5	225	0.0062	0.372	27.00544465
270	309.3	0.209	23.1	312.9	0.2105	6.2	0.0041	22.7	270	0.0061	0.366	26.56987296
315	313.8	0.2113	23.3	318.1	0.2133	5.3	0.0036	22.6	315	0.006	0.36	26.13430127
360	314.9	0.2119	23.2	320.5	0.2153	4.9	0.0034	21.9	360	0.0057	0.342	24.82758621
405	318	0.2153	23	323.1	0.218	5.4	0.0037	21.6	405	0.0055	0.33	23.95644283
450	322.4	0.2185	22.8	325.9	0.2211	5.8	0.0039	21.3	450	0.0054	0.324	23.52087114
495	326.1	0.222	22.6	328.7	0.2236	5.2	0.0036	21.1	495	0.0052	0.312	22.64972777
540	328.5	0.2244	22.5	332	0.2267	5.4	0.0038	20.9	540	0.0051	0.306	22.21415608
585	330.9	0.2273	22.3	334.7	0.2293	5	0.0036	20.8	585	0.005	0.3	21.77858439
630	333.9	0.2301	22.2	337	0.2317	5.4	0.0039	20.5	630	0.005	0.3	21.77858439
675	338.4	0.2332	22	341.1	0.2348	5.6	0.004	20.4	675	0.005	0.3	21.77858439
720	342	0.2369	21.8	344.2	0.2381	5.3	0.0039	20.1	720	0.005	0.3	21.77858439
765	344.5	0.239	21.7	346.9	0.2408	4.8	0.0035	19.9	765	0.005	0.3	21.77858439
810	347.4	0.2422	21.5	349.5	0.243	4.5	0.0033	19.8	810	0.005	0.3	21.77858439



**Table B.1-3: Experimental run duplicate**

Time (min)	Feed			Brine		Permeate						
	EC F (µS)	TDS F (g/L)	Temperature F (°C)	EC (µS)	TDS (g/L)	EC P (µS)	TDS P (g/L)	Temperature (°C)	Time (min)	Volume (L)	Flow Rate (l/h)	Flux (L/h m <sup>2</sup> )
0	282.7	0.1964	21.7	282.6	0.1946	2.4	0.0017	21.5	0	0.008	0.48	34.84573503
45	286.6	0.1986	21.9	288.4	0.1991	2.3	0.0016	21.3	45	0.0075	0.45	32.66787659
90	293.6	0.2014	22.3	295.8	0.2023	2.6	0.0018	22	90	0.007	0.42	30.49001815
135	299.9	0.2044	22.6	302.1	0.2051	2.5	0.0017	22	135	0.007	0.42	30.49001815
180	305.1	0.2069	22.9	306.7	0.2076	2.1	0.0015	22	180	0.0068	0.408	29.61887477
225	309.7	0.2093	23.1	311.2	0.2102	2.3	0.0016	22.2	225	0.0063	0.378	27.44101633
270	315.7	0.2123	23.2	318	0.2131	2.7	0.002	22.5	270	0.0061	0.366	26.56987296
315	320.7	0.2145	23.5	324.5	0.2169	3.5	0.0024	22.5	315	0.0059	0.354	25.69872958
360	323.5	0.217	23.6	329	0.2191	4.6	0.0032	22.6	360	0.0058	0.348	25.26315789
405	329.7	0.2195	23.7	332.3	0.2214	4.7	0.0032	22.4	405	0.0055	0.33	23.95644283
450	333.6	0.2225	23.7	338.4	0.2249	4	0.0028	22.4	450	0.0054	0.324	23.52087114
495	336.4	0.2248	23.8	342.7	0.2278	4.1	0.0028	22.4	495	0.0053	0.318	23.08529946
540	343.3	0.229	23.8	346.5	0.2305	3.7	0.0026	22.3	540	0.0052	0.312	22.64972777
585	348.2	0.2318	23.8	351	0.2333	3.8	0.0026	22.3	585	0.0051	0.306	22.21415608
630	351.6	0.2342	23.8	355	0.2358	4.2	0.0028	22.3	630	0.005	0.3	21.77858439
675	355.3	0.2368	23.7	360.5	0.24	4.1	0.0028	22.2	675	0.005	0.3	21.77858439
720	357.4	0.2387	23.6	364.2	0.2424	4.3	0.003	22.1	720	0.005	0.3	21.77858439
765	359.2	0.2406	23.6	369.1	0.246	4.6	0.0032	22	765	0.005	0.3	21.77858439
810	363.5	0.2447	23.5	372.8	0.2492	5.3	0.0037	21.9	810	0.005	0.3	21.77858439

## Data analysis report on the two ranges of data of unmodified membranes

Data analysis using Microsoft Excel was performed to assess the significance of data of an experimental run and the 'duplicate run' has a significant difference or not.

### F-Test Two-Sample for Variances

	<i>Variable 1</i>	<i>Variable 2</i>
Mean	25.12560894	25.65287993
Variance	12.37524528	17.24146599
Observations	19	19
df	18	18
F	0.717760618	
P(F<=f) one-tail	0.244401058	
F Critical one-tail	0.451019887	

### t-Test: Two-Sample Assuming Unequal Variances

	<i>Variable 1</i>	<i>Variable 2</i>
Mean	25.12560894	25.65287993
Variance	12.37524528	17.24146599
Observations	19	19
Hypothesized Mean Difference	0	
df	35	
t Stat	0.422320597	
P(T<=t) one-tail	0.337687095	
t Critical one-tail	1.68957244	
P(T<=t) two-tail	0.67537419	
t Critical two-tail	2.030107915	

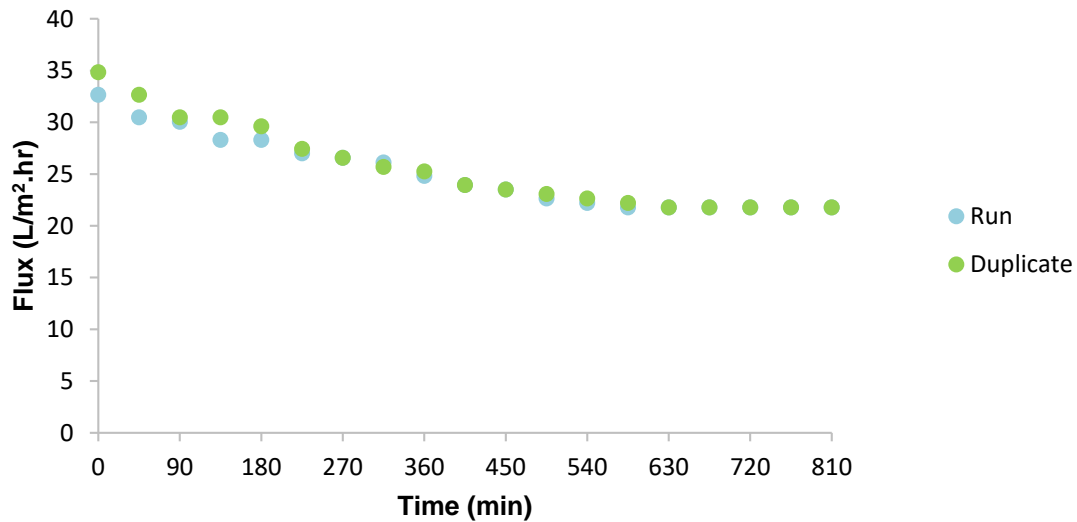


Figure B.1-1: Permeate flux decline of experimental run and duplication

Table B.1-4: Average experimental flux and FDR

Experimental Run 1			Average	Experimental Run 2		
Time (min)	Flux (L/m <sup>2</sup> .hr)	FDR (%)	Flux (L/m <sup>2</sup> .hr)	Time (min)	Flux (L/m <sup>2</sup> .hr)	FDR (%)
0	32.67	0.00	33.76	0	34.85	0.00
45	30.49	6.67	31.58	45	32.67	6.25
90	30.05	8.00	30.27	90	30.49	12.50
135	28.31	13.33	29.40	135	30.49	12.50
180	28.31	13.33	28.97	180	29.62	15.00
225	27.01	17.33	27.22	225	27.44	21.25
270	26.57	18.67	26.57	270	26.57	23.75
315	26.13	20.00	25.92	315	25.70	26.25
360	24.83	24.00	25.05	360	25.26	27.50
405	23.96	26.67	23.96	405	23.96	31.25
450	23.52	28.00	23.52	450	23.52	32.50
495	22.65	30.67	22.87	495	23.09	33.75
540	22.21	32.00	22.43	540	22.65	35.00
585	21.78	33.33	22.00	585	22.21	36.25
630	21.78	33.33	21.78	630	21.78	37.50
675	21.78	33.33	21.78	675	21.78	37.50
720	21.78	33.33	21.78	720	21.78	37.50
765	21.78	33.33	21.78	765	21.78	37.50
810	21.78	33.33	21.78	810	21.78	37.50

## **Appendix B.2**

Data from batch experiments

**RO cell experimental runs with 19.8 mL Laundry Detergent and 4 ppm  
anti-scalant**

Kinetic data for the RO cell experimental runs with 19.8 mL Laundry Detergent and 4 ppm anti-scalant, measuring operation parameters in the feed, brine and permeate.

Below in Table B.2-1 the operating conditions is illustrated for the RO process and included are the membrane specification:

**Table B.2-1: Membrane specification and initial operating conditions of experimental run.**

Dimensions	14.5 cm x 9.5 cm
Active Area	0.013775 m <sup>2</sup>
Nomination	XLE-4040
Feed Pressure:	10 bar
Piston Pressure:	14 bar
Feed flow rate:	0.56 L/hr
Brine Pressure:	10 bar

**Table B.2-2: Experimental run**

Time (min)	Feed			Brine		Permeate					
	EC F (µS)	TDS F (g/L)	Temperature F (°C)	EC (µS)	TDS (g/L)	EC P (µS)	TDS P (g/L)	Temperature (°C)	Volume (L)	Flow Rate (l/h)	Flux (L/h m <sup>2</sup> )
0	289.8	0.1963	22.8	296	0.1997	11.8	0.008	22.7	0.0091	0.546	39.63702359
45	297.1	0.2001	23.2	301.5	0.2015	11.1	0.0075	22.8	0.009	0.54	39.20145191
90	303.3	0.2036	23.4	307.4	0.2056	12.5	0.0085	22.9	0.0089	0.534	38.76588022
135	310.8	0.2079	23.6	314.4	0.2093	12.7	0.0086	23	0.009	0.54	39.20145191
180	317.5	0.2117	23.7	420.6	0.2135	11.8	0.0083	23.9	0.008	0.48	34.84573503
225	326.8	0.2177	23.8	324.5	0.218	14.4	0.0096	23.1	0.0082	0.492	35.7168784
270	334.4	0.2222	23.8	337	0.2232	12.3	0.0086	23.1	0.008	0.48	34.84573503
315	340.7	0.2265	23.9	344.9	0.2277	13.1	0.0089	22.5	0.008	0.48	34.84573503
360	347.8	0.2308	24	350.1	0.2313	13.4	0.0094	22.3	0.0078	0.468	33.97459165
405	354.5	0.2359	23.8	356.7	0.2363	14	0.0096	22.5	0.0078	0.468	33.97459165
450	359.9	0.2405	23.7	365.2	0.2425	11.2	0.0077	22.4	0.0071	0.426	30.92558984
495	368.5	0.2458	23.7	370.8	0.2474	9.5	0.0065	22.2	0.0069	0.414	30.05444646
540	375.5	0.2509	23.6	378	0.2523	10	0.0068	22.2	0.0069	0.414	30.05444646
585	382.4	0.2553	23.5	384.4	0.2582	10.5	0.0072	22.1	0.0063	0.378	27.44101633
630	389.5	0.0261	23.5	393.3	0.2632	10.3	0.0071	22.2	0.0062	0.372	27.00544465
675	397.3	0.2661	23.5	400	0.2673	9.2	0.0063	22.2	0.0062	0.372	27.00544465
720	408.5	0.2726	23.7	411.5	0.2738	8.9	0.0061	22.4	0.006	0.36	26.13430127
765	416.2	0.2774	23.7	419.2	0.279	9.8	0.0066	22.6	0.006	0.36	26.13430127
810	422.6	0.2821	23.7	426.4	0.2839	9.3	0.0063	22.2	0.006	0.36	26.13430127

**Table B.2-3: Experimental run duplicate**

Time (min)	Feed			Brine		Permeate					
	EC F (µS)	TDS F (g/L)	Temperature F (°C)	EC (µS)	TDS (g/L)	EC P (µS)	TDS P (g/L)	Temperature (°C)	Volume (L)	Flow Rate (l/h)	Flux (L/h m <sup>2</sup> )
0	274.8	0.1965	20.2	278.7	0.1977	9	0.0065	20.3	0.0085	0.51	37.02359347
45	281.8	0.1997	20.7	285.4	0.2005	10.8	0.0076	20.7	0.008	0.48	34.84573503
90	287.9	0.2032	21.1	292.7	0.204	11.1	0.0079	21	0.0072	0.432	31.36116152
135	295.9	0.2071	21.4	299.8	0.2081	12.1	0.0082	21	0.0072	0.432	31.36116152
180	302.2	0.2106	21.7	307.4	0.2123	10.3	0.0073	20.9	0.007	0.42	30.49001815
225	310.7	0.2146	21.9	312.7	0.2155	13.2	0.0091	20.9	0.007	0.42	30.49001815
270	316.9	0.2181	22.2	318.5	0.2188	13.5	0.0098	21.2	0.007	0.42	30.49001815
315	323.7	0.2226	22.3	325.9	0.2228	15	0.0106	21.1	0.007	0.42	30.49001815
360	331.1	0.2262	22.5	332.3	0.2269	11.9	0.0109	21.2	0.0068	0.408	29.61887477
405	337.6	0.2304	22.6	339	0.231	11.6	0.0091	21.1	0.0065	0.39	28.31215971
450	344.2	0.2345	22.6	348.5	0.2375	11.1	0.0079	20.8	0.006	0.36	26.13430127
495	350.1	0.2384	22.6	353	0.2401	11.9	0.0084	20.8	0.006	0.36	26.13430127
540	355	0.2422	22.5	357.1	0.2441	11.5	0.0082	20.9	0.006	0.36	26.13430127
585	361.2	0.2465	22.5	365.5	0.2488	11.4	0.0081	20.7	0.006	0.36	26.13430127
630	366.6	0.2507	22.4	368.5	0.2522	13	0.0092	20.6	0.006	0.36	26.13430127
675	372.4	0.2545	22.4	374.2	0.2565	12.4	0.0088	20.6	0.0055	0.33	23.95644283
720	378.1	0.2596	22.3	384.2	0.2609	11.5	0.0083	20.3	0.0055	0.33	23.95644283
765	383.9	0.2639	22.2	386.3	0.2656	11.3	0.0081	20.2	0.0054	0.324	23.52087114
810	389.2	0.268	22.1	391.6	0.2696	11.8	0.0085	20.2	0.0054	0.324	23.52087114

## Data analysis report on the two ranges of data of unmodified membranes

Data analysis using Microsoft Excel was performed to assess the significance of data of an experimental run and the 'duplicate run' has a significant difference or not.

### F-Test Two-Sample for Variances

	<i>Variable 1</i>	<i>Variable 2</i>
Mean	32.41570351	28.42678384
Variance	24.05927864	14.73180087
Observations	19	19
df	18	18
F	1.633152583	
P(F<=f) one-tail	0.153583195	
F Critical one-tail	2.217197134	

### t-Test: Two-Sample Assuming Unequal Variances

	<i>Variable 1</i>	<i>Variable 2</i>
Mean	32.41570351	28.42678384
Variance	24.05927864	14.73180087
Observations	19	19
Hypothesized Mean Difference	0	
df	34	
t Stat	2.79168336	
P(T<=t) one-tail	0.004270726	
t Critical one-tail	1.690924198	
P(T<=t) two-tail	0.008541451	
t Critical two-tail	2.032244498	



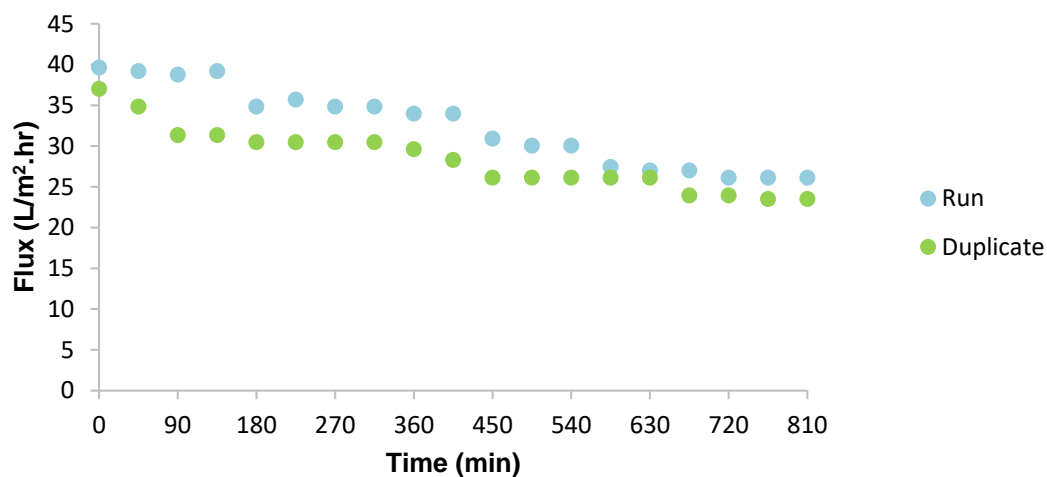


Figure B.2-1: Permeate flux decline of experimental run and duplication

Table B.2-4: Average experimental flux and FDR

Experimental Run 1			Average	Experimental Run 2		
Time (min)	Flux (L/m <sup>2</sup> .hr)	FDR (%)	Flux (L/m <sup>2</sup> .hr)	Time (min)	Flux (L/m <sup>2</sup> .hr)	FDR (%)
0	39.64	0.00	38.33	0	37.02	0.00
45	39.20	1.10	37.02	45	34.85	5.88
90	38.77	2.20	35.06	90	31.36	15.29
135	39.20	1.10	35.28	135	31.36	15.29
180	34.85	12.09	32.67	180	30.49	17.65
225	35.72	9.89	33.10	225	30.49	17.65
270	34.85	12.09	32.67	270	30.49	17.65
315	34.85	12.09	32.67	315	30.49	17.65
360	33.97	14.29	31.80	360	29.62	20.00
405	33.97	14.29	31.14	405	28.31	23.53
450	30.93	21.98	28.53	450	26.13	29.41
495	30.05	24.18	28.09	495	26.13	29.41
540	30.05	24.18	28.09	540	26.13	29.41
585	27.44	30.77	26.79	585	26.13	29.41
630	27.01	31.87	26.57	630	26.13	29.41
675	27.01	31.87	25.48	675	23.96	35.29
720	26.13	34.07	25.05	720	23.96	35.29
765	26.13	34.07	24.83	765	23.52	36.47
810	26.13	34.07	24.83	810	23.52	36.47

## **Appendix B.3**

Data from batch experiments

**RO cell experimental runs with 19.8 mL Laundry Detergent and 8 ppm  
anti-scalant**

Kinetic data for the RO cell experimental runs with 19.8 mL Laundry Detergent and 8 ppm anti-scalant, measuring operation parameters in the feed, brine and permeate.

Below in Table B.3-1 the operating conditions is illustrated for the RO process and included are the membrane specification:

**Table B.3-1: Membrane specification and initial operating conditions of experimental run.**

Dimensions	14.5 cm x 9.5 cm
Active Area	0.013775 m <sup>2</sup>
Nomination	XLE-4040
Feed Pressure:	10 bar
Piston Pressure:	14 bar
Feed flow rate:	0.56 L/hr
Brine Pressure:	10 bar

**Table B.3-2: Experimental run**

Time (min)	Feed			Brine		Permeate						
	EC F (μS)	TDS F (g/L)	Temperature F (°C)	EC (μS)	TDS (g/L)	EC P (μS)	TDS P (g/L)	Temperature (°C)	Time (min)	Volume (L)	Flow Rate (l/h)	Flux (L/h m <sup>2</sup> )
0	287.8	0.1974	22.3	292.4	0.199	11.7	0.0063	22.6	0	0.011	0.66	47.91288566
45	298.4	0.2026	22.9	305.8	0.2053	10.3	0.0074	23.1	45	0.01	0.6	43.55716878
90	308.9	0.2073	23.4	314.1	0.2089	8.2	0.0063	23	90	0.009	0.54	39.20145191
135	319.6	0.2127	23.8	324.1	0.2146	18.8	0.0125	23.6	135	0.0085	0.51	37.02359347
180	330.1	0.2178	24.2	334.4	0.2194	15.6	0.0091	23.9	180	0.0085	0.51	37.02359347
225	339.1	0.223	24.5	344	0.2239	10.7	0.007	24.1	225	0.0085	0.51	37.02359347
270	351.7	0.2291	24.9	354.1	0.23	12.9	0.0088	24.5	270	0.0085	0.51	37.02359347
315	363.2	0.235	25.1	366.4	0.236	10.6	0.0095	24.9	315	0.0085	0.51	37.02359347
360	374.3	0.2412	25.5	376.3	0.2419	10.9	0.0101	24.2	360	0.0085	0.51	37.02359347
405	384.6	0.2477	25.5	386	0.2482	10.7	0.0104	23.9	405	0.0085	0.51	37.02359347
450	393.8	0.2538	25.5	396.2	0.2561	23.4	0.0155	23.7	450	0.0075	0.45	32.66787659
495	409.8	0.2651	25.3	413.1	0.267	16.9	0.0113	23.4	495	0.0073	0.438	31.79673321
540	412.6	0.267	25.3	415.2	0.2702	16.4	0.011	23.4	540	0.007	0.42	30.49001815
585	420.8	0.2729	25.1	423.8	0.2754	16	0.0108	23.3	585	0.007	0.42	30.49001815
630	429.5	0.28	25	433.4	0.2829	15.7	0.0107	23	630	0.0065	0.39	28.31215971
675	439.8	0.287	24.8	442	0.2894	13.2	0.009	22.9	675	0.006	0.36	26.13430127
720	449.6	0.295	24.6	452.2	0.297	11.5	0.0079	22.6	720	0.006	0.36	26.13430127
765	455.7	0.3	24.4	460	0.3032	12	0.0081	22.7	765	0.006	0.36	26.13430127
810	463	0.3045	24.5	472.5	0.31	10.7	0.0073	23.1	810	0.006	0.36	26.13430127

**Table B.3-3: Experimental run duplicate**

Time (min)	Feed			Brine		Permeate						
	EC F (μS)	TDS F (g/L)	Temperature F (°C)	EC (μS)	TDS (g/L)	EC P (μS)	TDS P (g/L)	Temperature (°C)	Time (min)	Volume (L)	Flow Rate (l/h)	Flux (L/h m <sup>2</sup> )
0	308.9	0.2007	25.1	314	0.2029	11.9	0.0072	24.8	0	0.009	0.54	39.20145191
45	317.8	0.2051	25.4	323.4	0.2066	10.6	0.0068	25.4	45	0.009	0.54	39.20145191
90	329	0.2103	25.9	332.6	0.2115	11.8	0.0077	25.8	90	0.009	0.54	39.20145191
135	338.1	0.215	26.2	341	0.2157	10.8	0.0055	25.6	135	0.0082	0.492	35.7168784
180	345.6	0.2191	26.4	348.2	0.2194	10.6	0.0066	25.4	180	0.0083	0.498	36.15245009
225	354.9	0.2244	26.5	356.2	0.2248	10.3	0.0075	25	225	0.008	0.48	34.84573503
270	359.7	0.2288	26.3	363	0.2315	12.7	0.0089	24	270	0.007	0.42	30.49001815
315	365.5	0.234	25.9	368.5	0.237	13	0.0091	23.9	315	0.007	0.42	30.49001815
360	371.9	0.2381	25.9	378.8	0.2426	17.7	0.0114	24.7	360	0.007	0.42	30.49001815
405	378.1	0.2418	25.9	388	0.2473	18.6	0.0121	24.8	405	0.007	0.42	30.49001815
450	388.3	0.2479	26.1	399.3	0.254	18.9	0.0128	25.2	450	0.007	0.42	30.49001815
495	396.5	0.2343	25.9	402.3	0.2584	18.4	0.0125	23	495	0.007	0.42	30.49001815
540	400.3	0.2585	25.4	406.1	0.2637	14.7	0.01	22.5	540	0.0061	0.366	26.56987296
585	407.9	0.2658	25	413	0.27	15.4	0.0107	22.3	585	0.0061	0.366	26.56987296
630	412.5	0.2708	24.7	419	0.2755	12.4	0.0086	21.9	630	0.0058	0.348	25.26315789
675	417.9	0.2754	24.4	424.1	0.2805	12.2	0.0084	21.6	675	0.0058	0.348	25.26315789
720	428.9	0.2843	24.1	431.2	0.2863	10.3	0.0072	21.5	720	0.0055	0.33	23.95644283
765	434.9	0.29	23.8	437.3	0.2924	12.9	0.0091	21.1	765	0.0055	0.33	23.95644283
810	445.7	0.2964	23.9	451	0.2985	11.7	0.0078	23.1	810	0.0055	0.33	23.95644283

## Data analysis report on the two ranges of data of unmodified membranes

Data analysis using Microsoft Excel was performed to assess the significance of data of an experimental run and the 'duplicate run' has a significant difference or not.

### F-Test Two-Sample for Variances

	<i>Variable 1</i>	<i>Variable 2</i>
Mean	34.11214061	30.67341675
Variance	38.15645154	28.82342633
Observations	19	19
df	18	18
F	1.323799992	
P(F<=f) one-tail	0.278972498	
F Critical one-tail	2.217197134	

### t-Test: Two-Sample Assuming Unequal Variances

	<i>Variable 1</i>	<i>Variable 2</i>
Mean	34.11214061	30.67341675
Variance	38.15645154	28.82342633
Observations	19	19
Hypothesized Mean Difference	0	
df	35	
t Stat	1.831478926	
P(T<=t) one-tail	0.03777588	
t Critical one-tail	1.68957244	
P(T<=t) two-tail	0.075551761	
t Critical two-tail	2.030107915	

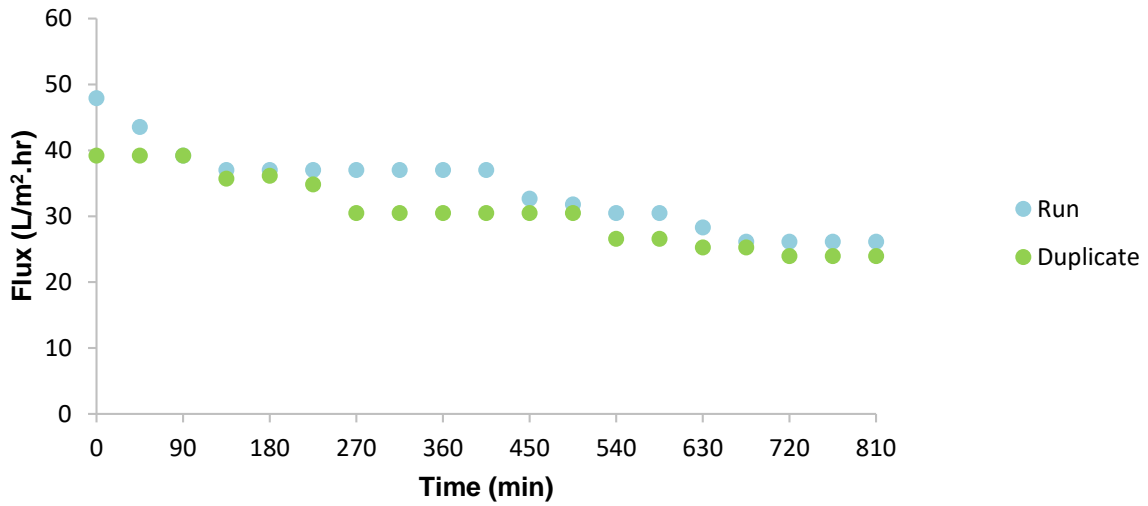


Figure B.3-1: Permeate flux decline of experimental run and duplication

Table B.3-4: Average experimental flux and FDR

Experimental Run 1			Average	Experimental Run 2		
Time (min)	Flux (L/m <sup>2</sup> .hr)	FDR (%)	Flux (L/m <sup>2</sup> .hr)	Time (min)	Flux (L/m <sup>2</sup> .hr)	FDR (%)
0	47.91	0.00	43.56	0	39.20	0.00
45	43.56	9.09	41.38	45	39.20	0.00
90	39.20	18.18	39.20	90	39.20	0.00
135	37.02	22.73	36.37	135	35.72	8.89
180	37.02	22.73	36.59	180	36.15	7.78
225	37.02	22.73	35.93	225	34.85	11.11
270	37.02	22.73	33.76	270	30.49	22.22
315	37.02	22.73	33.76	315	30.49	22.22
360	37.02	22.73	33.76	360	30.49	22.22
405	37.02	22.73	33.76	405	30.49	22.22
450	32.67	31.82	31.58	450	30.49	22.22
495	31.80	33.64	31.14	495	30.49	22.22
540	30.49	36.36	28.53	540	26.57	32.22
585	30.49	36.36	28.53	585	26.57	32.22
630	28.31	40.91	26.79	630	25.26	35.56
675	26.13	45.45	25.70	675	25.26	35.56
720	26.13	45.45	25.05	720	23.96	38.89
765	26.13	45.45	25.05	765	23.96	38.89
810	26.13	45.45	25.05	810	23.96	38.89

# Appendix C

Data from batch experiments

**RO cell experimental runs with 26.4 mL Laundry Detergent and  
variable anti-scalant dosage concentration  
(0, 4, and 8 ppm)**



## **Appendix C.1**

Data from batch experiments

**RO cell experimental runs with 26.4 mL Laundry Detergent and 0 ppm  
anti-scalant**

Kinetic data for the RO cell experimental runs with 26.4 mL Laundry Detergent and 0 ppm anti-scalant, measuring operation parameters in the feed, brine and permeate.

Below in Table C.1-1 the operating conditions is illustrated for the RO process and included are the membrane specification:

**Table C.1-1: Membrane specification and initial operating conditions of experimental run.**

Dimensions	14.5 cm x 9.5 cm
Active Area	0.013775 m <sup>2</sup>
Nomination	XLE-4040
Feed Pressure:	10 bar
Piston Pressure:	14 bar
Feed flow rate:	0.56 L/hr
Brine Pressure:	10 bar

**Table C.1-2: Experimental run**

Time (min)	Feed			Brine		Permeate						
	EC F (μS)	TDS F (g/L)	Temperature F (°C)	EC (μS)	TDS (g/L)	EC P (μS)	TDS P (g/L)	Temperature (°C)	Time (min)	Volume (L)	Flow Rate (l/h)	Flux (L/h m <sup>2</sup> )
0	278.8	0.2051	18.9	281	0.2053	9.6	0.0071	18.7	0	0.0069	0.414	30.05444646
45	285.8	0.2088	19.2	289.9	0.2104	11.6	0.0086	18.7	45	0.0068	0.408	29.61887477
90	291.5	0.2122	19.5	294.6	0.2138	15.8	0.0116	19	90	0.0065	0.39	28.31215971
135	295.5	0.2148	19.6	299.6	0.2165	15.6	0.0116	18.5	135	0.0063	0.378	27.44101633
180	299.9	0.2177	19.6	304	0.2198	16.2	0.012	18.6	180	0.006	0.36	26.13430127
225	304.8	0.2213	19.6	307.3	0.2225	16.3	0.0121	18.5	225	0.0059	0.354	25.69872958
270	309.3	0.2237	19.6	310.8	0.2251	13	0.0097	18.3	270	0.0055	0.33	23.95644283
315	312.6	0.2273	19.5	314	0.228	11.5	0.0086	18	315	0.0053	0.318	23.08529946
360	315.4	0.2295	19.4	317.9	0.2309	5.6	0.0042	17.9	360	0.0051	0.306	22.21415608
405	319.5	0.2327	19.3	321	0.2337	5.3	0.004	17.6	405	0.005	0.3	21.77858439
450	321.9	0.2354	19.2	324.3	0.237	3.8	0.0028	17.5	450	0.005	0.3	21.77858439
495	325.3	0.2384	19.1	327.3	0.2397	3.6	0.0027	17.4	495	0.005	0.3	21.77858439
540	328.3	0.2416	19	329.9	0.2425	3.2	0.0024	17.2	540	0.005	0.3	21.77858439
585	331.3	0.2435	18.9	331.6	0.2436	5.8	0.0045	17.1	585	0.005	0.3	21.77858439
630	334.3	0.2466	18.8	334.1	0.2466	2.5	0.0018	17.2	630	0.005	0.3	21.77858439
675	336.8	0.2494	18.7	337.8	0.2493	2.9	0.0021	17.2	675	0.005	0.3	21.77858439
720	339.5	0.2509	18.7	341.9	0.252	2.7	0.002	17.2	720	0.005	0.3	21.77858439
765	344.5	0.254	18.8	346.4	0.2548	2.4	0.0018	17.4	765	0.005	0.3	21.77858439
810	351.1	0.258	18.9	350.4	0.2567	2.9	0.0023	17.4	810	0.005	0.3	21.77858439

**Table C.1-3: Experimental run duplicate**

Time (min)	Feed			Brine		Permeate						
	EC F (µS)	TDS F (g/L)	Temperature F (°C)	EC (µS)	TDS (g/L)	EC P (µS)	TDS P (g/L)	Temperature (°C)	Time (min)	Volume (L)	Flow Rate (l/h)	Flux (L/h m <sup>2</sup> )
0	288.4	0.2116	19.1	293.9	0.2141	5.3	0.004	18.8	0	0.008	0.48	34.84573503
45	290	0.2137	19.3	295.9	0.2146	4.3	0.0032	18.9	45	0.007	0.42	30.49001815
90	298.7	0.2164	19.7	302	0.2179	8	0.0058	19.3	90	0.0065	0.39	28.31215971
135	302.5	0.2183	19.8	306.1	0.2203	6.2	0.0045	19.1	135	0.006	0.36	26.13430127
180	308.3	0.2209	20	310.5	0.2227	6.4	0.0048	19.1	180	0.0059	0.354	25.69872958
225	311.2	0.2235	20.1	314.6	0.2257	6.2	0.0045	19.1	225	0.0055	0.33	23.95644283
270	316.3	0.2271	20.1	318	0.2279	8.2	0.0061	19.2	270	0.0054	0.324	23.52087114
315	320.4	0.2291	20.2	323.1	0.2314	7.5	0.0056	19	315	0.0053	0.318	23.08529946
360	324.1	0.2328	20.2	326.7	0.2336	8.7	0.0065	19	360	0.0052	0.312	22.64972777
405	327.8	0.2352	20.2	330.2	0.2362	5.8	0.0043	19	405	0.0051	0.306	22.21415608
450	331.4	0.2376	20.2	334.2	0.2385	7.2	0.0053	18.9	450	0.005	0.3	21.77858439
495	336.2	0.2402	20.2	338.7	0.2418	6.2	0.0045	19	495	0.005	0.3	21.77858439
540	339.6	0.2423	20.3	343.7	0.2448	6.4	0.0046	19.2	540	0.005	0.3	21.77858439
585	343.7	0.2456	20.2	346.2	0.2472	5.7	0.0041	18.8	585	0.005	0.3	21.77858439
630	347.4	0.2493	20.1	349.3	0.2501	5.7	0.0042	18.7	630	0.005	0.3	21.77858439
675	350.8	0.2514	20.1	353.8	0.2533	5.7	0.0042	19	675	0.005	0.3	21.77858439
720	356.1	0.2555	20.2	358.3	0.2565	6.5	0.0048	19	720	0.005	0.3	21.77858439
765	359.2	0.2577	20.1	362.6	0.2594	5.9	0.0043	18.7	765	0.005	0.3	21.77858439
810	363.4	0.2615	20.1	365.4	0.2622	4.7	0.0034	18.7	810	0.005	0.3	21.77858439

## Data analysis report on the two ranges of data of unmodified membranes

Data analysis using Microsoft Excel was performed to assess the significance of data of an experimental run and the 'duplicate run' has a significant difference or not.

### F-Test Two-Sample for Variances

	<i>Variable 1</i>	<i>Variable 2</i>
Mean	23.91059318	24.04814213
Variance	8.851506799	13.12415066
Observations	19	19
df	18	18
F	0.674444163	
P(F<=f) one-tail	0.205710373	
F Critical one-tail	0.451019887	

### t-Test: Two-Sample Assuming Unequal Variances

	<i>Variable 1</i>	<i>Variable 2</i>
Mean	23.91059318	24.04814213
Variance	8.851506799	13.12415066
Observations	19	19
Hypothesized Mean Difference	0	
df	35	
t Stat	0.127897824	
P(T<=t) one-tail	0.449480944	
t Critical one-tail	1.68957244	
P(T<=t) two-tail	0.898961889	
t Critical two-tail	2.030107915	

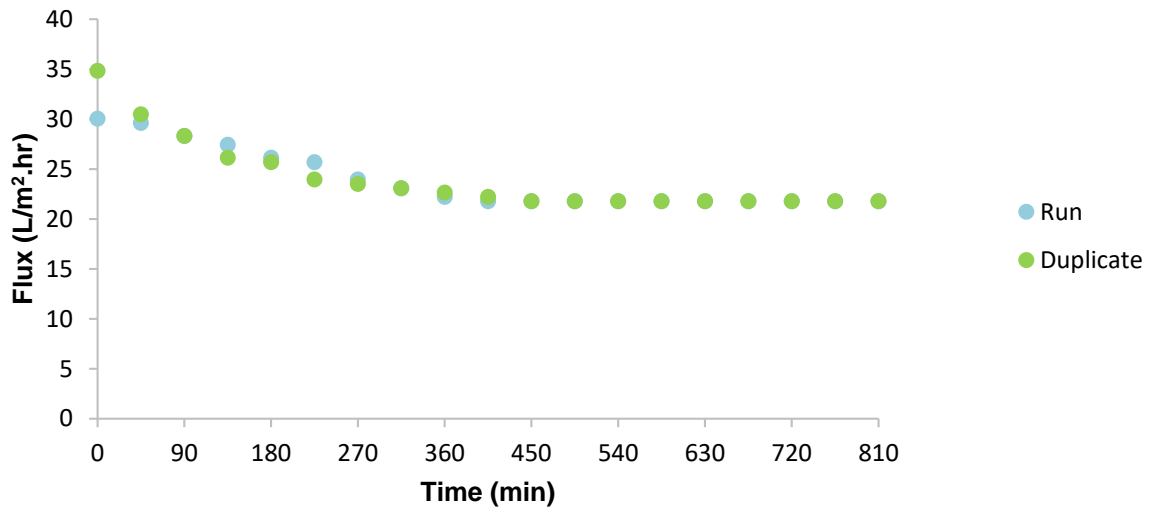


Figure C.1-1: Permeate flux decline of experimental run and duplication

Table C.1-4: Average experimental flux and FDR

Experimental Run 1			Average	Experimental Run 2		
Time (min)	Flux (L/m <sup>2</sup> .hr)	FDR (%)	Flux (L/m <sup>2</sup> .hr)	Time (min)	Flux (L/m <sup>2</sup> .hr)	FDR (%)
0	30.05	0.00	32.45	0	34.85	0.00
45	29.62	1.45	30.05	45	30.49	12.50
90	28.31	5.80	28.31	90	28.31	18.75
135	27.44	8.70	26.79	135	26.13	25.00
180	26.13	13.04	25.92	180	25.70	26.25
225	25.70	14.49	24.83	225	23.96	31.25
270	23.96	20.29	23.74	270	23.52	32.50
315	23.09	23.19	23.09	315	23.09	33.75
360	22.21	26.09	22.43	360	22.65	35.00
405	21.78	27.54	22.00	405	22.21	36.25
450	21.78	27.54	21.78	450	21.78	37.50
495	21.78	27.54	21.78	495	21.78	37.50
540	21.78	27.54	21.78	540	21.78	37.50
585	21.78	27.54	21.78	585	21.78	37.50
630	21.78	27.54	21.78	630	21.78	37.50
675	21.78	27.54	21.78	675	21.78	37.50
720	21.78	27.54	21.78	720	21.78	37.50
765	21.78	27.54	21.78	765	21.78	37.50
810	21.78	27.54	21.78	810	21.78	37.50

## **Appendix C.2**

Data from batch experiments

**RO cell experimental runs with 26.4 mL Laundry Detergent and 4 ppm  
anti-scalant**

Kinetic data for the RO cell experimental runs with 26.4 mL Laundry Detergent and 4 ppm anti-scalant, measuring operation parameters in the feed, brine and permeate.

Below in Table C.2-1 the operating conditions is illustrated for the RO process and included are the membrane specification:

**Table C.2-1: Membrane specification and initial operating conditions of experimental run.**

Dimensions	14.5 cm x 9.5 cm
Active Area	0.013775 m <sup>2</sup>
Nomination	XLE-4040
Feed Pressure:	10 bar
Piston Pressure:	14 bar
Feed flow rate:	0.56 L/hr
Brine Pressure:	10 bar



**Table C.2-2: Experimental run**

Time (min)	Feed			Brine		Permeate						
	EC F (μS)	TDS F (g/L)	Temperature F (°C)	EC (μS)	TDS (g/L)	EC P (μS)	TDS P (g/L)	Temperature (°C)	Time (min)	Volume (L)	Flow Rate (l/h)	Flux (L/h m <sup>2</sup> )
0	318.7	0.2157	23.2	320.1	0.2162	10.7	0.0073	22.7	0	0.01	0.6	43.55716878
45	326.9	0.2191	23.4	330.8	0.2209	9.1	0.0068	23	45	0.008	0.48	34.84573503
90	335.4	0.2231	23.7	338.6	0.2249	9.4	0.0064	23.1	90	0.008	0.48	34.84573503
135	341.3	0.2271	23.8	342.5	0.2272	9	0.0062	23.2	135	0.0079	0.474	34.41016334
180	346.9	0.2302	24	351.5	0.2319	8.4	0.0052	23.3	180	0.0078	0.468	33.97459165
225	356.4	0.2352	24.2	359.9	0.2359	8.8	0.0056	23.5	225	0.0078	0.468	33.97459165
270	364.1	0.2393	24.4	366.1	0.24	7.8	0.0049	23.3	270	0.0078	0.468	33.97459165
315	371.1	0.2438	24.5	372.6	0.2445	7.5	0.0046	23.5	315	0.0078	0.468	33.97459165
360	381.4	0.2503	24.5	382.3	0.2505	6.6	0.0042	22.6	360	0.0078	0.468	33.97459165
405	384.5	0.2531	24.5	386.7	0.2537	17.5	0.0138	23.2	405	0.0078	0.468	33.97459165
450	391.6	0.2579	24.4	394.8	0.2613	20.9	0.0145	22.5	450	0.007	0.42	30.49001815
495	399.4	0.2627	24.4	402.1	0.2655	23.5	0.0161	22.5	495	0.007	0.42	30.49001815
540	404.9	0.2672	24.3	408.8	0.2699	27.6	0.0189	22.5	540	0.007	0.42	30.49001815
585	412.3	0.2725	24.2	414	0.2745	23.8	0.0164	22.2	585	0.0065	0.39	28.31215971
630	417.6	0.2769	24.1	421.7	0.2792	26.8	0.0182	22.6	630	0.0065	0.39	28.31215971
675	425.2	0.2821	23.9	429.1	0.2846	23.1	0.0159	22	675	0.006	0.36	26.13430127
720	430.4	0.2867	23.8	433.3	0.2889	27.6	0.0188	22	720	0.006	0.36	26.13430127
765	438.5	0.2922	23.7	440	0.2944	26	0.0181	21.9	765	0.006	0.36	26.13430127
810	443.9	0.2974	23.6	447.3	0.3	20.6	0.0145	21.6	810	0.0055	0.33	23.95644283

**Table C.2-3: Experimental run duplicate**

Time (min)	Feed			Brine		Permeate						
	EC F (µS)	TDS F (g/L)	Temperature F (°C)	EC (µS)	TDS (g/L)	EC P (µS)	TDS P (g/L)	Temperature (°C)	Time (min)	Volume (L)	Flow Rate (l/h)	Flux (L/h m <sup>2</sup> )
0	312.4	0.213	22.8	321.1	0.2162	13.8	0.0094	22.4	0	0.009	0.54	39.20145191
45	321.8	0.2176	23.1	329.6	0.2206	14.7	0.01	22.8	45	0.009	0.54	39.20145191
90	330.4	0.2218	23.4	336.5	0.2245	14.5	0.0097	22.8	90	0.008	0.48	34.84573503
135	337.8	0.2256	23.5	342.8	0.2279	13.5	0.009	23	135	0.0077	0.462	33.53901996
180	338.9	0.226	23.6	341.4	0.2266	14.5	0.0099	23	180	0.0075	0.45	32.66787659
225	347.6	0.231	23.9	352.5	0.233	13.4	0.0091	23.1	225	0.007	0.42	30.49001815
270	359.3	0.2356	23.9	357.2	0.2366	13	0.0092	23	270	0.007	0.42	30.49001815
315	362.5	0.24	24.1	365.1	0.2412	13.5	0.009	23.1	315	0.007	0.42	30.49001815
360	370.2	0.2448	24.2	372.7	0.2453	14.2	0.0096	23.2	360	0.007	0.42	30.49001815
405	377.7	0.249	24.3	379.5	0.2496	14	0.0095	23.1	405	0.007	0.42	30.49001815
450	384.9	0.2533	24.3	386	0.253	13.5	0.0091	23.1	450	0.0068	0.408	29.61887477
495	393	0.2588	24.4	397.7	0.261	16.4	0.011	23.2	495	0.0061	0.366	26.56987296
540	400	0.2629	24.4	404.3	0.265	16.6	0.0112	23.1	540	0.0061	0.366	26.56987296
585	405.3	0.2667	24.4	408.3	0.2695	15.8	0.0108	23	585	0.0061	0.366	26.56987296
630	411.3	0.2707	24.4	415.6	0.2737	17.8	0.0121	22.8	630	0.006	0.36	26.13430127
675	419.7	0.2764	24.3	421.2	0.278	14	0.0095	22.6	675	0.006	0.36	26.13430127
720	423.9	0.28	24.2	427.3	0.2825	15	0.0103	22.5	720	0.0059	0.354	25.69872958
765	429.1	0.2839	24.1	433.2	0.2871	13.3	0.0091	22.4	765	0.0055	0.33	23.95644283
810	437.6	0.2903	24	442	0.2927	14.6	0.01	22.4	810	0.0055	0.33	23.95644283

## Data analysis report on the two ranges of data of unmodified membranes

Data analysis using Microsoft Excel was performed to assess the significance of data of an experimental run and the 'duplicate run' has a significant difference or not.

### F-Test Two-Sample for Variances

	<i>Variable 1</i>	<i>Variable 2</i>
Mean	31.68210908	29.84812303
Variance	21.0558907	20.56105842
Observations	19	19
df	18	18
F	1.024066479	
P(F<=f) one-tail	0.480160003	
F Critical one-tail	2.217197134	

### t-Test: Two-Sample Assuming Unequal Variances

	<i>Variable 1</i>	<i>Variable 2</i>
Mean	31.68210908	29.84812303
Variance	21.0558907	20.56105842
Observations	19	19
Hypothesized Mean Difference	0	
df	36	
t Stat	1.239189456	
P(T<=t) one-tail	0.11164687	
t Critical one-tail	1.688297694	
P(T<=t) two-tail	0.223293739	
t Critical two-tail	2.028093987	

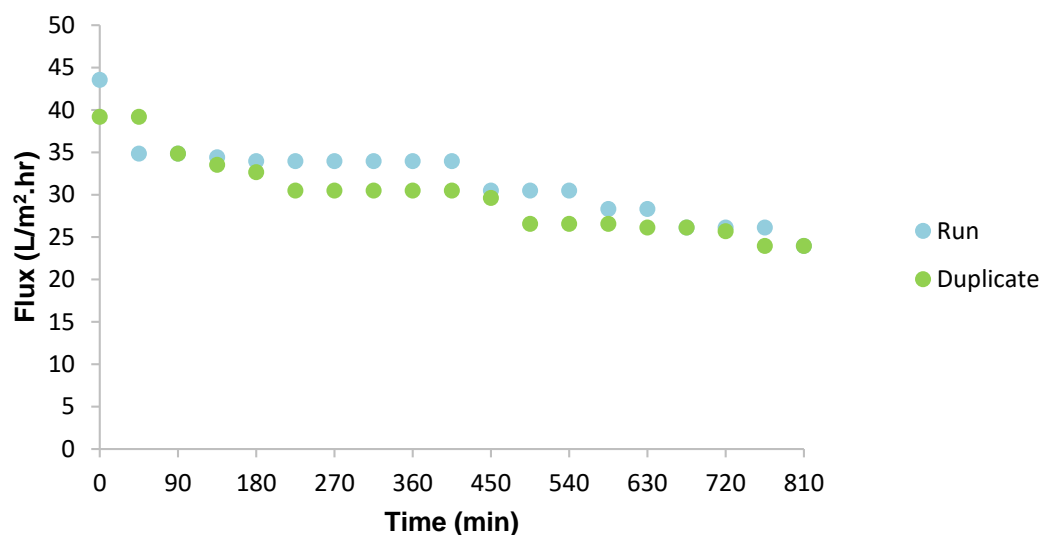


Figure C.2-1: Permeate flux decline of experimental run and duplication

Table C.2-4: Average experimental flux and FDR

Experimental Run 1			Average	Experimental Run 2		
Time (min)	Flux (L/m <sup>2</sup> .hr)	FDR (%)	Flux (L/m <sup>2</sup> .hr)	Time (min)	Flux (L/m <sup>2</sup> .hr)	FDR (%)
0	43.56	0.00	41.38	0	39.20	0.00
45	34.85	20.00	37.02	45	39.20	0.00
90	34.85	20.00	34.85	90	34.85	11.11
135	34.41	21.00	33.97	135	33.54	14.44
180	33.97	22.00	33.32	180	32.67	16.67
225	33.97	22.00	32.23	225	30.49	22.22
270	33.97	22.00	32.23	270	30.49	22.22
315	33.97	22.00	32.23	315	30.49	22.22
360	33.97	22.00	32.23	360	30.49	22.22
405	33.97	22.00	32.23	405	30.49	22.22
450	30.49	30.00	30.05	450	29.62	24.44
495	30.49	30.00	28.53	495	26.57	32.22
540	30.49	30.00	28.53	540	26.57	32.22
585	28.31	35.00	27.44	585	26.57	32.22
630	28.31	35.00	27.22	630	26.13	33.33
675	26.13	40.00	26.13	675	26.13	33.33
720	26.13	40.00	25.92	720	25.70	34.44
765	26.13	40.00	25.05	765	23.96	38.89
810	23.96	45.00	23.96	810	23.96	38.89

## **Appendix C.3**

Data from batch experiments

**RO cell experimental runs with 26.4 mL Laundry Detergent and 8 ppm  
anti-scalant**

Kinetic data for the RO cell experimental runs with 26.4 mL Laundry Detergent and 8 ppm anti-scalant, measuring operation parameters in the feed, brine and permeate.

Below in Table C.3-1 the operating conditions is illustrated for the RO process and included are the membrane specification:

**Table C.3-1: Membrane specification and initial operating conditions of experimental run.**

Dimensions	14.5 cm x 9.5 cm
Active Area	0.013775 m <sup>2</sup>
Nomination	XLE-4040
Feed Pressure:	10 bar
Piston Pressure:	14 bar
Feed flow rate:	0.56 L/hr
Brine Pressure:	10 bar

**Table C.3-2: Experimental run**

Time (min)	Feed			Brine		Permeate						
	EC F (µS)	TDS F (g/L)	Temperature F (°C)	EC (µS)	TDS (g/L)	EC P (µS)	TDS P (g/L)	Temperature (°C)	Time (min)	Volume (L)	Flow Rate (l/h)	Flux (L/h m <sup>2</sup> )
0	312.7	0.2136	22.5	319.7	0.217	9.2	0.0063	22.5	0	0.009	0.54	39.20145191
45	324.9	0.2199	23	330.6	0.2215	12.7	0.0086	22.6	45	0.0083	0.498	36.15245009
90	333.6	0.2242	23.3	337.7	0.2253	11.3	0.0077	22.6	90	0.008	0.48	34.84573503
135	344.7	0.23	23.6	349.1	0.2318	14	0.0094	23	135	0.0078	0.468	33.97459165
180	353.8	0.2348	23.8	358.5	0.2366	13.5	0.0091	22.8	180	0.0072	0.432	31.36116152
225	357.6	0.2373	24.1	359.1	0.2375	16.1	0.0111	22.8	225	0.0072	0.432	31.36116152
270	367.4	0.243	24.2	368.4	0.2428	15.9	0.0106	22.9	270	0.0072	0.432	31.36116152
315	376.4	0.2484	24.3	376.3	0.2479	16.8	0.0114	22.7	315	0.0072	0.432	31.36116152
360	384.8	0.2541	24.3	386.1	0.254	17.8	0.012	22.5	360	0.0072	0.432	31.36116152
405	392.8	0.2596	24.2	396.2	0.2616	14.8	0.0103	22.1	405	0.0072	0.432	31.36116152
450	398.1	0.264	24	400.6	0.2667	13.9	0.0096	21.8	450	0.006	0.36	26.13430127
495	405.6	0.27	23.8	406.2	0.2711	14.7	0.0102	21.6	495	0.006	0.36	26.13430127
540	409.7	0.2738	23.7	414.2	0.277	12	0.0084	21.6	540	0.006	0.36	26.13430127
585	416.6	0.2793	23.5	420.5	0.2828	11.8	0.0083	21.3	585	0.0056	0.336	24.39201452
630	425.2	0.2861	23.4	428.2	0.2888	11.8	0.0083	21.2	630	0.0056	0.336	24.39201452
675	434.6	0.2925	23.2	436.8	0.2944	11.9	0.0084	21.3	675	0.0053	0.318	23.08529946
720	439	0.296	23.2	446.7	0.3	11.8	0.0083	21.9	720	0.0053	0.318	23.08529946
765	454	0.3045	23.4	457.3	0.3064	11.9	0.0083	22	765	0.0053	0.318	23.08529946
810	464	0.3108	23.5	466.5	0.3138	12.5	0.0087	21.5	810	0.0053	0.318	23.08529946

**Table C.3-3: Experimental run duplicate**

Time (min)	Feed			Brine		Permeate						
	EC F (µS)	TDS F (g/L)	Temperature F (°C)	EC (µS)	TDS (g/L)	EC P (µS)	TDS P (g/L)	Temperature (°C)	Time (min)	Volume (L)	Flow Rate (l/h)	Flux (L/h m <sup>2</sup> )
0	310.5	0.2138	22	315.7	0.2151	15.7	0.0101	21.8	0	0.009	0.54	39.20145191
45	320.6	0.2194	22.4	325.4	0.221	13.5	0.0093	21.8	45	0.0085	0.51	37.02359347
90	325.7	0.2235	22.4	332	0.2256	12.9	0.0089	21.7	90	0.0079	0.474	34.41016334
135	334.8	0.2287	22.7	340.6	0.23	12.5	0.0088	22	135	0.007	0.42	30.49001815
180	345.1	0.2337	22.9	349.8	0.2352	11	0.0077	21.9	180	0.007	0.42	30.49001815
225	352.9	0.2388	23	356.7	0.2397	11.5	0.008	21.9	225	0.0069	0.414	30.05444646
270	357.3	0.2413	23.1	359.7	0.2418	12.9	0.0089	22.1	270	0.007	0.42	30.49001815
315	366.5	0.2465	23.2	367.5	0.2464	13.1	0.0091	22	315	0.0069	0.414	30.05444646
360	375.3	0.252	23.4	377.1	0.2527	13.3	0.0092	22	360	0.0069	0.414	30.05444646
405	383	0.2579	23.3	385	0.283	13.8	0.0093	21.6	405	0.0069	0.414	30.05444646
450	390.3	0.2625	23.3	392.5	0.2629	13.4	0.0092	21.3	450	0.0065	0.39	28.31215971
495	397.8	0.268	23.2	400.4	0.2703	12.5	0.0089	21.1	495	0.0065	0.39	28.31215971
540	404.2	0.273	23	407.3	0.2752	11.8	0.0083	20.9	540	0.006	0.36	26.13430127
585	412.4	0.2798	22.9	414.4	0.2814	10.4	0.0074	20.9	585	0.006	0.36	26.13430127
630	420.4	0.2856	22.8	422.3	0.288	11	0.0078	21	630	0.0055	0.33	23.95644283
675	425.1	0.29	22.7	430	0.2927	9.4	0.0067	20.8	675	0.0052	0.312	22.64972777
720	435.1	0.2967	22.6	437.2	0.2985	10.2	0.0073	20.8	720	0.005	0.3	21.77858439
765	442.8	0.3024	22.4	446.5	0.305	10	0.0071	20.6	765	0.005	0.3	21.77858439
810	452.1	0.3094	22.4	454.4	0.3107	9.1	0.0065	20.5	810	0.005	0.3	21.77858439



## Data analysis report on the two ranges of data of unmodified membranes

Data analysis using Microsoft Excel was performed to assess the significance of data of an experimental run and the 'duplicate run' has a significant difference or not.

### F-Test Two-Sample for Variances

	<i>Variable 1</i>	<i>Variable 2</i>
Mean	29.04575413	28.58725762
Variance	25.25530826	24.73162925
Observations	19	19
df	18	18
F	1.021174464	
P(F<=f) one-tail	0.48251768	
F Critical one-tail	2.217197134	

### t-Test: Two-Sample Assuming Unequal Variances

	<i>Variable 1</i>	<i>Variable 2</i>
Mean	29.04575413	28.58725762
Variance	25.25530826	24.73162925
Observations	19	19
Hypothesized Mean Difference	0	
df	36	
t Stat	0.282673159	
P(T<=t) one-tail	0.389523188	
t Critical one-tail	1.688297694	
P(T<=t) two-tail	0.779046376	
t Critical two-tail	2.028093987	

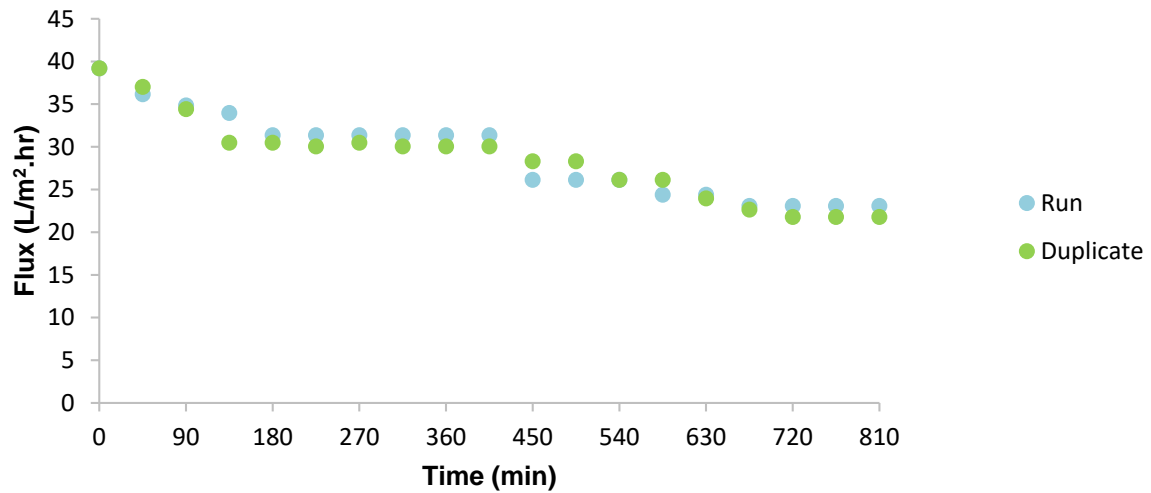


Figure C.3-1: Permeate flux decline of experimental run and duplication

Table C.3-4: Average experimental flux and FDR

Experimental Run 1			Average	Experimental Run 2		
Time (min)	Flux (L/m <sup>2</sup> .hr)	FDR (%)	Flux (L/m <sup>2</sup> .hr)	Time (min)	Flux (L/m <sup>2</sup> .hr)	FDR (%)
0	39.20	0.00	39.20	0	39.20	0.00
45	36.15	7.78	36.59	45	37.02	5.56
90	34.85	11.11	34.63	90	34.41	12.22
135	33.97	13.33	32.23	135	30.49	22.22
180	31.36	20.00	30.93	180	30.49	22.22
225	31.36	20.00	30.71	225	30.05	23.33
270	31.36	20.00	30.93	270	30.49	22.22
315	31.36	20.00	30.71	315	30.05	23.33
360	31.36	20.00	30.71	360	30.05	23.33
405	31.36	20.00	30.71	405	30.05	23.33
450	26.13	33.33	27.22	450	28.31	27.78
495	26.13	33.33	27.22	495	28.31	27.78
540	26.13	33.33	26.13	540	26.13	33.33
585	24.39	37.78	25.26	585	26.13	33.33
630	24.39	37.78	24.17	630	23.96	38.89
675	23.09	41.11	22.87	675	22.65	42.22
720	23.09	41.11	22.43	720	21.78	44.44
765	23.09	41.11	22.43	765	21.78	44.44
810	23.09	41.11	22.43	810	21.78	44.44

# Appendix D

Data from batch experiments

**RO cell experimental Long run with 13.2 mL Laundry Detergent and 0 ppm anti-scalant**

Kinetic data for the RO cell experimental Long run with 13.2 mL Laundry Detergent and 0 ppm anti-scalant, measuring operation parameters in the feed, brine and permeate.

Below in Table D-1 the operating conditions is illustrated for the RO process and included are the membrane specification:

**Table D-1: Membrane specification and initial operating conditions of experimental run.**

Dimensions	14.5 cm x 9.5 cm
Active Area	0.013775 m <sup>2</sup>
Nomination	XLE-4040
Feed Pressure:	10 bar
Piston Pressure:	14 bar
Feed flow rate:	0.56 L/hr
Brine Pressure:	10 bar

**Table D-2: Experimental run**

Time (min)	Feed			Brine		Permeate						
	EC F (µS)	TDS F (g/L)	Temperature F (°C)	EC (µS)	TDS (g/L)	EC P (µS)	TDS P (g/L)	Temperature (°C)	Time (min)	Volume (L)	Flow Rate (l/h)	Flux (L/h m <sup>2</sup> )
0	270.1	0.1807	23.5	273.1	0.1817	25.5	0.0169	24	0	0.0105	0.63	45.73502722
300	290.9	0.1895	24.9	293	0.19	25	0.0166	24.2	300	0.0095	0.57	41.37931034
600	303.8	0.1973	23.1	308.5	0.1995	24	0.0159	24.1	600	0.0072	0.432	31.36116152
900	314.5	0.2043	25.1	318.8	0.2067	21.7	0.0144	23.9	900	0.0062	0.372	27.00544465
1200	323.1	0.2133	24.2	327.6	0.2163	8.2	0.0056	23	1200	0.0054	0.324	23.52087114
1500	343.6	0.2235	25	349.1	0.225	7.1	0.0047	24.6	1500	0.0055	0.33	23.95644283
1800	364.4	0.2338	25.7	371	0.2373	6.7	0.0044	24.9	1800	0.005	0.3	21.77858439
2100	377.5	0.2441	25.3	381.2	0.2464	4.3	0.0029	23.2	2100	0.005	0.3	21.77858439
2400	380.9	0.253	23.8	383	0.2551	3.5	0.0025	21.5	2400	0.0041	0.246	17.8584392
2700	392.6	0.263	23.4	394.1	0.2634	3.9	0.0027	22.7	2700	0.0041	0.246	17.8584392
3000	417.2	0.2745	24.2	421.6	0.2754	4.3	0.0028	23.7	3000	0.004	0.24	17.42286751
3300	441.1	0.2878	24.9	447.7	0.2904	4.3	0.0029	23.4	3300	0.004	0.24	17.42286751
3600	462.3	0.3019	24.8	468.1	0.3048	4.2	0.0028	23.5	3600	0.004	0.24	17.42286751
3900	482.2	0.3156	24.7	488.6	0.3183	5.1	0.0035	23.3	3900	0.0035	0.21	15.24500907
4200	506	0.324	25	513	0.335	5.8	0.0039	23.9	4200	0.0035	0.21	15.24500907
4500	547	0.349	25.9	552	0.351	4.6	0.003	24.4	4500	0.0033	0.198	14.3738657
4800	570	0.365	25.5	572	0.367	5.2	0.0035	23	4800	0.0031	0.186	13.50272232
5100	576	0.38	24.3	580	0.381	5.1	0.0035	22.2	5100	0.003	0.18	13.06715064
5400	587	0.394	23.3	589	0.396	4.4	0.0031	21.1	5400	0.003	0.18	13.06715064
5700	628	0.413	24.3	635	0.417	5.3	0.0036	23.3	5700	0.0029	0.174	12.63157895
6000	675	0.434	25.5	685	0.438	5.4	0.0037	24.3	6000	0.0029	0.174	12.63157895

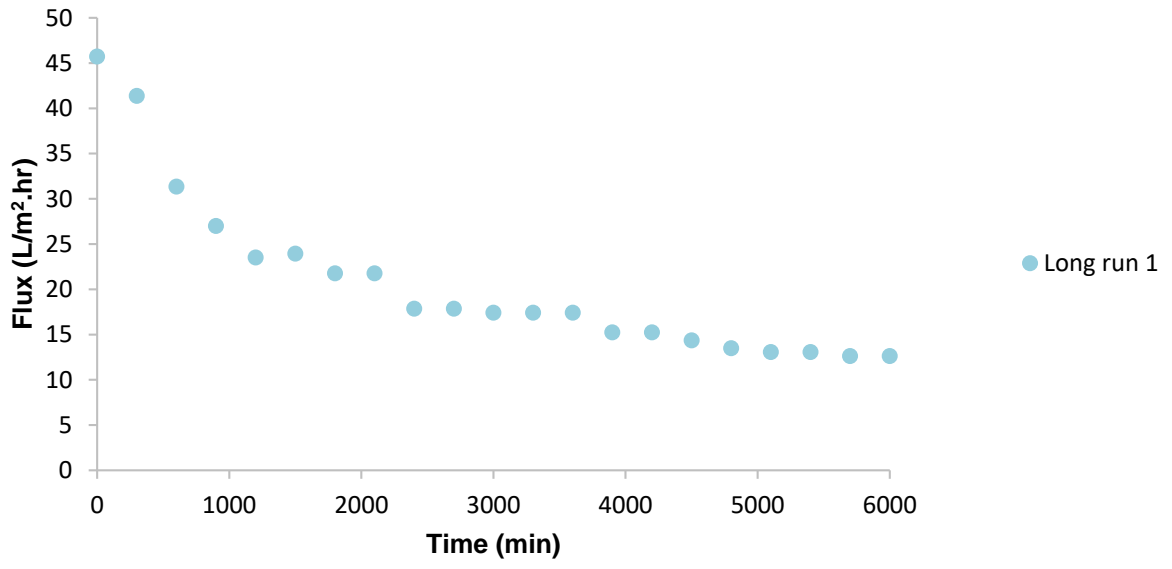


Figure D-1: Permeate flux decline of experimental run

# Appendix E

Data from batch experiments

**RO cell experimental Long run with 13.2 mL Laundry Detergent and 8 ppm anti-scalant**

Kinetic data for the RO cell experimental Long run with 13.2 mL Laundry Detergent and 8 ppm anti-scalant, measuring operation parameters in the feed, brine and permeate.

Below in Table E-1 the operating conditions is illustrated for the RO process and included are the membrane specification:

**Table E-1: Membrane specification and initial operating conditions of experimental run.**

Dimensions	14.5 cm x 9.5 cm
Active Area	0.013775 m <sup>2</sup>
Nomination	XLE-4040
Feed Pressure:	10 bar
Piston Pressure:	14 bar
Feed flow rate:	0.56 L/hr
Brine Pressure:	10 bar



**Table E-2: Experimental run**

Time (min)	Feed			Brine		Permeate						
	EC F (µS)	TDS F (g/L)	Temperature F (°C)	EC (µS)	TDS (g/L)	EC P (µS)	TDS P (g/L)	Temperature (°C)	Time (min)	Volume (L)	Flow Rate (l/h)	Flux (L/h m <sup>2</sup> )
0	234.3	0.1681	20.1	237.8	0.1696	10.7	0.0078	19.8	0	0.008	0.48	34.84573503
300	249.3	0.1758	20.9	252.1	0.1781	22	0.016	19.5	300	0.0079	0.474	34.41016334
600	257.5	0.1828	20.6	260.1	0.1842	20.6	0.015	19.2	600	0.007	0.42	30.49001815
900	266.6	0.1889	20.7	269.6	0.1905	14.5	0.0106	19.2	900	0.006	0.36	26.13430127
1200	277.7	0.1974	20.5	280.4	0.1984	10.1	0.0074	19.1	1200	0.006	0.36	26.13430127
1500	290.4	0.2052	20.9	296.4	0.2081	9.7	0.007	20.1	1500	0.0055	0.33	23.95644283
1800	309.3	0.2154	21.5	315.3	0.2194	6.6	0.0047	20.3	1800	0.005	0.3	21.77858439
2100	323.4	0.2249	21.7	328	0.2276	12.1	0.0086	20.4	2100	0.005	0.3	21.77858439
2400	337.5	0.2357	21.4	341.1	0.2377	7.5	0.0054	19.8	2400	0.005	0.3	21.77858439
2700	350.6	0.2464	21.1	356.2	0.2493	6.9	0.0049	20.1	2700	0.0045	0.27	19.60072595
3000	375	0.26	21.9	380	0.262	10.5	0.0074	20.8	3000	0.0045	0.27	19.60072595
3300	391.9	0.2694	22.3	396.6	0.271	7.4	0.0053	20.9	3300	0.0045	0.27	19.60072595
3600	403.2	0.2792	21.8	407.8	0.2814	7.4	0.0053	20.6	3600	0.0043	0.258	18.72958258
3900	420.3	0.292	21.6	424	0.2936	10.4	0.0075	19.8	3900	0.0041	0.246	17.8584392
4200	438.3	0.3042	21.9	441.2	0.3039	7.5	0.0053	21	4200	0.0041	0.246	17.8584392
4500	478.7	0.3191	23.7	483.5	0.3202	4.5	0.0031	22.6	4500	0.004	0.24	17.42286751
4800	498.7	0.3337	23.5	504	0.337	7.2	0.0051	21.7	4800	0.004	0.24	17.42286751
5100	522	0.349	23.4	527	0.352	5.6	0.0039	21.9	5100	0.0038	0.228	16.55172414
5400	536	0.362	23	541	0.365	7.3	0.0053	21.3	5400	0.0038	0.228	16.55172414
5700	565	0.378	23.5	573	0.38	5.4	0.0037	23	5700	0.0035	0.21	15.24500907
6000	596	0.394	24.2	605	0.397	7.3	0.0049	22.8	6000	0.0035	0.21	15.24500907

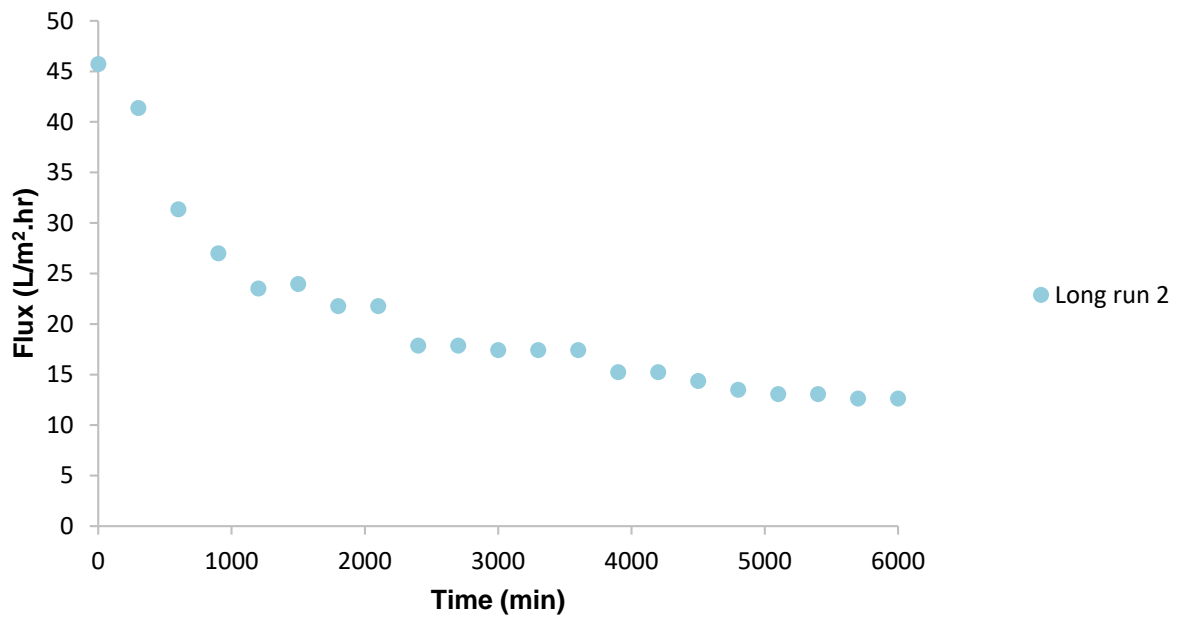


Figure E-1: Permeate flux decline of experimental run

# Appendix F

## **Sample calculations of RO parameters**

Sample calculations are based on short run data in Appendix A.1:

### Flux

The permeate flux was calculated using the following formula:

$$Flux = J_v = \frac{Q}{A} = \frac{V}{A \times \Delta t} = \frac{0.009L}{0.013775m^2 \times 0.016667hr} = 39.2 \frac{L}{m^2 \cdot hr}$$

### Salt Rejection

The observed salt rejection was calculated using the conductivities of the feed and the permeate, according to Kucera (2015):

$$R = \left(1 - \frac{EC_{permeate}}{EC_{Feed}}\right) * 100 = \left(1 - \frac{2.7\mu S}{231.2\mu S}\right) * 100 = 98.83\%$$

### Flux Decline Ratio (FDR)

The flux decline ratio (in %) was recorded to evaluate the severity of fouling using the initial flux of permeate ( $J_i$ ) and time dependent flux of permeate ( $J_t$ ) all in  $L/m^2 \cdot hr$  in the following formula:

$$FDR = \frac{Q}{A} = \left(\frac{J_i - J_t}{J_i}\right) \times 100 = \left(\frac{39.2 - 35.72}{39.2}\right) \times 100 = 8.89\%$$

# Appendix G

Data from batch experiments

**COD and Surfactant data**

**Table G-1: COD and Surfactant data**

Run	COD Feed	COD Permeate	COD Permeate Duplicate	% COD removed	Surfactant Feed	Surfactant Permeate	Surfactant Permeate Duplicate	% Surfactant removed
	(mg/L)	(mg/L)	(mg/L)	(%)	(mg/L)	(mg/L)	(mg/L)	(%)
13.2 mL								
0 ppm	460	36.5	42.5	91.41304348	83	0.125	0.125	99.84939759
4 ppm	460	29.2	29.2	93.65217391	83	0.1	0.1	99.87951807
8 ppm	460	29.2	29.2	93.65217391	83	0.1	0.1	99.87951807
19.8 mL								
0 ppm	629	29.2	29.2	95.35771065	103.5	0.1	0.1	99.90338164
4 ppm	629	32	46	93.79968203	103.5	0.1	0.1	99.90338164
8 ppm	629	52	36	93.00476948	103.5	0.1	0.22	99.84541063
26.4 mL								
0 ppm	815	48.66666667	29.2	95.22290389	128	0.166666667	0.1	99.89583333
4 ppm	815	84	46.25	92.00920245	128	0.1	0.0625	99.93652344
8 ppm	815	50	45	94.17177914	128	0.1	0.0625	99.93652344
Long run 1	460	16.22222222	-	96.47342995	83	0.055555556	-	99.9330656
Long run 2	460	21.42857143	-	95.34161491	83	0.051020408	-	99.93852963

# Appendix H

**Testing procedure of physical and chemical parameters**

## **Flux**

Permeate was collected in a small cylinder for a 15 second and the volume was noted. This value was used to determine the flux as shown in appendix A, B, C, D and E. Note that this was taken every 45 min during the experimental short runs and every 5 hours during the experimental long runs.

## **Electrical Conductivity (EC)**

The EC was read off the EC meters (feed or permeate meter) when the probe of the EC meter was placed inside the feed tank or the permeate samples. This was also taken every 45 minutes the experimental short runs and every 5 hours during the experimental long runs.

## **Total Dissolved Solids (TDS)**

Again the TDS was read off the EC meters as well, also taken every 45 minutes the experimental short runs and every 5 hours during the experimental long runs.

## **Temperature**

The temperature was read off the EC meters as well, also taken every 45 minutes the experimental short runs and every 5 hours during the experimental long runs.



# Appendix I

## **EDX Raw Data**

Sample: Virgin

Processing option : All elements analysed (Normalised)

All results in weight%

Spectrum	In stats.	C	O	S	Total
Spectrum 1	Yes	77.22	16.83	5.95	100
Spectrum 2	Yes	77.5	16.32	6.18	100
Spectrum 3	Yes	77.11	16.8	6.09	100
Spectrum 4	Yes	77.26	16.76	5.97	100
Spectrum 5	Yes	77.38	16.44	6.17	100
Mean		77.3	16.63	6.07	100
Std. deviation		0.15	0.23	0.11	
Max.		77.5	16.83	6.18	
Min.		77.11	16.32	5.95	

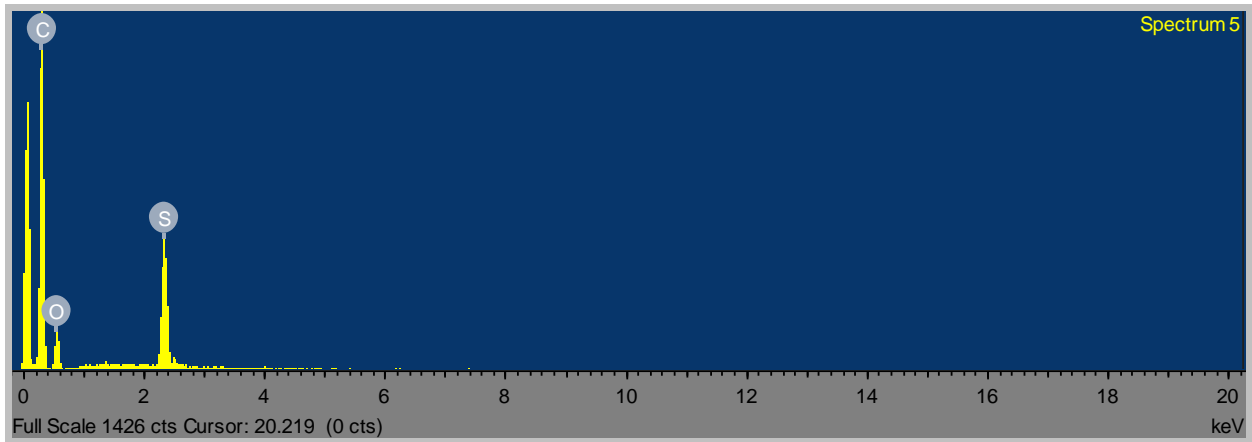


Figure I-1: EDX Spectrum (virgin)

Sample: Long run 1

Processing option : All elements analysed (Normalised)

All results in weight%

Spectrum	In stats.	C	O	S	Total
Spectrum 1	Yes	71.73	22.85	5.43	100
Spectrum 2	Yes	72.42	21.94	5.63	100
Spectrum 3	Yes	70.78	24.58	4.64	100
Spectrum 4	Yes	71.67	23.17	5.16	100
Spectrum 5	Yes	73.1	21.48	5.42	100
Mean		71.94	22.8	5.26	100
Std. deviation		0.87	1.2	0.38	
Max.		73.1	24.58	5.63	
Min.		70.78	21.48	4.64	

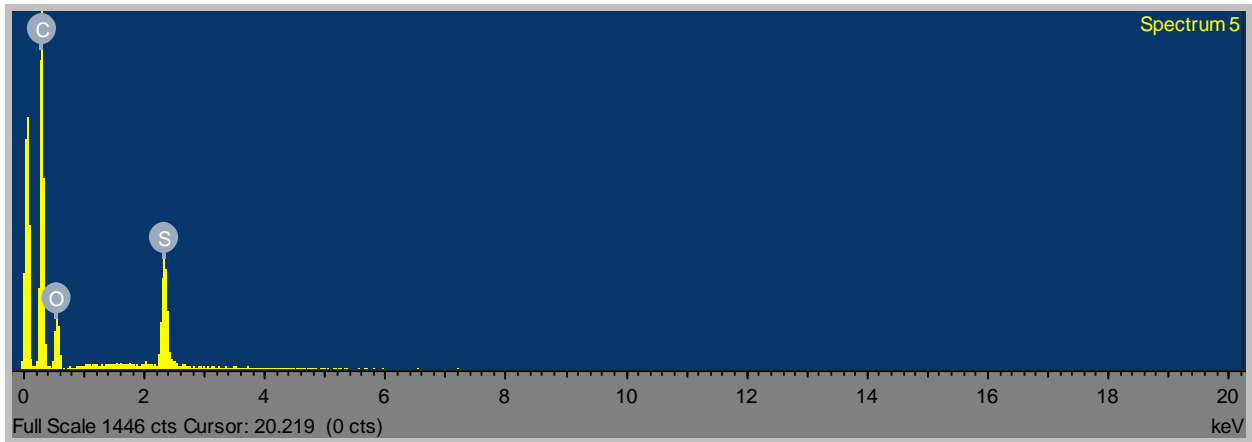


Figure I-2: EDX Spectrum (long run 1)

Sample: Long run 2

Processing option : All elements analysed (Normalised)

All results in weight%

Spectrum	In stats.	C	O	S	Total
Spectrum 1	Yes	75.53	18.15	6.32	100
Spectrum 2	Yes	74.74	18.99	6.27	100
Spectrum 3	Yes	75.56	18.13	6.31	100
Spectrum 4	Yes	75.62	17.87	6.51	100
Spectrum 5	Yes	75.25	18.38	6.37	100
Mean		75.34	18.3	6.35	100
Std. deviation		0.36	0.42	0.09	
Max.		75.62	18.99	6.51	
Min.		74.74	17.87	6.27	

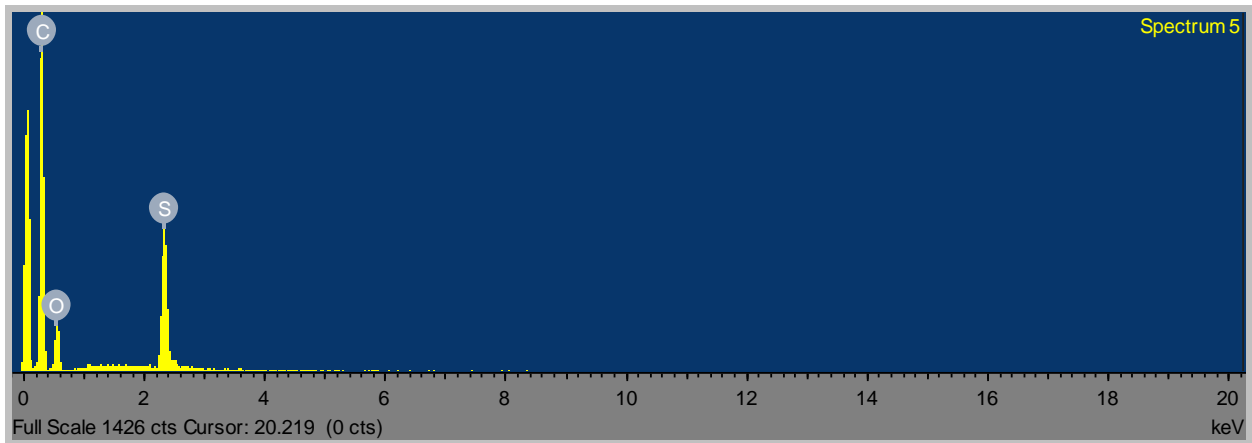


Figure I-3: EDX Spectrum (long run 2)

Sample: 13.2 ml Laundry detergent; 0 ppm anti-scalant dosage

Processing option : All elements analysed (Normalised)

All results in weight%

Spectrum	In stats.	C	O	S	Total
Spectrum 1	Yes	77.14	16.71	6.15	100
Spectrum 2	Yes	75.87	18.26	5.86	100
Spectrum 3	Yes	77.56	16.57	5.87	100
Spectrum 4	Yes	77.34	16.71	5.94	100
Spectrum 5	Yes	77.26	16.81	5.93	100
Mean		77.04	17.01	5.95	100
Std. deviation		0.67	0.7	0.11	
Max.		77.56	18.26	6.15	
Min.		75.87	16.57	5.86	

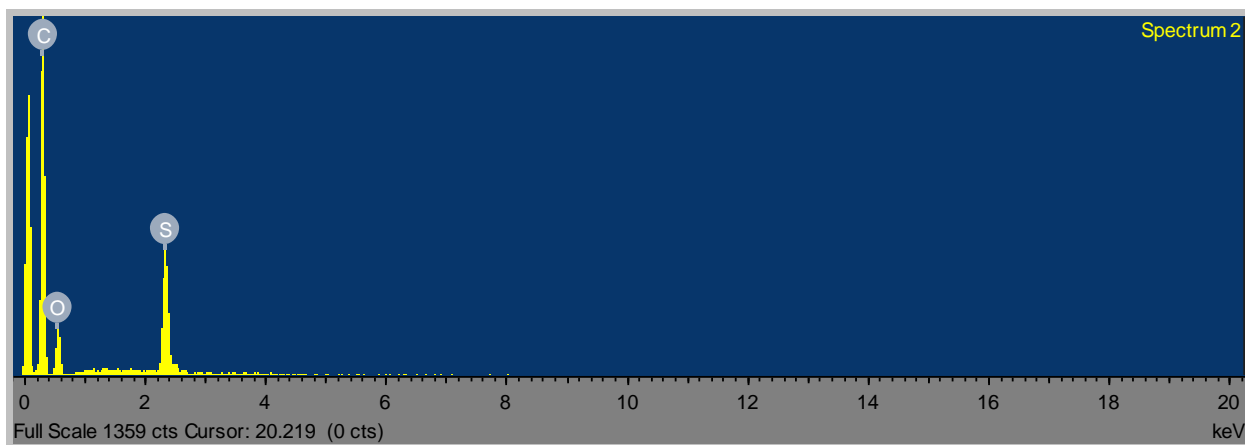


Figure I-4: EDX Spectrum (13.2 ml Laundry detergent; 0 ppm anti-scalant dosage)

Sample: 13.2 ml Laundry detergent; 4 ppm anti-scalant dosage

Processing option : All elements analysed (Normalised)

All results in weight%

Spectrum	In stats.	C	O	S	Total
Spectrum 1	Yes	75.92	18.48	5.6	100
Spectrum 2	Yes	76.28	17.94	5.78	100
Spectrum 3	Yes	75.18	19.19	5.63	100
Spectrum 4	Yes	75.56	18.49	5.95	100
Spectrum 5	Yes	75.91	18.37	5.72	100
Mean		75.77	18.49	5.74	100
Std. deviation		0.42	0.45	0.14	
Max.		76.28	19.19	5.95	
Min.		75.18	17.94	5.6	

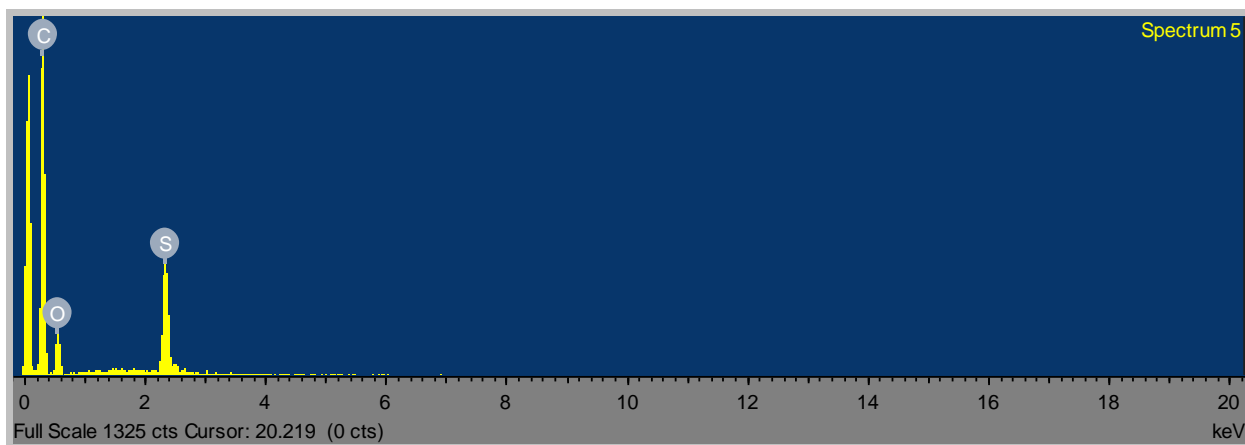


Figure I-5: EDX Spectrum (13.2 ml Laundry detergent; 4 ppm anti-scalant dosage)

Sample: 13.2 ml Laundry detergent; 8 ppm anti-scalant dosage

Processing option : All elements analysed (Normalised)

All results in weight%

Spectrum	In stats.	C	O	S	Total
Spectrum 1	Yes	74.82	19.34	5.84	100
Spectrum 2	Yes	75.15	18.88	5.96	100
Spectrum 3	Yes	74.79	19.59	5.62	100
Spectrum 4	Yes	75.85	18.33	5.83	100
Spectrum 5	Yes	75.12	18.91	5.97	100
Mean		75.15	19.01	5.84	100
Std. deviation		0.43	0.49	0.14	
Max.		75.85	19.59	5.97	
Min.		74.79	18.33	5.62	

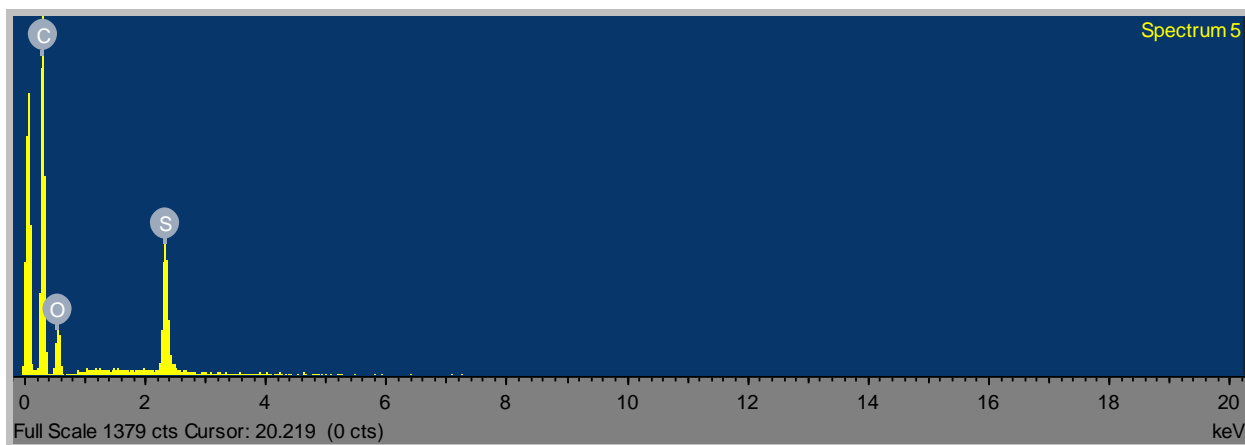


Figure I-6: EDX Spectrum (13.2 ml Laundry detergent; 8 ppm anti-scalant dosage)

Sample: 19.8 ml Laundry detergent; 0 ppm anti-scalant dosage

Processing option : All elements analysed (Normalised)

All results in weight%

Spectrum	In stats.	C	O	S	Total
Spectrum 1	Yes	76.15	18.06	5.79	100
Spectrum 2	Yes	77.01	17.06	5.93	100
Spectrum 3	Yes	77.14	17.1	5.76	100
Spectrum 4	Yes	77.52	16.55	5.92	100
Spectrum 5	Yes	76.7	17.46	5.84	100
Mean		76.9	17.25	5.85	100
Std. deviation		0.52	0.56	0.08	
Max.		77.52	18.06	5.93	
Min.		76.15	16.55	5.76	

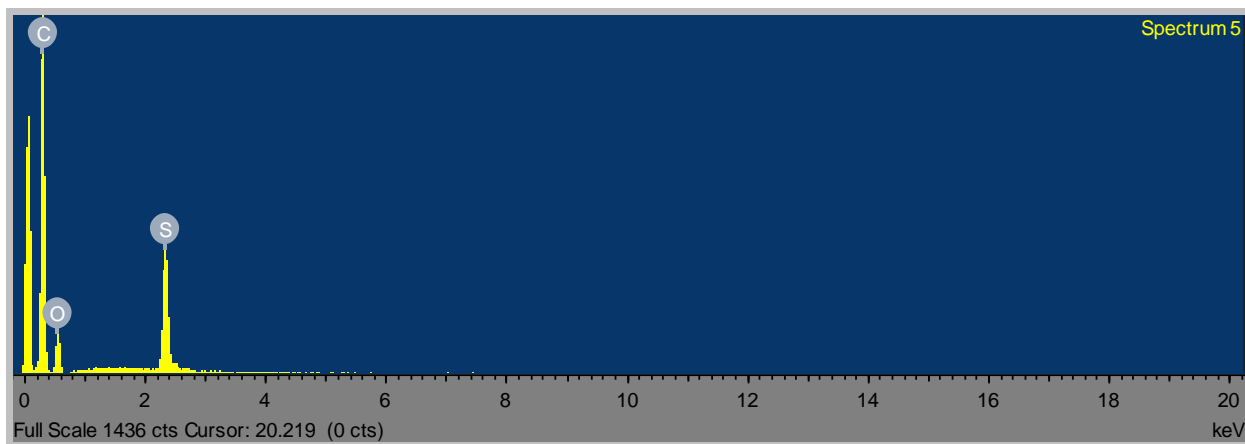


Figure I-7: EDX Spectrum (19.8 ml Laundry detergent; 0 ppm anti-scalant dosage)



Sample: 19.8 ml Laundry detergent; 4 ppm anti-scalant dosage

Processing option : All elements analysed (Normalised)

All results in weight%

Spectrum	In stats.	C	O	S	Total
Spectrum 1	Yes	75.39	18.67	5.94	100
Spectrum 2	Yes	74.6	19.39	6.02	100
Spectrum 3	Yes	75.59	18.58	5.83	100
Spectrum 4	Yes	75.66	18.32	6.02	100
Spectrum 5	Yes	76.27	17.73	6	100
Mean		75.5	18.54	5.96	100
Std. deviation		0.6	0.6	0.08	
Max.		76.27	19.39	6.02	
Min.		74.6	17.73	5.83	

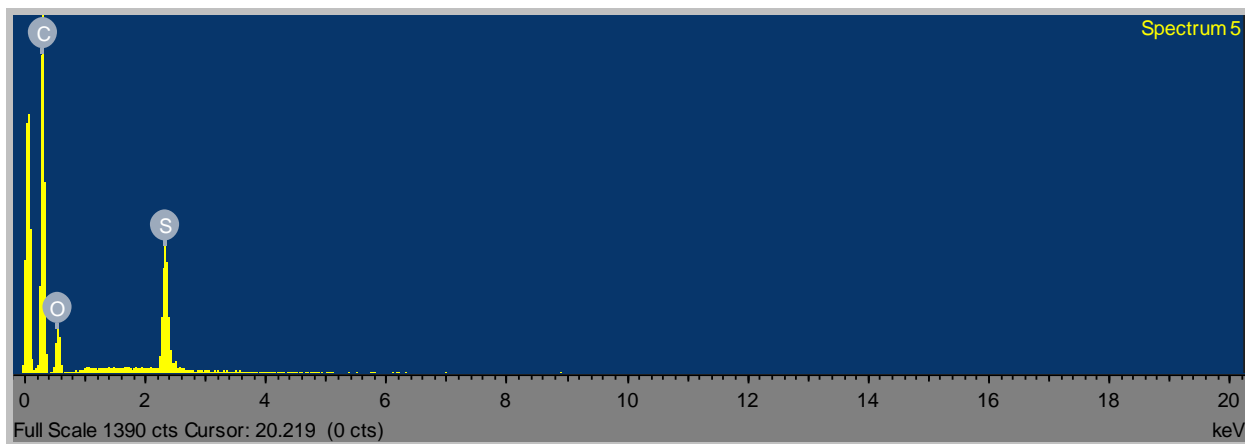


Figure I-8: EDX Spectrum (19.8 ml Laundry detergent; 4 ppm anti-scalant dosage)

Sample: 19.8 ml Laundry detergent; 8 ppm anti-scalant dosage

Processing option : All elements analysed (Normalised)

All results in weight%

Spectrum	In stats.	C	O	S	Total
Spectrum 1	Yes	76.82	16.69	6.49	100
Spectrum 2	Yes	75.49	18.14	6.37	100
Spectrum 3	Yes	75.8	17.92	6.28	100
Spectrum 4	Yes	76.22	17.24	6.54	100
Spectrum 5	Yes	76.63	17.07	6.3	100
Mean		76.19	17.41	6.4	100
Std. deviation		0.56	0.6	0.11	
Max.		76.82	18.14	6.54	
Min.		75.49	16.69	6.28	

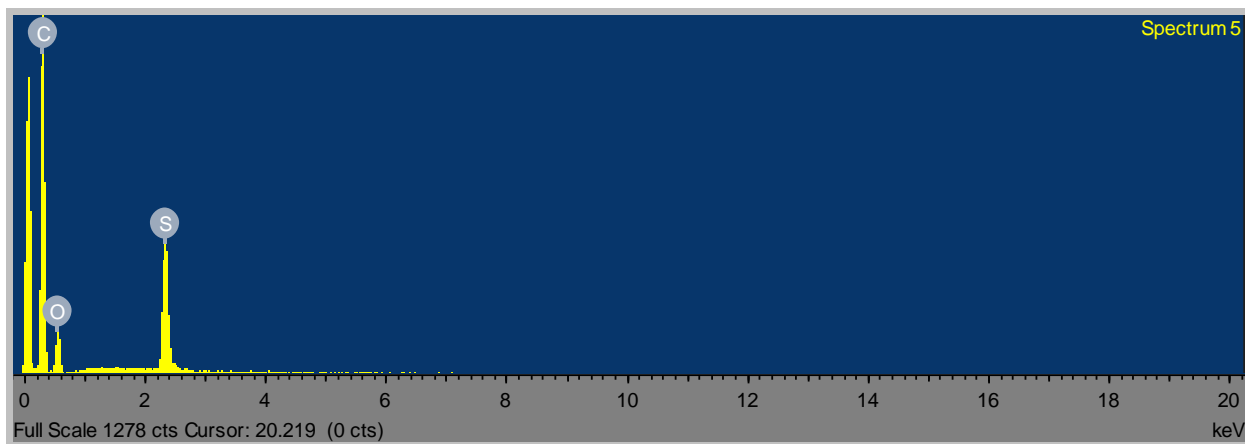


Figure I-9: EDX Spectrum (19.8 ml Laundry detergent; 8 ppm anti-scalant dosage)

Sample: 26.4 ml Laundry detergent; 0 ppm anti-scalant dosage

Processing option : All elements analysed (Normalised)

All results in weight%

Spectrum	In stats.	C	O	S	Cl	Total
Spectrum 1	Yes	76.7	17.19	5.91	0.2	100
Spectrum 2	Yes	75.7	18.07	6.23		100
Spectrum 3	Yes	75.38	18.38	6.24		100
Spectrum 4	Yes	75.26	18.63	6.11		100
Spectrum 5	Yes	75.75	18.25	6		100
ave		75.758	18.104	6.098		
Max.		76.7	18.63	6.24	0.2	
Min.		75.26	17.19	5.91	0.2	

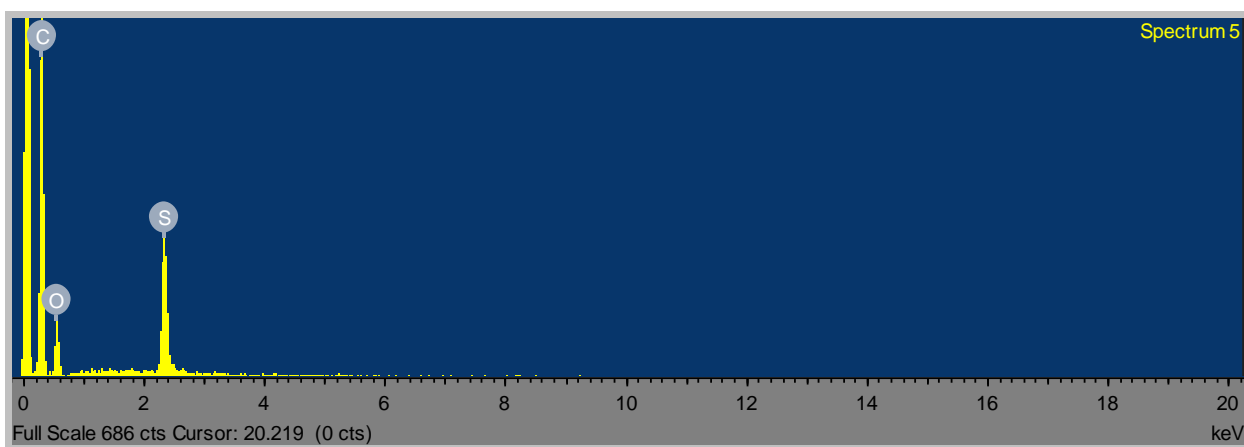


Figure I-10: EDX Spectrum (26.4 ml Laundry detergent; 0 ppm anti-scalant dosage)

Sample: 26.4 ml Laundry detergent; 4 ppm anti-scalant dosage

Processing option : All elements analysed (Normalised)

All results in weight%

Spectrum	In stats.	C	O	S	Total
Spectrum 1	Yes	77.34	16.03	6.63	100
Spectrum 2	Yes	76.85	16.54	6.61	100
Spectrum 3	Yes	77.36	16.19	6.44	100
Spectrum 4	Yes	77.83	15.6	6.57	100
Spectrum 5	Yes	77.14	15.94	6.92	100
Mean		77.31	16.06	6.63	100
Std. deviation		0.36	0.34	0.17	
Max.		77.83	16.54	6.92	
Min.		76.85	15.6	6.44	

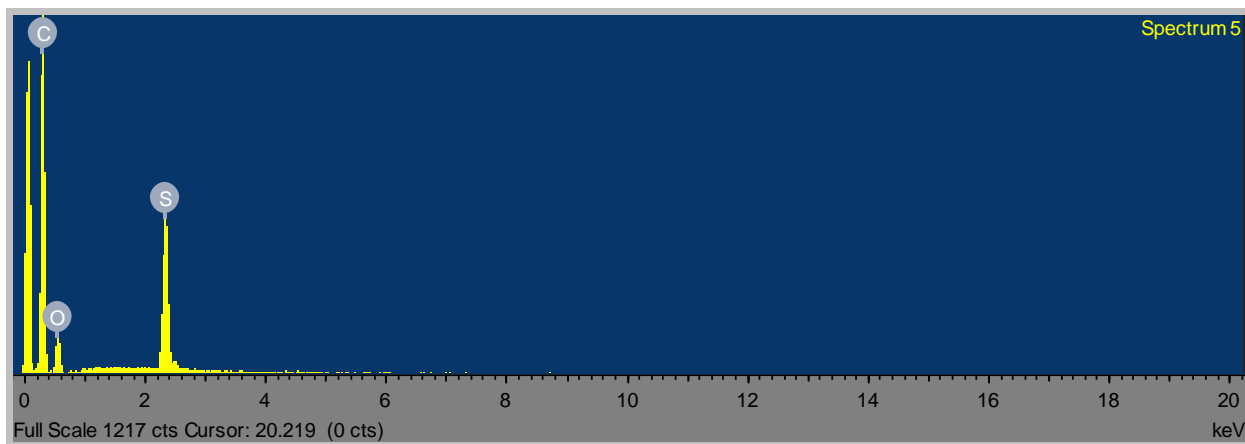


Figure I-11: EDX Spectrum (26.4 ml Laundry detergent; 4 ppm anti-scalant dosage)

Sample: 26.4 ml Laundry detergent; 8 ppm anti-scalant dosage

Processing option : All elements analysed (Normalised)

All results in weight%

Spectrum	In stats.	C	O	S	Cl	Total
Spectrum 1	Yes	76.49	17.36	6.15		100
Spectrum 2	Yes	76.74	17.02	6.23		100
Spectrum 3	Yes	76.44	17.29	6.27		100
Spectrum 4	Yes	77.86	15.95	6	0.2	100
Spectrum 5	Yes	76.92	16.65	6.43		100
Max.		77.86	17.36	6.43	0.2	
Min.		76.44	15.95	6	0.2	
ave		76.89	16.854	6.216		

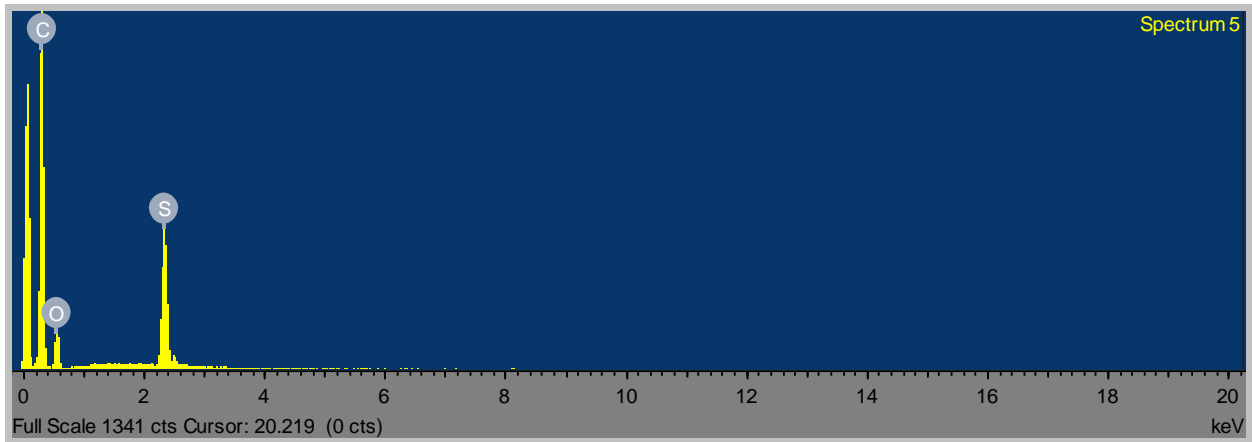


Figure I-12: EDX Spectrum (26.4 ml Laundry detergent; 8 ppm anti-scalant dosage)

# Appendix J

## ATR FTIR Raw Data

Data of FTIR analysis presented below are 10 points obtained for each experimental run. The ATR-FTIR spectra were recorded at a resolution of  $8\text{ cm}^{-1}$  during 64 scans at a nominal incident angle of  $45^\circ$  with wave numbers ranging between  $4000$  and  $400\text{ cm}^{-1}$ . To capture certain functionalities in both the clean and fouled membrane samples, spectra were zoomed into a region of  $2000$ - $400\text{ cm}^{-1}$ .

**Table J-1: FTIR data (virgin; 13.2 ml laundry detergent @ 0ppm, 4ppm, 8ppm anti-scalant)**

Virgin		13.2 mL Laundry detergent; 0 ppm anti-scalant		13.2 mL Laundry detergent; 4 ppm anti-scalant		13.2 mL Laundry detergent; 8 ppm anti-scalant	
Wave number (cm <sup>-1</sup> )	Absorbance	Wave number (cm <sup>-1</sup> )	Absorbance	Wave number (cm <sup>-1</sup> )	Absorbance	Wave number (cm <sup>-1</sup> )	Absorbance
700.0334	0.3659219	700.0334	0.1514154	700.0334	0.15748755	700.0334	0.29203295
700.9977	0.35541545	700.9977	0.1412052	700.9977	0.1472439	700.9977	0.28158995
701.9619	0.34622745	701.9619	0.13168225	701.9619	0.13768465	701.9619	0.2722345
702.9261	0.3387069	702.9261	0.12325827	702.9261	0.1292186	702.9261	0.26434725
703.8904	0.33315395	703.8904	0.116328725	703.8904	0.1222441	703.8904	0.2582702
704.8546	0.32980385	704.8546	0.11124837	704.8546	0.1171226	704.8546	0.2542849
705.8188	0.3287986	705.8188	0.10829905	705.8188	0.11414505	705.8188	0.2525823
706.7831	0.33014505	706.7831	0.107647615	706.7831	0.11348665	706.7831	0.25322185
707.7473	0.33366435	707.7473	0.10929946	707.7473	0.1151581	707.7473	0.25608525
708.7115	0.338953	708.7115	0.11305655	708.7115	0.1189622	708.7115	0.2608395
709.6758	0.3453789	709.6758	0.11849934	709.6758	0.1244742	709.6758	0.26692915

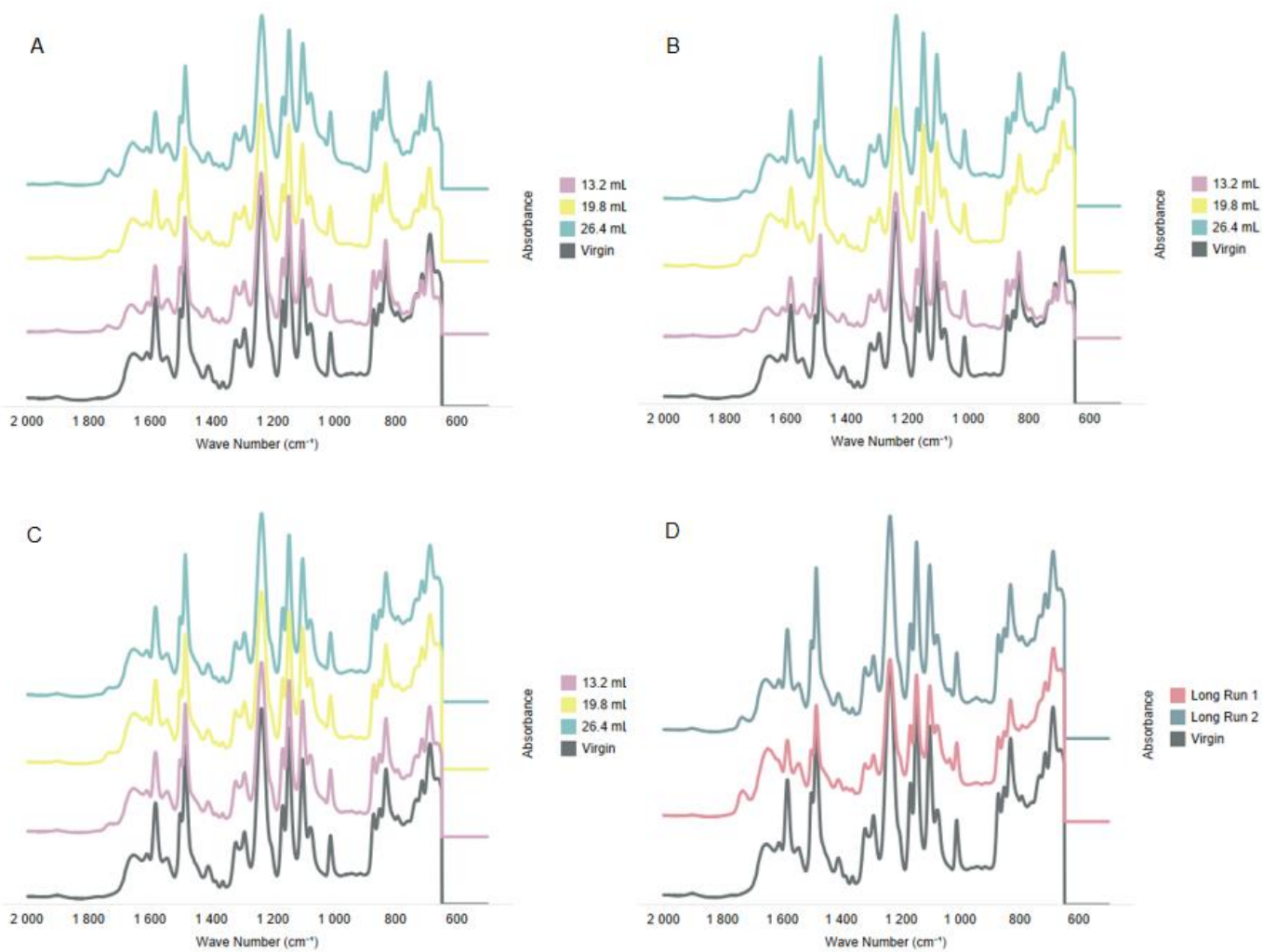
**Table J-2: FTIR data (long run 1; 19.8ml laundry detergent @ 0ppm, 4ppm, 8ppm anti-scalant)**

Long run 1		19.8 mL Laundry detergent; 0 ppm anti-scalant		19.8 mL Laundry detergent; 4 ppm anti-scalant		19.8 mL Laundry detergent; 8 ppm anti-scalant	
Wave number (cm <sup>-1</sup> )	Absorbance	Wave number (cm <sup>-1</sup> )	Absorbance	Wave number (cm <sup>-1</sup> )	Absorbance	Wave number (cm <sup>-1</sup> )	Absorbance
700.0334	0.33620285	700.0334	0.18751645	700.0334	0.35826505	700.0334	0.3564861
700.9977	0.32985105	700.9977	0.1778165	700.9977	0.3496694	700.9977	0.3474079
701.9619	0.32442265	701.9619	0.168858	701.9619	0.3422426	701.9619	0.33956575
702.9261	0.3201077	702.9261	0.1610242	702.9261	0.3362761	702.9261	0.3332666
703.8904	0.31706365	703.8904	0.15467965	703.8904	0.33201425	703.8904	0.3287702
704.8546	0.31540005	704.8546	0.150146	704.8546	0.3296339	704.8546	0.3262701
705.8188	0.3151601	705.8188	0.14767185	705.8188	0.32921805	705.8188	0.3258684
706.7831	0.31629375	706.7831	0.14739245	706.7831	0.33072175	706.7831	0.32753925
707.7473	0.3186333	707.7473	0.1492852	707.7473	0.3339378	707.7473	0.3310884
708.7115	0.32187875	708.7115	0.15312985	708.7115	0.33847515	708.7115	0.3361243
709.6758	0.3256088	709.6758	0.15849315	709.6758	0.34376855	709.6758	0.34206035



**Table J-3: FTIR data (long run 2; 26.4ml laundry detergent @ 0ppm, 4ppm, 8ppm anti-scalant)**

Long run 2		26.4 mL Laundry detergent; 0 ppm anti-scalant		26.4 mL Laundry detergent; 4 ppm anti-scalant		26.4 mL Laundry detergent; 8 ppm anti-scalant	
Wave number (cm <sup>-1</sup> )	Absorbance	Wave number (cm <sup>-1</sup> )	Absorbance	Wave number (cm <sup>-1</sup> )	Absorbance	Wave number (cm <sup>-1</sup> )	Absorbance
700.0334	0.3471237	700.0334	0.2068399	700.0334	0.352219	700.0334	0.3569273
700.9977	0.33753795	700.9977	0.19544745	700.9977	0.3415873	700.9977	0.34704375
701.9619	0.329172	701.9619	0.18496105	701.9619	0.33228565	701.9619	0.33844685
702.9261	0.32235695	702.9261	0.175827	702.9261	0.32468165	702.9261	0.3314696
703.8904	0.31738015	703.8904	0.16847405	703.8904	0.31909855	703.8904	0.326397
704.8546	0.31446295	704.8546	0.16328195	704.8546	0.3157911	704.8546	0.323445
705.8188	0.31372825	705.8188	0.1605411	705.8188	0.314911	705.8188	0.32273265
706.7831	0.3151606	706.7831	0.160402	706.7831	0.3164619	706.7831	0.32424315
707.7473	0.3185642	707.7473	0.1628216	707.7473	0.32024885	707.7473	0.32778
708.7115	0.32353655	708.7115	0.16751975	708.7115	0.32584275	708.7115	0.33293575
709.6758	0.32947545	709.6758	0.1739647	709.6758	0.33258195	709.6758	0.3390937



**Figure J-1: Zoomed in ATR-FTIR Spectra for varying concentrations of Anti-scalant. A: 0 ppm; B: 4 ppm; C: 8 ppm & D: Long Runs**